IEEE Access
Multidisciplinary | Rapid Review | Open Access Journal

Received 18 May 2023, accepted 17 June 2023, date of publication 28 June 2023, date of current version 6 July 2023.

Digital Object Identifier 10.1109/ACCESS.2023.3290306

RESEARCH ARTICLE

Robust Decentralized H_∞ Attack-Tolerant Observer-Based Team Formation Network Control of Large-Scale Quadrotor UAVs: HJIE-Reinforcement Learning-Based Deep Neural Network Method

BOR-SEN CHEN, (Life Fellow, IEEE), AND PO-CHUN CHAO
Department of Electrical Engineering, National Tsing Hua University, Hsinchu 30013, Taiwan
Corresponding author: Bor-Sen Chen (bschen@ee.nthu.edu.tw)

ABSTRACT In this paper, a robust decentralized H_∞ attack-tolerant observer-based team formation tracking control scheme is proposed for large-scale quadrotor unmanned aerial vehicle (UAV) systems under external disturbance, measurement noise, couplings from other neighboring quadrotor UAVs, and malicious attacks on actuator and sensor of the network control system (NCS) via wireless communication. First, we constructed a smoothed model of attack signals to describe their behavior. Then, by integrating the smoothed dynamic model with the system dynamic model of each quadrotor UAV, we can simultaneously estimate the attack signals and the system state of each quadrotor UAV through a traditional Luenberger observer for the efficient robust decentralized H_∞ attack-tolerant observer-based team formation tracking control of large-scale quadrotor UAVs. For the design of robust decentralized H_∞ attack-tolerant observer-based team formation tracking control of large-scale quadrotor UAVs, a very difficult independent nonlinear partial differential observer/controller-coupled Hamilton Jacobi Issac equation (HJIE) must be solved for the observer and controller design of each quadrotor UAV. Nowadays, there are no analytical and numerical methods to resolve HJIE. Thus, an HJIE-reinforcement learning-based deep neural network (DNN) is trained to directly solve the observer/controller-coupled HJIE for robust decentralized H_∞ attack-tolerant observer-based team formation tracking control of each quadrotor UAV. Since the system model of the quadrotor UAV and HJIE have been adopted for the HJIE-reinforcement Adam learning algorithm DNN training, compared to the traditional DNN big data-driven training schemes, we save a lot of training data and time to achieve the robust decentralized H_∞ attack-tolerant observer-based team formation tracking control design. As the Adam algorithm converges, we could show that the proposed HJIE-reinforcement DNN-based decentralized H_∞ attack-tolerant observer-based tracking control scheme can achieve the theoretical result. Finally, the simulation results are presented with a comparison to verify the effectiveness of the proposed method.

INDEX TERMS Network control system (NCS), attack-tolerant observer-based tracking control, team formation NCS of large-scale quadrotor UAVs, observer/controller-coupled HJIE, HJIE-reinforcement learning deep neural network (DNN), H_∞ decentralized reference tracking control of large-scale systems.

I. INTRODUCTION

In this generation, along with technological development, automation systems and the internet of things (IOTs) have attracted more attention in a future smart city. The unmanned aerial vehicle (UAV) has become a hot topic due to its wide applications such as agriculture, military, rescuing, humanitarian relief, and wireless communication [1], [3]. To successfully complete the above tasks, a UAV is needed to track the specified trajectory. Among all types of UAVs,

The associate editor coordinating the review of this manuscript and approving it for publication was Yang Tang.

This work is licensed under a Creative Commons Attribution-NonCommercial-NoDerivatives 4.0 License.
For more information, see https://creativecommons.org/licenses/by-nc-nd/4.0/

quadrotor UAVs have vertical take-off and landing (VTOL) capabilities [4]. In accordance with this maneuverability, quadrotor UAVs can follow a wider variety of trajectories than other types of UAVs. Although quadrotor UAVs have many appealing advantages in practical applications, the power consumption of quadrotor UAVs during flight is a key issue that needs further consideration. Recently, as the need to implement more complex tasks continues to increase, the team formation tracking control problem of multi-quadrotor UAVs is more appealing than the tracking control problem of a single quadrotor UAV in the future.

Currently, common team formation methods include the behavior-based control method [5], the leader-follower (L-F) method [6], and the virtual leader structure (V-S) method [7]. Among the above-mentioned methods, the (V-S) method is considered to be the most recognized strategy for team formation tracking control design problems. Since the leader is virtualized, it avoids the problem of the L-F approach, where the desired team formation shape cannot be maintained once the leader collides during the flight process.

Generally, the control designs of the large-scale team formation system are divided into two kinds: centralized control [8] and decentralized control [9]. The centralized control strategy is that all quadrotor UAV subsystems are coordinated by a single controller. With an increase in the number of quadrotor UAV subsystems to a large scale, the computational complexity of implementing the centralized formation control strategy will be large and even lead the formation control design to being infeasible. Hence, the decentralized V-S formation control strategy is preferred when considering the formation of large-scale quadrotor UAVs.

Recently, with the advancement of communication technology [10], [11], the control signals of physical plants are not calculated by themselves, but by remote computing units via wireless network channels from the ground control system (GCS). In a large-scale quadrotor UAV team formation, a network control system (NCS) is applied to the formation tracking control. Specifically, NCS is divided into two parts: the local side (physical controlled system) and the remote side (computing unit). When the state information of the quadrotor UAV team is transmitted to the GCS, GCS calculates control commands and then sends the control input back to the quadrotor UAV, which can effectively reduce power consumption and provide greater flexibility and maintainability during tasks. Although the network-based control strategy can optimize the calculation process of control commands, it also creates some problems that need to be dealt with. First, as a result of the uncertainty of quality of service (QoS) in wireless network communication, packet dropout may occur [12], [16]. When packets are lost from the transmission, signal information cannot travel over the wireless network communication channel, so the receiver will not be able to receive any signal from the sender [14]. Second, if the signal is affected by the network-induced delay, it cannot be delivered to the receiver on time [16]. According to the above mention, the entire NCS is delay-dependent, and the corresponding control problem is tougher than a delay-free network.

On the flip side, since the rapid development of wireless network-based communication technology and widespread applications in recent years, network security has become a major issue, which has attracted the attention of many researchers and research institutions. Moreover, hackers may attack the network control system to interfere with the transmission of information or even cause the system to crash. Even though various methods have been proposed to resist malicious attacks [17], [19], they may still enter the network through security breaches. These malicious attacks interfere with the correctness of signals in wireless network channels, thus disrupting the operation of the entire network system. Due to the fact that these malicious attacks are unavailable signals to the designer, the impact of malicious attacks on NCS is not easily eliminated. To deal with this problem, an attack-tolerant control strategy has been developed to compensate for the impact of unavailable malicious attack signals on the system [20], [21]. This strategy constructs a specific observer to simultaneously estimate state variables and malicious attack signals. After that, through the estimated malicious attack signals, a control strategy can be implemented to compensate for the impact of actual malicious attack signals on NCS. Even the causes of actuator and sensor fault are different from the causes of actuator and sensor attack signal, their effects on the control and observer are described by the similar mathematic equations and are always discussed together by many papers. Traditionally, to estimate these malicious attack signals, singular descriptor-based observers have been widely used in the field of fault estimation (FE) [22], [23]. Nevertheless, the above descriptor-based observers are difficult to implement in most practical applications due to complex algebraic equation constraints. Recently, a novel intermediate observer design method is proposed to estimate the system states, actuator faults and sensor faults of nonlinear multi-agent system [24] and a novel adaptive adjustable dimension observer-based fault estimation for switched fuzzy system is proposed in [25].

Except for malicious attacks, in practice, unexpected external disturbances will inevitably interfere with quadrotor UAVs, e.g., a wind gust. Additionally, quadrotor UAVs may suffer unknown coupling effects from other quadrotor UAVs in the large-scale quadrotor UAV team formation system such as trailing vortex coupling from other neighboring quadrotor UAVs. Therefore, in a non-ideal environment, the formation controller design of the quadrotor UAVs should consider the external disturbance, measurement noise, and trailing vortex coupling of other quadrotor UAVs in the team; otherwise, it may lead to instability or even crashes, especially for a large-scale quadrotor UAVs team formation system. Based on the above discussion, the attenuation of these effects should be further considered in the formation tracking control scheme to ameliorate the formation tracking

control performance of the NCS of quadrotor UAVs. Hence, in this study, we should deal with malicious attack signal estimation and attack-tolerant tracking control problems for large-scale team formation quadrotor UAVs NCS under malicious attack via wireless channel, external disturbance, and trailing vortex coupling from neighor UAVs.

Over several decades, the robust H_∞ observer-based output feedback control strategies have been adopted and widely used to address the attenuation problem of these non-ideal effects [26], [27], [28]. Through the smoothing model [29], malicious attacks on quadrotor UAV actuators and sensors through network channels can be effectively described and embedded into the augmented state of the augmented system of each quadrotor UAV model and the malicious attack signal smoothing model to avoid the destruction of the state estimate of each quadrotor UAV by the malicious attack signal. Thus, the malicious attack signals and state variables of each quadrotor UAV can be estimated by the traditional Luenberger observer. And then, the estimated state variables and malicious attack signals are adopted for the robust decentralized H_∞ attack-tolerant observer-based team formation tracking control design of the NCS of large-scale quadrotor UAVs by compensating for the effect of malicious attacks. Taking advantage of tracking the desired virtual leader with a desired team formation shape, the tracking error and estimation error of each quadrotor UAV system can be considered independently by the proposed robust decentralized H_∞ attack-tolerant observer-based tracking control strategy. Therefore, the original robust decentralized H_∞ attack-tolerant observer-based team formation tracking control problem of the large-scale quadrotor UAV NCS under malicious attack, external disturbance, measurement noise, and trailing vortex coupling can be converted into an independent robust H_∞ attack-tolerant observer-based tracking control design problem for each quadrotor UAV in the team formation. Furthermore, the robust decentralized H_∞ attack-tolerant observer-based team formation tracking control design problem of large-scale quadrotor UAVs can be further converted into the problem of solving an equivalent highly nonlinear partial differential observer/controller-coupled Hamilton Jacobi Isaacs Equation (HJIE) problem for robust H_∞ attack-tolerant controller and observer design of each quadrotor UAV in the team formation.

However, observer/controller-coupled HJIE is difficult to solve analytically and numerically. Therefore, instead of solving HJIE directly, several interpolation methods (e.g., the global linearization method [30] and the Takagi-Sugeno (T-S) fuzzy interpolation method [31]) have been proposed to interpolate N local linearized systems at different operations to approximate a nonlinear quadrotor UAV system. Then, with the adoption of the quadratic Lyapunov function, observer/controller-coupled HJIE can be replaced by a set of observer/controller-coupled N^2 Riccati-like Equations (RLEs). By utilizing the Schur's complement technique, N^2 Riccati-like inequalities can be transformed into a set of N^2 observer/controller-coupled linear matrix inequalities (LMIs), which can be solved by a two steps procedure (one for observer and another for controller of each quadrotor UAV) with the assistance of LMI Toolbox in MATLAB. However, these interpolation methods need to solve a large number of LMIs, especially for a highly nonlinear system such as a quadrotor UAV. Further, we need to calculate H_∞ observer-based controller laws for each quadrotor UAV by interpolating N^2 local linearized observer-based control laws via N^2 interpolation functions at every time instant, which makes the design complexity and computational load dramatically increase. Besides, the solution of HJIE is based on a quadratic Lyapunov function, resulting in a more conservative solution for nonlinear HJIE. Lately, an HJIE-embedded DNN learning approach is proposed to solve HJIE for robust H_∞ stabilization control of nonlinear time-varying systems by a HJIE-embedded Adam learning algorithm [32] and the robust H_∞ observer-based reference tracking control design of nonlinear systems under external disturbance and measurement noise directly through the observer/control coupled HJIE-embedded DNN-based learning algorithm [33]. Recently, it is appealing to extend to the more complicated robust H_∞ attack-tolerant observer-based team formation tracking design of large-scale NCS under coupling of neighor UAVs and malicious attack signal through wireless channel for more practical applications in future 5G and 6G era.

In this paper, an HJIE-reinforcement learning DNN observer-based control scheme is proposed to achieve robust decentralized H_∞ attack-tolerant observer-based team formation tracking control of large-scale quadrotor UAV NCS to ensure that the network-controlled quadrotor UAVs can progressively approach the desired formation of the large-scale quadrotor UAVs under the effect of external disturbance, malicious attack, trailing vortex coupling, and measurement noise. Instead of conventional interpolation methods, a DNN-based observer-based control scheme is trained by HJIE-reinforcement Adam learning algorithm [34] to solve the nonlinear partial differential observer/controller-coupled HJIE directly for the robust decentralized H_∞ attack-tolerant observer-based team formation tracking control law of each quadrotor UAV under the worst-case effects of external disturbance, malicious attack, measurement noise, and trailing vortex coupling, which are employed for generating output signals to produce the state signal, state estimation, estimation error and tracking error to train DNN for observer gain and control gain of H_∞ observer-based formation control of each quadrotor UAV by HJIE-reinforcement learning-based Adam learning algorithm in the offline training phase as shown in Fig.3. This HJIE-reinforcement DNN-based observer-based control scheme trained based the worse-case external disturbance, measurement noise and coupling in the offline training phase will not influence the H_∞ attack-tolerant observer-based control tracking performance of each UAV because the robust decentralized H_∞ attack-tolerant observer-based team formation control design is based on the worst-case external disturbances, malicious attacks, coupling

of neighor UAVs, and measurement noise. In the online operation phase, external disturbances, malicious attacks, coupling, and measurement noise are available, as shown in Fig.2. A simulation example with comparison is provided to confirm the team formation tracking performance of the proposed robust decentralized H_∞ attack-tolerant observer-based team formation tracking control scheme of 25 UAVs.

The main contributions of this study are summarized as follows:

(I) A novel smoothed dynamic model is employed to model malicious attack signals that are not available for the NCS. Thence, the malicious attack signals are embedded via smooth dynamic model in large-scale UAV NCS so that the malicious attack signals and state variables of quadrotor UAVs can be estimated via a traditional Luenberger observer simultaneously to compensate for the effect to achieve the attack-tolerant control. The worst-case effects of external disturbance, malicious attacks, measurement noise, and couplings from other quadrotor UAVs on the state estimation and formation tracking control strategy of each quadrotor UAV are minimized to achieve robust decentralized H_∞ attack-tolerant observer-based team formation network tracking control of large-scale quadrotor UAVs. By argumenting each UAV NCS system in the team with smoothed dynamic model, reference tracking error dynamic, and estimation error dynamic so that the decentralized attack-tolerant observer-based team formation control design becomes a robust stabilization control problem to significantly simplify the design procedure.

(II) An observer/controller-coupled HJIE is developed for each quadrotor UAV to accomplish the robust decentralized H_∞ attack-tolerant observer-based team formation tracking control design of large-scale quadrotor UAVs, which becomes how to solve an independent observer/controller-coupled HJIE for the decentralized H_∞ attack-tolerant observer-based reference tracking control of each UAV in the team formation.

(III) An HJIE-reinforcement DNN scheme is proposed to solve the observer/controller-coupled HJIE directly for the robust decentralized H_∞ attack-tolerant observer-based team formation tracking control design of the large-scale quadrotor UAV NCS to simplify the design complexity. Moreover, the proposed HJIE-reinforcement-based DNN learning scheme can reduce a lot of training data and training time compared to conventional big data-driven learning approaches to enlarge the domain of application for DNN via the HJIE-reinforcement learning scheme.

The structure of this paper is described below. The large-scale quadrotor UAV team formation network control system, smoothed models that are used to describe malicious attack signals, and problem formulation are introduced in Section II. In Section III, a robust decentralized H_∞ attack-tolerant observer-based team formation tracking control strategy is provided. HJIE-reinforcement DNN-based decentralized H_∞ attack-tolerant observer-based team formation tracking control design of large-scale quadrotor UAV NCS in Section IV. In this section, we also propose a reinforcement learning-based Adam algorithm to train the DNN control scheme. A simulation example with comparison is given in Section V. The conclusion is drawn in Section VI.

Notation: $M > 0 (M \geq 0)$: The positive definite symmetric (semi-definite symmetric) matrix M,respectively; M^T: The transpose of the matrix M; I_a: The identity matrix with dimension $a \times a$;$\mathbb{R}^n$: the set of n-tuple real vectors; $\mathbb{R}^{n\times m}$: The set of all real $n \times m$ matrices; $\|.\|_2$: The Euclidean norm; $\pounds_2[0, \infty)$: A set of real stochastic functions $x(t) \in \mathbb{R}^n$ with finite energy, that is, $E\left\{\int_0^\infty x^T(t)x(t)dt\right\} < \infty$; $E\{\cdot\}$: The expectation operator; $diag(A_1, \ldots A_n)$: A block diagonal matrix with the main diagonal $A_1, \ldots A_n$.

II. SYSTEM DESCRIPTION AND PRELIMINARIES

A. SYSTEM MODEL OF QUADROTOR UAV IN LARGE-SCALE TEAM FORMATION

In this subsection, we consider the position and attitude of the quadrotor UAV simultaneously in the dynamic model. The position of the quadrotor UAV w.r.t. inertial frame is described by Cartesian coordinates (x, y, z) of its mass center, and the attitude of the quadrotor UAV in the body frame is described by three rotation Euler angles (ϕ, θ, ψ) on the body of the quadrotor UAV, which represent the roll angle $(-\frac{\pi}{2} < \phi < \frac{\pi}{2})$, the pitch angle $(-\frac{\pi}{2} < \theta < \frac{\pi}{2})$, and the yaw angle $(-\pi < \psi < \pi)$ related to the orientation of the quadrotor UAV, respectively, as shown in Fig.1.

For a large-scale quadrotor UAV team formation system, it is indicated as a set $S = \{S_1, S_2, \ldots, S_N\}$, consisting of single quadrotor UAV subsystems $S_i, i = 1, \ldots N$. In practice, each single quadrotor UAV suffers not only from external disturbances but also from the effect of interconnected couplings by non-ideal communications or aerodynamics from other nearby quadrotor UAVs. Taking these effects into consideration, the ith team formation quadrotor UAV subsystem can be formulated as follows:

$$\begin{aligned} S_i : \dot{X}_i(t) &= F_i(X_i(t)) + G_i(X_i(t))U_i(t) + D_i(X_i(t))v_i(t) \\ &\quad + \sum_{j\in N_i} F_{ij}(X_i(t))X_j(t - \tau_{ij}(t)) \\ Y_i(t) &= C_i(X_i(t)) + n_i(t), for\ i, j = 1, \ldots, N; i \neq j \end{aligned} \quad (1)$$

where $X_i(t) = [x_1^i(t), x_2^i(t), y_1^i(t), y_2^i(t), z_1^i(t), z_2^i(t), \phi_1^i(t), \phi_2^i(t), \theta_1^i(t), \theta_2^i(t), \psi_1^i(t), \psi_2^i(t)]^T$ is the state vector of the system, $x_1^i(t), y_1^i(t), z_1^i(t) \in \mathbb{R}$ are the positions of the ith quadrotor UAV, $x_2^i(t), y_2^i(t), z_2^i(t) \in \mathbb{R}$ are the velocities of the ith quadrotor UAV, $\phi_1^i(t), \theta_1^i(t), \psi_1^i(t) \in \mathbb{R}$ are the attitudes of the i th quadrotor UAV, and $\phi_2^i(t), \theta_2^i(t), \psi_2^i(t) \in \mathbb{R}$ are the angular velocities of the ith quadrotor UAV. $U_i(t) = [F^i(t), \tau_\phi^i(t), \tau_\theta^i(t), \tau_\psi^i(t)]^T$ is the control input of the ith quadrotor UAV in the formation team, $F^i(t) \in \mathbb{R}$ is the total thrust acting on the ith quadrotor UAV, the rotational forces $\tau_\phi^i(t), \tau_\theta^i(t), \tau_\psi^i(t) \in \mathbb{R}$ are generated by four rotors of the ith quadrotor UAV, $v_i(t) = [v_x^i(t), v_y^i(t), v_z^i(t), v_\phi^i(t), v_\theta^i(t), v_\psi^i(t)]^T$ is the external disturbance of the ith quadrotor UAV. $Y_i(t)$ is the measurement output of the ith quadrotor UAV. $n_i(t)$ is the measurement

noise. $C_i(X_i(t))$ is the nonlinear output matrix. N denotes the number of quadrotor UAVs in the team. The system matrices of the ith quadrotor UAV in (1) are given as:

$$F_i(X_i(t)) = \begin{bmatrix} x_2^i(t), \\ -\frac{K_x^i}{m_i} x_2^i(t), \\ y_2^i(t), \\ -\frac{K_y^i}{m_i} y_2^i(t), \\ z_2^i(t), \\ -\frac{K_z^i}{m_i} z_2^i(t) - g, \\ \phi_2^i(t), \\ \frac{J_y^i - J_z^i}{J_x^i}\theta_1^i(t)\psi_1^i(t) - \frac{K_\phi^i}{J_x^i}\phi_2^i(t), \\ \theta_2^i(t), \\ \frac{J_z^i - J_x^i}{J_x^i}\phi_1^i(t)\psi_1^i(t) - \frac{K_\theta^i}{J_y^i}\theta_2^i(t), \\ \psi_2^i(t), \\ \frac{J_x^i - J_y^i}{Jz}\phi_1^i(t)\theta_1^i(t) - \frac{K_\psi^i}{J_z^i}\psi_2^i(t) \end{bmatrix}$$

$$G_i(X_i(t)) = \begin{bmatrix} 0 & 0 & 0 & 0 \\ (\cos\phi_1^i(t)\sin\theta_1^i(t)\cos\psi_1^i(t) + \sin\phi_1^i(t)\sin\psi_1^i(t))\frac{1}{m_i} & 0 & 0 & 0 \\ 0 & 0 & 0 & 0 \\ (\cos\phi_1^i(t)\sin\theta_1^i(t)\sin\psi_1^i(t) - \sin\phi_1^i(t)\sin\psi_1^i(t))\frac{1}{m_i} & 0 & 0 & 0 \\ 0 & 0 & 0 & 0 \\ \frac{1}{m_i}\cos\phi_1^i(t)\cos\theta_1^i(t) & 0 & 0 & 0 \\ 0 & 0 & 0 & 0 \\ 0 & \frac{1}{J_x^i} & 0 & 0 \\ 0 & 0 & 0 & 0 \\ 0 & 0 & \frac{1}{J_y^i} & 0 \\ 0 & 0 & 0 & 0 \\ 0 & 0 & 0 & \frac{1}{J_z^i} \end{bmatrix}$$

$$D_i(X_i(t)) = \begin{bmatrix} 0&0&0&0&0&0 \\ 1&0&0&0&0&0 \\ 0&0&0&0&0&0 \\ 0&1&0&0&0&0 \\ 0&0&0&0&0&0 \\ 0&0&1&0&0&0 \\ 0&0&0&0&0&0 \\ 0&0&0&1&0&0 \\ 0&0&0&0&0&0 \\ 0&0&0&0&1&0 \\ 0&0&0&0&0&0 \\ 0&0&0&0&0&1 \end{bmatrix}$$

where $F_i(X_i(t))$ is the system function matrix of the ith quadrotor UAV. g is the gravitational acceleration, J_x^i, J_y^i, J_z^i are the moments of inertia of the ith quadrotor UAV, $K_x^i, K_y^i, K_z^i, K_\phi^i, K_\theta^i, K_\psi^i$ represent aerodynamic damping coefficient of the ith quadrotor UAV, m_i is the total mass of the ith quadrotor UAV. $G_i(X_i(t)) \in \mathbb{R}^{12\times 4}$ is the input matrix of the ith quadrotor UAV. $D_i(X_i(t))$ is the influence matrix of the external disturbance. $F_{ij}(X_i(t)) \in \mathbb{R}^{12\times 12}$ is the coupling matrix between the ith quadrotor UAV to the jth quadrotor UAV. $X_j(t-\tau_{ij}(t)) \in \mathbb{R}^{12}$ is the coupling term from the jth quadrotor UAV to the ith quadrotor UAV with a time-varying delay $\tau_{ij}(t)$.N_i denotes the neighboring quadrotor UAVs coupling with the ith quadrotor UAV.

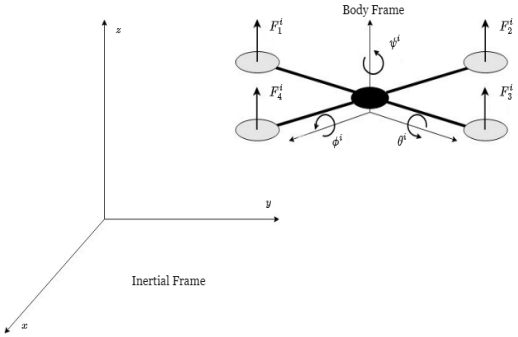

FIGURE 1. Structure of the ith quadrotor UAV in the large-scale UAV formation team under the inertial frame and body frame.

B. A LARGE-SCALE QUADROTOR UAV TEAM FORMATION NETWORK CONTROL SYSTEM

Under the structure of the network control system (NCS) of large-scale quadrotor UAV team formation as shown in Fig.2, each quadrotor UAV is controlled through an observer-based controller on the remote side. Through the sensor, output measurement data $Y_i(t)$ of the ith quadrotor UAV is sampled and transmitted to the observer on the remote side. Then, the control signals are computed at each observer-based controller on the remote side and transmitted via a wireless network channel to the zero-order holder (ZOH),which is set on the quadrotor UAV at the local side as shown in Fig.2 at every sampling period. Once the sampled data with control commands arrives at the ZOH of the quadrotor UAV, the ZOH will convert the sampled data into continuous control signals and transmits them to the actuator to control the quadrotor UAV. The control commands are stored in ZOH and kept until new control signals are received to update.

For NCS, when signals are transmitted through the wireless network channels, some hackers may attack NCS, which can even make NCS unstable. Hence, we need to take these malicious attacks into consideration in the NCS of the large-scale quadrotor UAV team formation system via a wireless network. In Fig.2, two malicious attack signals $\gamma_a^i(t)$ and $\gamma_s^i(t)$ will interfere with the performance of both the reference tracking and the state estimation of the NCS of the large-scale quadrotor UAV team formation system via wireless network channels, respectively. In this case, the sensor and actuator would receive erroneous information from the wireless network channel, and their corruption could lead to the entire team formation system of large-scale quadrotor UAVs being out of control. That is, the two malicious attack signals $\gamma_a^i(t)$ and $\gamma_s^i(t)$ can be equivalently referred to as the sensor attack signal and the actuator attack signal in each quadrotor UAV NCS of team formation of large-scale quadrotor UAVs. Then, the ith quadrotor UAV NCS in (1) under actuator attack and sensor attack via the

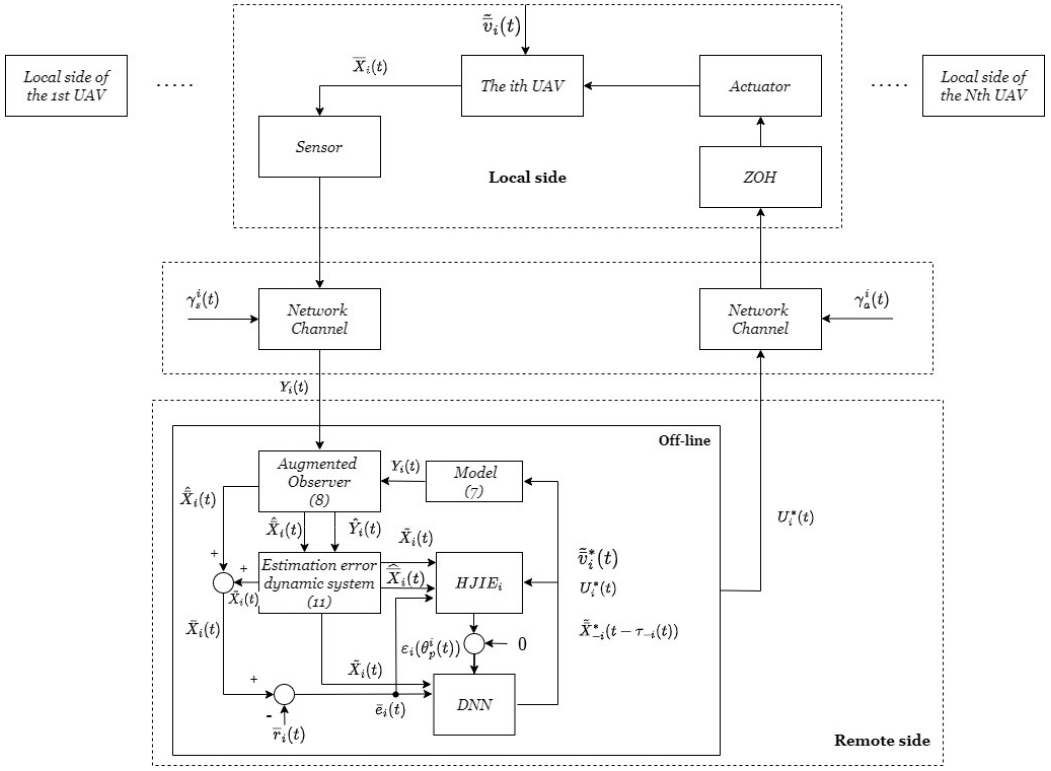

FIGURE 2. The structure of robust decentralized DNN-based H_∞ attack-tolerant observer-based team formation NCS of large-scale quadrotor UAVs. In the offline training phase, we need the stochastic augmented model of each quadrotor UAV to produce $Y_i(t)$ with the worst-case external disturbance $\tilde{\bar{v}}_i^*(t)$ and worst-case coupling $\tilde{\bar{X}}_{-i}^*(t-\tau_{-i})$, and then augmented Luenberger observer and estimation error model are employed to produce $\hat{\bar{X}}_i(t)$ and $\tilde{\bar{X}}_i(t)$ to obtain $\bar{X}_i(t) = \hat{\bar{X}}_i(t) + \tilde{\bar{X}}_i(t)$ and to get formation tracking error $\bar{e}_i(t) = \bar{X}_i(t) - \bar{r}_i(t)$. Then, $\bar{e}_i(t)$ and $\tilde{\bar{X}}_i(t)$ are transmitted into DNN to train DNN by HJIE-reinforcement learning to output $\frac{\partial V(\tilde{\bar{X}}_i(t), \bar{e}_i(t), t)}{\partial [\tilde{\bar{X}}_i^T(t)\ \bar{e}_i^T(t)\ t]^T}$ to produce H_∞ tracking control $U_i^*(t)$ and observer gain $L_i^*(\hat{\bar{X}}_i(t))$ until HJIE-reinforcement learning converge as shown in Fig.3. In the online operation phase, the output $Y_i(t)$ can be obtained from the real quadrotor UAV.

wireless network channel should be modified as follows:

$$\begin{aligned}\dot{X}_i(t) &= F_i(X_i(t)) + G_i(X_i(t))(U_i(t) + \gamma_a^i(t)) + D_i(X_i(t))v_i(t) \\ &\quad + \sum_{j\in N_i} F_{ij}(X_i(t))X_j(t - \tau_{ij}(t)) \\ Y_i(t) &= C_i(X_i(t)) + n_i(t) + D_s^i(X_i(t))\gamma_s^i(t), \\ &\quad for\ i, j = 1, \ldots, N; i \neq j \end{aligned} \tag{2}$$

where $\gamma_a^i(t)$ denotes the actuator attack signal, $\gamma_s^i(t)$ denotes the sensor attack signal and $D_s^i(X_i(t))$ denotes the effect matrix of sensor attack signal $\gamma_s^i(t)$.

Assumption 1: Before the start of state estimation and team formation tracking control process of quadrotor UAVs, the system state $X_i(t)$, actuator attack signal $\gamma_a^i(t)$, sensor attack signal $\gamma_s^i(t)$ and external disturbance $v_i(t)$ of the ith quadrotor UAV in nonlinear NCS of team formation of quadrotor UAVs are assumed to be zero, i.e., $X_i(t) = 0$, $\gamma_a^i(t) = 0$, $\gamma_s^i(t) = 0$ and $v_i(t) = 0$, $\forall t < 0$, for $i = 1, \ldots, N$.

As the actuator attack $\gamma_a^i(t)$ and the sensor attack $\gamma_s^i(t)$ are not available, they cannot be estimated directly by the traditional Luenberger observer. In order to estimate attack signals $\gamma_a^i(t)$ and $\gamma_s^i(t)$, the novel dynamic smoothed models of the attack signals $\gamma_a^i(t)$ and $\gamma_s^i(t)$ in [29] are employed for avoiding their corruption on state estimation and tracking control of quadrotor UAVs. By the novel dynamic smoothed models of the attack signals $\gamma_a^i(t)$ and $\gamma_s^i(t)$, the state of the system and the attack signals can be estimated by the traditional Luenberger observer simultaneously. Similar to [29], the dynamic smoothed model is proposed for malicious attack signals $\gamma_a^i(t)$ and $\gamma_s^i(t)$. Initially, by the right derivative of the actuator attack signal $\dot{\gamma}_a^i(t) = \lim_{\tau\to 0} \frac{\gamma_a^i(t+\tau) - \gamma_a^i(t)}{\tau}$, we can construct the following approximations:

$$\begin{aligned}\dot{\gamma}_a^i(t) &= \tfrac{1}{\tau}(\gamma_a^i(t+\tau) - \gamma_a^i(t)) + \epsilon_{1,a}^i(t), \\ \dot{\gamma}_a^i(t-\tau) &= \tfrac{1}{\tau}(\gamma_a^i(t) - \gamma_a^i(t-\tau)) + \epsilon_{2,a}^i(t), \\ &\vdots \\ \dot{\gamma}_a^i(t-k\tau) &= \tfrac{1}{\tau}(\gamma_a^i(t-(k-1)\tau) - \gamma_a^i(t-k\tau)) + \epsilon_{k,a}^i(t)\end{aligned} \tag{3}$$

where $\epsilon_{1,a}^i(t), \epsilon_{2,a}^i(t), \ldots, \epsilon_{k,a}^i(t)$ denote the derivative approximation errors of $\dot{\gamma}_a^i(t), \dot{\gamma}_a^i(t-\tau), \ldots \dot{\gamma}_a^i(t-k\tau)$,

respectively, and $\tau > 0$ denotes a small time interval and $k \in \mathbb{N}$ denotes the number of delay samples. Moreover, the future attack signal $\gamma_a^i(t+\tau)$ could be extrapolated as follows:

$$\gamma_a^i(t+\tau) = \sum_{n=0}^{k} a_n \gamma_a^i(t-n\tau) + \delta_a^i(t), \tag{4}$$

where $\{a_n\}_{n=0}^k$ are extrapolation coefficients such as the Lagrange extrapolation approach [35] or other extrapolation approaches with $\sum_{n=0}^{k} a_n = 1$, $\delta_a^i(t)$ is the extrapolation error of $\gamma_a^i(t+\tau)$. By combing (3) and (4), the smoothed model of the actuator attack signal $\gamma_a^i(t)$ can be constructed as

$$\dot{\Gamma}_a^i(t) = A_{\gamma_a}\Gamma_a^i(t) + \epsilon_a^i(t) \tag{5}$$

where $\Gamma_a^i(t) = [\gamma_a^{iT}(t), \gamma_a^{iT}(t-\tau), \ldots, \gamma_a^{iT}(t-k\tau)]^T$, $\epsilon_a^i(t) = [(\epsilon_{1,a}^i(t) + \delta_a^i(t)/\tau)^T, \epsilon_{2,a}^{iT}(t), \ldots, \epsilon_{k,a}^{iT}(t)]^T$ denotes the derivative approximation error and

$$A_{\gamma_a} = \begin{bmatrix} \frac{\bar{a}_0}{\tau} I_{n_a} & \frac{a_1}{\tau} I_{n_a} & \frac{a_2}{\tau} I_{n_a} & \ldots & \frac{a_k}{\tau} I_{n_a} \\ \frac{1}{\tau} I_{n_a} & -\frac{1}{\tau} I_{n_a} & & \ldots & 0 \\ 0 & \frac{1}{\tau} I_{n_a} & -\frac{1}{\tau} I_{n_a} & \ldots & 0 \\ . & . & & & . \\ . & & . & & . \\ . & & & . & . \\ 0 & \ldots & 0 & \frac{1}{\tau} I_{n_a} & -\frac{1}{\tau} I_{n_a} \end{bmatrix},$$

with $\bar{a}_0 = -1 + a_0$. Similar to the above procedure, the smoothed model of the sensor attack signal $\gamma_s^i(t)$ can be constructed as

$$\dot{\Gamma}_s^i(t) = A_{\gamma_s}\Gamma_s^i(t) + \epsilon_s^i(t) \tag{6}$$

where $\Gamma_s^i(t) = [\gamma_s^{iT}(t), \gamma_s^{iT}(t-\tau), \ldots, \gamma_s^{iT}(t-k\tau)]^T$, $\epsilon_s^i(t) = [(\epsilon_{1,s}^i(t) + \delta_s^i(t)/\tau)^T, \epsilon_{2,s}^{iT}(t), \ldots, \epsilon_{k,s}^{iT}(t)]^T$, and

$$A_{\gamma s} = \begin{bmatrix} \frac{\bar{b}_0}{\tau} I_{n_a} & \frac{b_1}{\tau} I_{n_a} & \frac{b_2}{\tau} I_{n_a} & \ldots & \frac{b_k}{\tau} I_{n_a} \\ \frac{1}{\tau} I_{n_a} & -\frac{1}{\tau} I_{n_a} & & \ldots & 0 \\ 0 & \frac{1}{\tau} I_{n_a} & -\frac{1}{\tau} I_{n_a} & \ldots & 0 \\ . & . & & & . \\ . & & . & & . \\ . & & & . & . \\ 0 & \ldots & 0 & \frac{1}{\tau} I_{n_a} & -\frac{1}{\tau} I_{n_a} \end{bmatrix},$$

with $\bar{b}_0 = -1 + b_0$ and $b_i, i = 0, \ldots, k$ are the extrapolation coefficient with $\sum_{i=0}^{k} b_i = 1$. Then, to estimate $X_i(t)$, $\gamma_a^i(t)$, $\gamma_s^i(t)$ simultaneously, we can augment these states as $\bar{X}_i(t) = [X_i^T(t)\ \Gamma_a^{iT}(t)\ \Gamma_s^{iT}(t)]^T$, and the corresponding ith augmented quadrotor UAV NCS is given as follows:

$$\begin{aligned} \dot{\bar{X}}_i(t) &= \bar{F}_i(\bar{X}_i(t)) + \bar{G}_i(\bar{X}_i(t))U_i(t) + \bar{D}_i(\bar{X}_i(t))\bar{v}_i(t) \\ &\quad + \sum_{j\in N_i} \bar{F}_{ij}(\bar{X}_i(t))\bar{X}_j(t-\tau_{ij}(t)) \\ Y_i(t) &= \bar{C}_i(\bar{X}_i(t)) + n_i(t), \end{aligned}$$

$$for\ i, j = 1, \ldots, N; i \neq j \tag{7}$$

where

$$\bar{F}_i(\bar{X}_i(t)) = \begin{bmatrix} F_i(X_i(t)) + \bar{G}_i(\bar{X}_i(t))S_a\Gamma_a^i(t) \\ A_{\gamma a}^i\Gamma_a^i(t) \\ A_{\gamma s}^i\Gamma_s^i(t) \end{bmatrix},$$

$$S_a = [I_{na}, 0, \ldots, 0],$$

$$\bar{G}_i(\bar{X}_i(t)) = \begin{bmatrix} G_i(X_i(t)) \\ 0 \\ 0 \end{bmatrix},$$

$$\bar{D}_i(\bar{X}_i(t)) = \begin{bmatrix} D_i(X_i(t)) & 0 & 0 \\ 0 & I & 0 \\ 0 & 0 & I \end{bmatrix},$$

$$\bar{v}_i(t) = \begin{bmatrix} v_i(t) \\ \epsilon_a^i(t) \\ \epsilon_s^i(t) \end{bmatrix}, \bar{F}_{ij}(\bar{X}_i(t)) = \begin{bmatrix} F_{ij}(X_i(t)) & 0 & 0 \\ 0 & I & 0 \\ 0 & 0 & I \end{bmatrix},$$

$$\bar{X}_j(t-\tau_{ij}(t)) = \begin{bmatrix} X_j^T(t-\tau_{ij}(t)), 0, 0 \end{bmatrix}^T,$$

$$\bar{C}_i(\bar{X}_i(t)) = C_i(X_i(t)) + D_s^i S_s \Gamma_s^i(t), S_s = [I_{ns}, 0, \ldots, 0].$$

In the ith augmented quadrotor UAV NCS of the team formation of large-scale quadrotor UAVs in (7), the attack signals $\gamma_a^i(t)$ and $\gamma_s^i(t)$ are embedded in the augmented state $\bar{X}_i(t)$ so that their corruption on state estimation and control can be avoided by the decentralized H_∞ attack-tolerant observer-based team formation tracking control strategy in the sequel. Generally, it is not easy to ensure the observability of the ith augmented nonlinear quadrotor UAV system in (7). To facilitate observer design in the sequel, the assumption is made as follows.

Assumption 2: Each augmented quadrotor UAV NCS in (7) is observable.

According to [39], if we denote the augmented vector $Z_i(t) = \left[Y_i^T(t), \dot{Y}_i^T(t), \cdots, Y^{(n)^T}(t)\right]$ and the corresponding Hessian matrix $H_i(\overline{X}_i(t)) = \frac{\partial^2 Z_i(t)}{\partial^2 \overline{X}_i(t)}$, then the *ith* augmented quadrotor UAV NCS in (7) is observerable at the equilibrium point $\bar{X}_i(t) = 0$, if there exist a constant $\varepsilon > 0$ and a constant matrix T such that the absolute values of the leading principle minors $\Delta_1(\bar{X}_i(t)), \cdots, \Delta_i(\bar{X}_i(t)), \cdots, \Delta_n(\bar{X}_i(t))$ satisfy with the following conditions:

$$\Delta_1(\bar{X}_i(t)) \geq \varepsilon, \cdots \Delta_i(\bar{X}_i(t)) \geq \varepsilon, \cdots \Delta_n(\bar{X}_i(t)) \geq \varepsilon, \forall \bar{X}_i(t)$$

where n is the dimension of $\bar{X}_i(t)$ and the principle minor $\Delta_i(\bar{X}_i(t))$ is the determinant of matrix by deleting the last $n-i$ columns and rows of Hessian matrix $T\ H_i(\bar{X}_i(t))$.

Then, under the above observerable assumption of each augmented quadrotor UAV NCS in (7), the Luenberger observer-based control law for each augmented quadrotor UAV NCS in (7) is proposed as

$$\begin{aligned} \dot{\hat{\bar{X}}}_i(t) &= \bar{F}_i(\hat{\bar{X}}_i(t)) + \bar{G}_i(\hat{\bar{X}}_i(t))U_i(t) \\ &\quad + L_i(\hat{\bar{X}}_i(t))\left(Y_i(t) - \hat{Y}_i(t)\right) \\ \hat{Y}_i(t) &= \bar{C}_i(\hat{\bar{X}}_i(t)) \end{aligned} \tag{8}$$

where $\hat{\bar{X}}_i(t)$ is the estimated state of the ith augmented quadrotor UAV NCS in (7), $\hat{Y}_i(t)$ denotes the estimated measurement output and $L_i(\hat{\bar{X}}_i(t))$ is the nonlinear observer gain.

In a practical application, we would like to control the state $X_i(t)$ of the ith quadrotor UAV to follow a specified reference $r_i(t)$ to achieve some tasks, where $[r_1(t), \ldots, r_i(t), \ldots, r_N(t)]^T$ is specified as the desired time-varying formation shape of N quadrotor UAVs by the designer. Then, the reference tracking error dynamic of the ith quadrotor UAV in the team formation is indicated as follows:

$$\begin{aligned}\dot{\bar{e}}_i(t) &= \dot{\bar{X}}_i(t) - \dot{\bar{r}}_i(t)\\ &= F_{e,i}(\bar{e}_i(t), t) + G_{e,i}(\bar{e}_i(t), t)U_i(t) + D_{e,i}(\bar{e}_i(t), t)\\ &\quad \times \bar{v}_i(t) + \sum_{j\in N_i} F_{e,ij}(\bar{e}_i(t), t)\bar{X}_j(t - \tau_{ij}(t)) \end{aligned} \tag{9}$$

where $\bar{r}_i(t) = [\, r_i^T(t)\ 0\ 0\,]^T$, $F_{e,i}(\bar{e}_i(t), t) = \bar{F}_i(\bar{e}_i(t) + \bar{r}_i(t)) - \dot{\bar{r}}_i(t)$, $G_{e,i}(\bar{e}_i(t), t) = \bar{G}_i(\bar{e}_i(t) + \bar{r}_i(t))$, $D_{e,i}(\bar{e}_i(t), t) = \bar{D}_i(\bar{e}_i(t) + \bar{r}_i(t))$,
$F_{e,ij}(\bar{e}_i(t), t) = \bar{F}_{ij}(\bar{e}_i(t) + \bar{r}_i(t))$

C. PROBLEM FORMULATION

In practical applications under some situations, certain tasks need to be achieved by multi-quadrotor UAVs. Thence, the formation tracking control problem of quadrotor UAVs should be solved. In this paper, we employed a virtual leader-based team formation structure to address the large-scale quadrotor UAVs team formation tracking control design problem. In order to construct the desired time-varying formation shape $[r_1(t), \ldots, r_i(t), \ldots, r_N(t)]^T$ of large-scale quadrotor UAVs, each quadrotor UAV should move a specific formation offset $r_i(t)$ from the virtual leader, respectively, and then the ith quadrotor UAV will follow the trajectory of the virtual leader and move the formation offset $r_i(t)$ to maintain the desired formation shape. Hence, the problem of team formation tracking control for large-scale quadrotor UAVs can be converted into N decentralized observer-based reference tracking control problems for each quadrotor UAV. In practice, malicious attacks may appear in the network formation control system. Then, we employed the decentralized nonlinear Luenberger observer in (8) to estimate each quadrotor UAV's state $X_i(t)$ as well as malicious attacks $\gamma_a^i(t)$ and $\gamma_s^i(t)$ on the actuator and sensor, respectively. If malicious attack signals on the actuator and sensor of each quadrotor UAV can be effectively estimated, their effects on the quadrotor UAV NCS can be reduced or even eliminated by the compensation of observer-based reference tracking control. On the other hand, intending to make each quadrotor UAV track the desired trajectory $r_i(t)$ efficiently, an attack-tolerant observer-based tracking controller $U_i(t) = K_i(\hat{\bar{X}}_i(t),\ \bar{e}_i(t))$ is needed based on $\hat{\bar{X}}_i(t)$ and $\bar{e}_i(t)$. Since the external disturbance, coupling effects from neighboring quadrotor UAVs, and measurement noise during the team flight process are unavoidable, too. The robust decentralized H_∞ attack-tolerant observer-based team formation tracking control strategy of large-scale quadrotor UAVs NCS is proposed to effectively minimize these undesired effects on the observer-based reference tracking control performance of each quadrotor UAV in the team formation system:

$$\min_{\substack{K_i(\hat{\bar{X}}_i(t),\ \bar{e}_i(t)),\\ L_i(\hat{\bar{X}}_i(t))}} \max_{\substack{\bar{v}_i(t),\\ n_i(t),\\ \bar{X}_j(t-\tau_{ij}(t))\\ \in \mathcal{L}_2[0,t_f]}} \frac{\begin{array}{c}E\{\int_0^{t_f} [(\bar{X}_i(t)-\hat{\bar{X}}_i(t))^T Q_{1,i}(\bar{X}_i(t)\\ -\hat{\bar{X}}_i(t))+\bar{e}_i^T(t)Q_{2,i}\bar{e}_i(t)\\ +U_i^T(t)R_iU_i(t)-V(\bar{X}_i(0),\bar{e}_i(0),0)]dt\}\end{array}}{\begin{array}{c}E\{\int_0^{t_f} [\bar{v}_i^T(t)\bar{v}_i(t)+n_i^T(t)n_i(t)\\ +\sum_{j\in N_j}\bar{X}_j^T(t-\tau_{ij}(t))\bar{X}_j(t-\tau_{ij}(t))]dt\}\end{array}}$$
$$\leq \rho_i^2,\ for\ i = 1, \ldots, N \tag{10}$$

where t_f denotes the terminal time; $Q_{1,i} \geq 0$, $Q_{2,i} \geq 0$ and $R_i = R_i^T \geq 0$ are the weighting matrices to trade-off between the estimation error, team formation tracking error and control input. ρ_i denotes the prescribed attenuation level; $V(\bar{X}_i(0) - \hat{\bar{X}}_i(0), \bar{e}_i(0), 0)$ represents the effect of nonzero initial condition of the augmented system in (7) to be extracted from the decentralized H_∞ attack-tolerant observer-based team formation tracking performance in (10). The physical meaning of the robust decentralized H_∞ attack-tolerant observer-based team formation tracking control strategy is how to attenuate the worst-case effect of external disturbance, measurement noise, and couplings from other quadrotor UAVs on the state estimation error of observer, team formation tracking error and control efforts below a prescribed level ρ_i^2 by specifying the observer-based control gain $K_i(\hat{\bar{X}}_i(t), \bar{e}_(t))$ and observer gain $L_i(\hat{\bar{X}}_i(t))$ for each quadrotor UAV from the mean energy perspective. Since the effect of all possible finite energy external disturbances, interconnected couplings from neighboring quadrotor UAVs, and measurement noise are minimized, the decentralized observer and controller of each quadrotor UAV will be achieved from the mean energy perspective, which will be confirmed in the sequel.

III. DECENTRALIZED H_∞ ATTACK-TOLERANT OBSERVER-BASED TEAM FORMATION TRACKING CONTROL OF LARGE-SCALE QUADROTOR UAV NCS

In this section, the decentralized H_∞ attack-tolerant observer-based team formation tracking control design of quadrotor UAV NCS is investigated. First, we formulate the state estimation error as $\tilde{\bar{X}}_i(t) = \bar{X}_i(t) - \hat{\bar{X}}_i(t)$ and the corresponding estimation error dynamic equation is derived as follows:

$$\begin{aligned}\dot{\tilde{\bar{X}}}_i(t) &= \tilde{F}_i(\tilde{\bar{X}}_i(t)) + \tilde{G}_i(\tilde{\bar{X}}_i(t))U_i(t) - L_i(\hat{\bar{X}}_i(t))\tilde{C}_i(\tilde{\bar{X}}_i(t))\\ &\quad + \sum_{j\in N_i} \bar{F}_{ij}(\bar{X}_i(t))\bar{X}_j(t - \tau_{ij}(t))\\ &\quad + \left[\, \bar{D}_i(\bar{X}_i(t)) \ - L_i(\hat{\bar{X}}_i(t))\,\right]\tilde{\bar{v}}_i(t) \end{aligned} \tag{11}$$

where

$$\tilde{F}_i(\tilde{\bar{X}}_i(t)) = \bar{F}_i(\bar{X}_i(t)) - \bar{F}_i(\hat{\bar{X}}_i(t)),\ \tilde{G}_i(\tilde{\bar{X}}_i(t)) = \bar{G}_i(\bar{X}_i(t)) - \bar{G}_i(\hat{\bar{X}}_i(t)),\ \tilde{C}_i(\tilde{\bar{X}}_i(t)) = \bar{C}_i(\bar{X}_i(t)) - \bar{C}_i(\hat{\bar{X}}_i(t)),$$
$$\tilde{\bar{v}}_i(t) = [\bar{v}_i^T(t)\ n_i^T(t)]^T$$

Moreover, we can augment the state estimation error $\tilde{X}_i(t)$ in (11) and team formation tracking error $\bar{e}_i(t)$ in (9), then the robust decentralized H_∞ attack-tolerant observer-based team formation tracking control strategy for large-scale quadrotor UAV NCS can be rewritten as the following Nash minmax game problem,

$$\min_{\substack{K_i(\hat{\tilde{X}}_i(t),\bar{e}_i(t))\\ L_i(\hat{\tilde{X}}_i(t))}} \max_{\substack{\tilde{\bar{v}}_i(t),\\ \tilde{\bar{X}}_{-i}(t-\tau_{-i}(t))\\ \in\mathcal{L}_2[0,tf]}} \frac{\begin{array}{c}E\{\int_0^{tf}[\tilde{\bar{X}}_i^T(t)\bar{Q}_i\tilde{\bar{X}}_i(t)\\ +U_i^T(t)R_iU_i(t)-V(\tilde{\bar{X}}_i(0),\bar{e}_i(0),0)]dt\}\end{array}}{\begin{array}{c}E\{\int_0^{tf}[\tilde{\bar{v}}_i^T(t)\tilde{\bar{v}}_i(t)\\ +\tilde{\bar{X}}_{-i}^T(t-\tau_{-i}(t))\tilde{\bar{X}}_{-i}(t-\tau_{-i}(t))]dt\}\end{array}} \le \rho_i^2,\ for\ i=1,\ldots,N \tag{12}$$

where $\tilde{\bar{X}}_i(t)=\left[\tilde{X}_i^T(t)\ \bar{e}_i^T(t)\right]^T$, $\bar{Q}_i=diag\{Q_{1,i},Q_{2,i}\}$, $\tilde{\bar{X}}_{-i}(t-\tau_{-i}(t))=\left[\cdots\tilde{X}_j^T(t-\tau_{ij}(t))\cdots\right]^T, j\in N_i$

Thus, the robust decentralized H_∞ attack-tolerant observer-based team formation tracking control strategy for large-scale quadrotor UAVs NCS in (10) is turned into the robust decentralized H_∞ stabilization strategy in (12) of the following augmented time-varying error system of quadrotor UAV team formation NCS

$$\begin{aligned}\dot{\tilde{\bar{X}}}_i(t)=&\begin{bmatrix}\tilde{F}_i(\tilde{X}_i(t))-L_i(\hat{\tilde{X}}_i(t))\tilde{C}_i(\tilde{X}_i(t))\\ F_{e,i}(\bar{e}_i(t),t)\end{bmatrix}\\&+\begin{bmatrix}\tilde{G}_i(\tilde{X}_i(t))\\ G_{e,i}(\bar{e}_i(t),t)\end{bmatrix}U_i(t)\\&+\begin{bmatrix}\bar{D}_i(\bar{X}_i(t)) & -L_i(\hat{\tilde{X}}_i(t))\\ D_{e,i}(\bar{e}_i(t),t) & 0\end{bmatrix}\tilde{\bar{v}}_i(t)\\&+\begin{bmatrix}\bar{F}_{-i}(\bar{X}_i(t))\\ F_{e,-i}(\bar{e}_i(t),t)\end{bmatrix}\tilde{\bar{X}}_{-i}(t-\tau_{-i}(t))\end{aligned} \tag{13}$$

where

$$F_{-i}(\bar{X}_i(t))=\left[\cdots\bar{F}_{ij}(\bar{X}_i(t))\cdots\right],$$
$$F_{e,-i}(\bar{e}_i(t),t)=\left[\cdots F_{e,ij}(\bar{e}_i(t),t)\cdots\right]$$

After the above operation, the complicated robust decentralized H_∞ attack-tolerant observer-based team formation control design problem in (10) is converted into how to solve min-max decentralized H_∞ stabilization design problem in (12) for the nonlinear coupled augmented system in (13) to simplify the design procedure.

Nevertheless, it is still difficult to directly solve the min-max game problem of the fractional payoff problem function in (12). Since $\tilde{\bar{v}}_i(t)$ and $\tilde{\bar{X}}_{-i}(t-\tau_{-i}(t))$ seek to maximize the payoff function, while other players $K_i(\hat{\tilde{X}}_i(t),\bar{e}_i(t))$ and $L_i(\hat{\tilde{X}}_i(t))$ seek to minimize the payoff function. Since the players $\tilde{\bar{v}}_i(t)$ and $\tilde{\bar{X}}_{-i}(t-\tau_{-i}(t))$ in the denominator $\tilde{\bar{v}}_i(t)$are independent of other players $K_i(\hat{\tilde{X}}_i(t),\bar{e}_i(t))$ and $L_i(\hat{\tilde{X}}_i(t))$. We employed the indirect two-step method [25] in the following to solve the min-max Nash game problem in (12). Thus, the min-max H_∞ game problem in (12) is equivalent to the following nonzero sum Nash min-max quadratic game problem [25], [28]

$$\begin{aligned}\min_{\substack{K_i(\hat{\tilde{X}}_i(t),\bar{e}_i(t))\\ L_i(\hat{\tilde{X}}_i(t))}} \max_{\substack{\tilde{\bar{v}}_i(t),\\ \tilde{\bar{X}}_{-i}(t-\tau_{-i}(t))\\ \in\mathcal{L}_2[0,tf]}} & E\{\int_0^{tf}\tilde{\bar{X}}_i^T(t)\bar{Q}_i\tilde{\bar{X}}_i(t)\\&+U_i^T(t)R_iU_i(t)-\rho_i^2(\tilde{\bar{v}}_i^T(t)\tilde{\bar{v}}_i(t)+\tilde{\bar{X}}_{-i}^T(t-\tau_{-i}(t))\\&\times\tilde{\bar{X}}_{-i}(t-\tau_{-i}(t)))dt\}\le E\{V(\tilde{\bar{X}}_i(0),\bar{e}_i(0),0)\},\\&for\ i=1,\ldots,N\end{aligned} \tag{14}$$

Then, the constrained min-max Nash quadratic game problem in (14) could be solved by a two-step method as follows. (i) At first, we solve the Nash min-max quadratic game problem as follows:

$$\begin{aligned}J_i=&\min_{\substack{K_i(\hat{\tilde{X}}_i(t),\bar{e}_i(t))\\ L_i(\hat{\tilde{X}}_i(t))}} \max_{\substack{\tilde{\bar{v}}_i(t),\\ \tilde{\bar{X}}_{-i}(t-\tau_{-i}(t))\\ \in\mathcal{L}_2[0,tf]}} E\{\int_0^{tf}\tilde{\bar{X}}_i^T(t)\bar{Q}_i\tilde{\bar{X}}_i(t)\\&+U_i^T(t)R_iU_i(t)-\rho_i^2(\tilde{\bar{v}}_i^T(t)\tilde{\bar{v}}_i(t)+\tilde{\bar{X}}_{-i}^T(t-\tau_{-i}(t))\\&\times\tilde{\bar{X}}_{-i}(t-\tau_{-i}(t)))dt\},\\&for\ i=1,\ldots,N\end{aligned} \tag{15}$$

(ii) In the second step, $J_i\le E\{V(\tilde{\bar{X}}_i(0),\bar{e}_i(0),0)\}$ needs to be guaranteed.

According to the above two-step method, the following theorem can solve the robust decentralized H_∞ attack-tolerant observer-based team formation tracking control strategy in (12).

Theorem 1: (*a*) *Given a prescribed attenuation level* ρ_i *the robust decentralized* H_∞ *attack-tolerant observer-based team formation tracking control strategy for large-scale quadrotor UAV NCS in (12) can be solved by the following* H_∞ *control* $U_i^*(t)$*, observer gain* $L_i^*(\hat{\tilde{X}}_i(t))$ *and the worst-case external disturbances* $\tilde{\bar{v}}_i^*(t)$*, interconnected coupling effects* $\tilde{\bar{X}}_{-i}^*(t-\tau_{-}i(t))$*:*

$$\begin{aligned}\tilde{\bar{v}}_i^*(t)=&\frac{1}{2\rho_i^2}\begin{bmatrix}\bar{D}_i(\bar{X}_i(t)) & -L_i(\hat{\tilde{X}}_i(t))\\ D_{e,i}(\bar{e}_i(t),t) & 0\end{bmatrix}^T\\&\times\left(\frac{\partial V(\tilde{X}_i(t),\bar{e}_i(t),t)}{\partial[\tilde{X}_i^T(t)\ \bar{e}_i^T(t)]^T}\right)\end{aligned} \tag{16}$$

$$\begin{aligned}U_i^*(t)=&K_i^*(\hat{\tilde{X}}_i(t),\bar{e}_i(t))\\=&-\frac{1}{2}R_i^{-1}\begin{bmatrix}\tilde{G}_i(\tilde{X}_i(t))\\ G_{e,i}(\bar{e}_i(t),t)\end{bmatrix}^T\\&\times\left(\frac{\partial V(\tilde{X}_i(t),\bar{e}_i(t),t)}{\partial[\tilde{X}_i^T(t)\ \bar{e}_i^T(t)]^T}\right)\end{aligned} \tag{17}$$

$$\begin{aligned}\tilde{\bar{X}}_{-i}^*(t-\tau_{-i}(t))=&\frac{1}{2\rho_i^2}\begin{bmatrix}\bar{F}_{-i}(\bar{X}_i(t))\\ F_{e,-i}(\bar{e}_i(t),t)\end{bmatrix}^T\\&\times\left(\frac{\partial V(\tilde{X}_i(t),\bar{e}_i(t),t)}{\partial[\tilde{X}_i^T(t)\ \bar{e}_i^T(t)]^T}\right)\end{aligned} \tag{18}$$

$$\begin{aligned}L_i^*(\hat{\tilde{X}}_i(t))=&\frac{1}{2}\frac{\frac{\partial V(\tilde{X}_i(t),\bar{e}_i(t),t)}{\partial\tilde{X}_i(t)}}{\left\|\frac{\partial V(\tilde{X}_i(t),\bar{e}_i(t),t)}{\partial\tilde{X}_i(t)}\right\|^2}\tilde{C}_i^T(\tilde{X}_i(t)),\\&for\ i=1,\ldots,N\end{aligned} \tag{19}$$

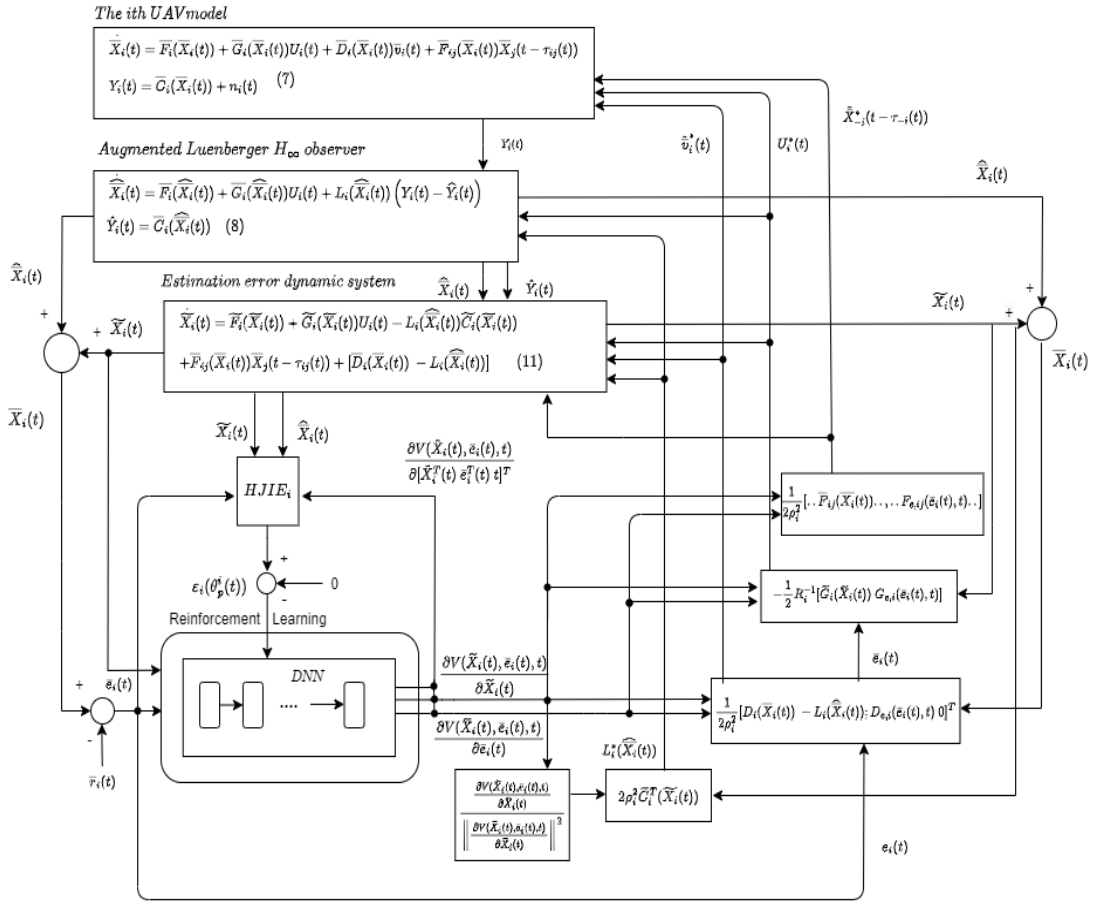

FIGURE 3. The flow chart of the offline training phase for the robust decentralized DNN-based H_∞ attack-tolerant observer-based team formation tracking control scheme of the large-scale quadrotor UAV NCS via HJIE-reinforcement learning algorithm in the remote side as shown in Fig.2. The detailed HJIE-reinforcement learning-based DNN architecture of robust H_∞ control in given in Fig.3.

where the Lyapunov function $V(\tilde{X}_i(t), \bar{e}_i(t), t) \geq 0$ with $V(0, 0, t) = 0$ is the solution of the observer/controller-coupled HJIE$_i$ as follows:

$$\begin{aligned} HJIE_i = & \frac{\partial V(\tilde{X}_i(t),\bar{e}_i(t),t)}{\partial t} + \tilde{\bar{X}}_i^T(t)\bar{Q}_i\tilde{\bar{X}}_i(t) \\ & - \frac{1}{4}\left(\frac{\partial V(\tilde{X}_i(t),\bar{e}_i(t),t)}{\partial[\tilde{X}_i^T(t)\ \bar{e}_i^T(t)]^T}\right)^T \tilde{G}_i(\tilde{X}_i(t), \bar{e}_i(t), t)R_i^{-1} \\ & \times \tilde{\bar{G}}_i^T(\tilde{X}_i(t), \bar{e}_i(t), t)\left(\frac{\partial V(\tilde{X}_i(t),\bar{e}_i(t),t)}{\partial[\tilde{X}_i^T(t)\ \bar{e}_i^T(t)]^T}\right) \\ & + \left(\frac{\partial V(\tilde{X}_i(t),\bar{e}_i(t),t)}{\partial[\tilde{X}_i^T(t)\ \bar{e}_i^T(t)]^T}\right)^T \tilde{\bar{F}}_i(\tilde{X}_i(t), \bar{e}_i(t), t) \\ & + \frac{1}{4\rho_i^2}\left(\frac{\partial V(\tilde{X}_i(t),\bar{e}_i(t),t)}{\partial[\tilde{X}_i^T(t)\ \bar{e}_i^T(t)]^T}\right)^T \tilde{D}_i(\tilde{X}_i(t), \bar{e}_i(t), t) \\ & \times \left(\frac{\partial V(\tilde{X}_i(t),\bar{e}_i(t),t)}{\partial[\tilde{X}_i^T(t)\ \bar{e}_i^T(t)]^T}\right) + \frac{1}{4\rho_i^2}\left(\frac{\partial V(\tilde{X}_i(t),\bar{e}_i(t),t)}{\partial[\tilde{X}_i^T(t)\ \bar{e}_i^T(t)]^T}\right)^T \\ & \times \bar{F}_{-i}(\tilde{\bar{X}}_i(t))\left(\frac{\partial V(\tilde{X}_i(t),\bar{e}_i(t),t)}{\partial[\tilde{X}_i^T(t)\ \bar{e}_i^T(t)]^T}\right) \\ & - \frac{1}{16\rho_i^2}\tilde{C}_i^T(\tilde{X}_i(t))\tilde{C}_i(\tilde{X}_i(t)) = 0 \end{aligned} \tag{20}$$

where

$$\frac{\partial V(\tilde{X}_i(t), \bar{e}_i(t), t)}{\partial[\tilde{X}_i^T(t)\ \bar{e}_i^T(t)\ ]^T} = \begin{bmatrix} \frac{\partial V(\tilde{X}_i(t),\bar{e}_i(t),t)}{\partial \tilde{X}_i^T(t)} \\ \frac{\partial V(\tilde{X}_i(t),\bar{e}_i(t),t)}{\partial \bar{e}_i^T(t)} \end{bmatrix},$$

$$\tilde{\bar{G}}_i(\tilde{X}_i(t), \bar{e}_i(t), t) = \begin{bmatrix} \tilde{G}_i(\tilde{X}_i(t)) \\ G_{e,i}(\bar{e}_i(t), t) \end{bmatrix},$$

$$\tilde{\bar{F}}_i(\tilde{X}_i(t), \bar{e}_i(t), t) = \begin{bmatrix} \tilde{F}_i(\tilde{X}_i(t)) \\ F_{e,i}(\bar{e}_i(t), t) \end{bmatrix},$$

$$\tilde{\bar{D}}_i(\tilde{X}_i(t), \bar{e}_i(t), t) = \begin{bmatrix} \bar{D}_i(\bar{X}_i(t))\bar{D}_i^T(\bar{X}_i(t)) & \bar{D}_i(\bar{X}_i(t))D_{e,i}^T(\bar{e}_i(t), t) \\ D_{e,i}(\bar{e}_i(t), t)\bar{D}_i^T(\bar{X}_i(t)) & D_{e,i}(\bar{e}_i(t), t)D_{e,i}^T(\bar{e}_i(t), t) \end{bmatrix},$$

$$\bar{F}_{-i}(\tilde{\bar{X}}_i(t), \bar{e}_i(t), t) = \begin{bmatrix} \bar{F}_{-i}(\bar{X}_i(t))\bar{F}_{-i}^T(\bar{X}_i(t)) & \bar{F}_{-i}(\bar{X}_i(t))F_{e,-i}^T(\bar{e}_i(t), t) \\ F_{e,-i}(\bar{e}_i(t), t)\bar{F}_{-i}^T(\bar{X}_i(t)) & F_{e,-i}(\bar{e}_i(t), t)F_{e,-i}^T(\bar{e}_i(t), t) \end{bmatrix}$$

(b) In each quadrotor UAV NCS, if external disturbances $\bar{v}_i(t) \in \mathcal{L}_2[0, \infty)$, measurement noise $n_i(t) \in \mathcal{L}_2[0, \infty)$ and couplings $\tilde{\bar{X}}_{-i}(t - \tau_{ij}(t)) \in \mathcal{L}_2[0, \infty)$, then the proposed robust decentralized H_∞ attack-tolerant observer-based team formation tracking control strategy of the ith quadrotor UAV network subsystem will achieve the asymptotical mean square team formation tracking and estimation ability, *i.e.*, $E\{U_i^T(t)U_i(t)\} \to 0$, $E\{\tilde{X}_i^T(t)\tilde{X}_i(t)\} \to 0$ and $E\{\bar{e}_i^T(t)\bar{e}_i(t)\} \to 0$ as $t \to \infty$.

Proof: Please refer to Appendix A. □

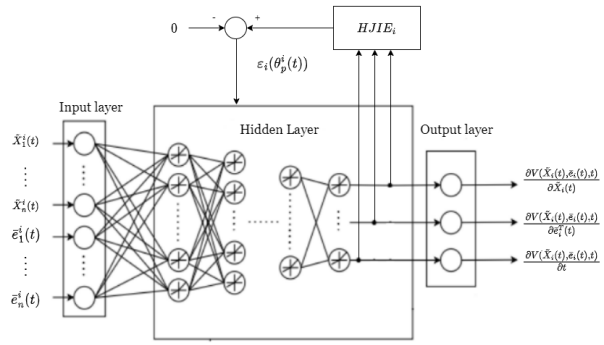

FIGURE 4. HJIE-reinforcement learning-based DNN architecture of robust H_∞ control of Fig.3 with input $\tilde{X}_i(t)$ and $\bar{e}_i(t)$ to output $\frac{\partial V(\tilde{X}_i(t),\bar{e}_i(t),t)}{\partial [\tilde{X}_i^T(t)\ \bar{e}_i^T(t)\ ]^T}$ and $\frac{\partial V(\tilde{X}_i(t),\bar{e}_i(t),t)}{\partial t}$ to solve HJIE$_i$ in (20) after the training by Adam learning algorithm in (25)-(28) according to the error $\varepsilon_i(\theta_p^i(t))$ of HJIE$_i$.

Remark 1: In the conventional H_∞ observer-based control problems, the H_∞ observer design and the H_∞ controller design are always separated based on their corresponding strategies [28], [38], i.e., $\min_{L_i(\hat{\tilde{X}}_i(t))} \max_{\substack{\tilde{\bar{v}}_i(t)\\ \in \pounds_2[0,t_f]}} \frac{E\{\int_0^{tf} \tilde{X}_i^T(t)Q_{1,i}\tilde{X}_i(t)dt\}}{E\{\int_0^{tf} \tilde{\bar{v}}_i^T(t)\tilde{\bar{v}}_i(t)dt\}}$ *and* $\min_{K_i(\hat{\tilde{X}}_i(t),\bar{e}_i(t))} \max_{\substack{\tilde{\bar{v}}_i(t)\\ \in \pounds_2[0,t_f]}} \frac{E\{\int_0^{tf} \bar{e}_i^T(t)Q_{2,i}\bar{e}_i(t)+U_i^T(t)R_iU_i(t)]dt\}}{E\{\int_0^{tf} \tilde{\bar{v}}_i^T(t)\tilde{\bar{v}}_i(t)dt\}}$, *respectively. In this situation, two coupled HJIEs are needed to be solved, which will be more complicated than HJIE$_i$ in (20).*

Remark 2: (i) From HJIE$_i = 0, i = 1, \ldots, N$ in (20), it is seen that each HJIE$_i = 0$ can be solved without the information of other quadrotor UAVs, i.e., the robust decentralized H_∞ attack-tolerant observer-based team formation tracking control is achieved for each quadrotor UAV by the proposed method in Theorem 1. (ii) Since $\overline{X}_j\left(t-\tau_{ij}\right)$ in (7) and (9) is the coupling from the jth neigboring UAV in the team, based on the robust decentralized H_∞ attack-tolerant observer-based team formation tracking control strategy in (10)(12), these effects of couplings $[\overline{\tilde{X}}_{-i}(t-\tau_i-i(t)) = [\cdots \overline{X}_j^T(t-\tau_{ij})\cdots]$ of neighboring UAVs in (12) are considered by the worst $[\hat{\tilde{X}}_{-i}^*(t-\tau_i(t))]$ in (18), which is independent on τ_{ij} but on the system characteristic of the ith UAV as shown in Theorem 1. Therefore, it does not exist constraint/assumptions on the coupling time delay τ_{ij}.

IV. ROBUST DECENTRALIZED H_∞ ATTACK-TOLERANT OBSERVER-BASED TEAM FORMATION TRACKING CONTROL DESIGN OF LARGE-SCALE QUADROTOR UAV NCS BASED ON HJIE-REINFORCEMENT DNN

For large-scale UAV NCS under external disturbance, malicious attacks, coupling effects and output measurement noise in (2), the robust decentralized H_∞ attack-tolerant observer-based team formation tracking control strategy in (12) is used to minimize the worst-case effect of all possible external disturbances $\bar{v}_i(t) \in \pounds_2[0,\infty)$, coupling effect $\bar{\tilde{X}}_{-i}(t-\tau_{-i}(t)) \in \pounds_2[0,\infty)$ and measurement noise $n_i(t) \in \pounds_2[0,\infty)$ on estimation error $\tilde{X}_i(t)$, tracking error $\bar{e}_i(t)$ and control input $U_i(t)$. From Theorem 1, in order to complete the decentralized H_∞ attack-tolerant observer-based formation tracking control design for each quadrotor UAV of large-scale UAV NCS, we have to solve the $\frac{\partial V(\tilde{X}_i(t),\bar{e}_i(t),t)}{\partial [\tilde{X}_i^T(t)\ \bar{e}_i^T(t)\ ]^T}$ and $\frac{\partial V(\tilde{X}_i(t),\bar{e}_i(t),t)}{\partial t}$ from the complicated time-varying partial differential HJIE$_i$ in (20) to obtain the optimal control gain $K_i^*(\hat{\tilde{X}}_i(t),\bar{e}_i(t))$ in (17), observer gain $L_i^*(\hat{\tilde{X}}_i(t))$ in (19), and the worst-case external disturbances $\bar{v}_i^*(t)$, measurement noise $n_i^*(t)$ in (16), and interconnected coupling effects $\bar{\tilde{X}}_{-i}^*(t-\tau_{-i}(t))$ in (18) for each quadrotor UAV in the team formation. In this study, in order to solve HJIE$_i$ in (20) directly and more efficiently for the decentralized H_∞ attack-tolerant observer-based team formation tracking control strategy of each quadrotor UAV, an HJIE-reinforcement learning DNN method is adopted to approach the theoretical solution $\frac{\partial V(\tilde{X}_i(t),\bar{e}_i(t),t)}{\partial [\tilde{X}_i^T(t)\ \bar{e}_i^T(t)\ ]^T}$ and $\frac{\partial V(\tilde{X}_i(t),\bar{e}_i(t),t)}{\partial t}$ in (20). The reason is that it is very hard to calculate $\frac{\partial V(\tilde{X}_i(t),\bar{e}_i(t),t)}{\partial [\tilde{X}_i^T(t)\ \bar{e}_i^T(t)\ ]^T}$ and $\frac{\partial V(\tilde{X}_i(t),\bar{e}_i(t),t)}{\partial t}$ in (20) for $K_i^*(\hat{\tilde{X}}_i(t),\bar{e}_i(t))$, $L_i^*(\hat{\tilde{X}}_i(t))$, $\bar{v}_i^*(t)$, $n_i^*(t)$, and $\bar{\tilde{X}}_{-i}^*(t-\tau_{-i}(t))$ in (16)-(19) in the real-time decentralized H_∞ attack-tolerant observer-based team formation control process even if the Lyapunov function $V(\tilde{X}_i(t),\bar{e}_i(t),t)$ of HJIE$_i$ in (20) is solved [27].

To simplify the design, we denote

$$\frac{\partial V(\tilde{X}_i(t),\bar{e}_i(t),t)}{\partial [\tilde{X}_i^T(t)\ \bar{e}_i^T(t)\ t]^T} = \begin{bmatrix} \frac{\partial V(\tilde{X}_i(t),\bar{e}_i(t),t)}{\partial \tilde{X}_i(t)} \\ \frac{\partial V(\tilde{X}_i(t),\bar{e}_i(t),t)}{\partial \bar{e}_i(t)} \\ \frac{\partial V(\tilde{X}_i(t),\bar{e}_i(t),t)}{\partial t} \end{bmatrix} \tag{21}$$

Then, according to HJIE$_i = 0$ in (20) and (21) can be reformulated as

$$\begin{aligned} HJIE_i = {} & \bar{\tilde{X}}_i^T(t)\bar{Q}_i\bar{\tilde{X}}_i(t) - \tfrac{1}{4}\left(\frac{\partial V(\tilde{X}_i(t),\bar{e}_i(t),t)}{\partial [\tilde{X}_i^T(t)\ \bar{e}_i^T(t)\ t]^T}\right)^T \\ & \times \begin{bmatrix} \tilde{\bar{G}}_i(\tilde{X}_i(t),\bar{e}_i(t),t) \\ 0 \end{bmatrix} R_i^{-1} \begin{bmatrix} \tilde{\bar{G}}_i(\tilde{X}_i(t),\bar{e}_i(t),t) \\ 0 \end{bmatrix}^T \\ & \times \left(\frac{\partial V(\tilde{X}_i(t),\bar{e}_i(t),t)}{\partial [\tilde{X}_i^T(t)\ \bar{e}_i^T(t)\ t]^T}\right) + \left(\frac{\partial V(\tilde{X}_i(t),\bar{e}_i(t),t)}{\partial [\tilde{X}_i^T(t)\ \bar{e}_i^T(t)\ t]^T}\right)^T \\ & \times \begin{bmatrix} \tilde{\bar{F}}_i(\tilde{X}_i(t),\bar{e}_i(t),t) \\ 1 \end{bmatrix} + \frac{1}{4\rho_i^2}\left(\frac{\partial V(\tilde{X}_i(t),\bar{e}_i(t),t)}{\partial [\tilde{X}_i^T(t)\ \bar{e}_i^T(t)\ t]^T}\right)^T \\ & \times \begin{bmatrix} \tilde{\bar{D}}_i(\tilde{X}_i(t),\bar{e}_i(t),t) & 0 \\ 0 & 0 \end{bmatrix} \left(\frac{\partial V(\tilde{X}_i(t),\bar{e}_i(t),t)}{\partial [\tilde{X}_i^T(t)\ \bar{e}_i^T(t)\ t]^T}\right) \\ & + \frac{1}{4\rho_i^2}\left(\frac{\partial V(\tilde{X}_i(t),\bar{e}_i(t),t)}{\partial [\tilde{X}_i^T(t)\ \bar{e}_i^T(t)\ t]^T}\right)^T \begin{bmatrix} \tilde{\bar{F}}_i(\tilde{X}_i(t),\bar{e}_i(t),t) & 0 \\ 0 & 0 \end{bmatrix} \\ & \times \left(\frac{\partial V(\tilde{X}_i(t),\bar{e}_i(t),t)}{\partial [\tilde{X}_i^T(t)\ \bar{e}_i^T(t)\ t]^T}\right) - \frac{1}{16\rho_i^2}\tilde{C}_i^T(\tilde{X}_i(t))\tilde{C}_i(\tilde{X}_i(t)) \\ = {} & 0, \quad for\ i = 1, \ldots, N \end{aligned} \tag{22}$$

Thus, in this study, we employ an HJIE-reinforcement learning-based DNN scheme to approach the partial differential $\frac{\partial V(\tilde{X}_i(t),\bar{e}_i(t),t)}{\partial [\tilde{X}_i^T(t)\ \bar{e}_i^T(t)\ t]^T}$ to obtain control input $K_i^*(\hat{\tilde{X}}_i(t),\bar{e}_i(t))$,

observer gain $L_i^*(\hat{\tilde{X}}_i(t))$, and the worst-case external disturbances $\bar{v}_i^*(t)$, coupling effects $\tilde{\bar{X}}_{-i}^*(t-\tau_{-i}(t))$, measurement noise $n_i^*(t)$. The training process of the deep learning approach of HJIE-reinforcement is separated into an offline training phase and an online operation phase. In the offline training period as shown in Fig.3, since the actual state, external disturbance, measurement noise, coupling effect, and malicious attack signals are unavailable, we substitute the worst-case $\bar{v}_i^*(t)$, $n_i^*(t)$, and $\tilde{\bar{X}}_{-i}^*(t-\tau_{-i}(t))$ for the actual $\bar{v}_i(t)$, $n_i(t)$, and $\tilde{\bar{X}}_{-i}(t-\tau_{-i}(t))$. This does not have any effect on the decentralized H_∞ attack-tolerant observer-based team formation tracking control strategy in (10) because this strategy is designed based on the worst-case $\bar{v}_i^*(t)$, $n_i^*(t)$, and $\tilde{\bar{X}}_{-i}^*(t-\tau_{-i}(t))$. Then, the Luenberger observer is proposed to produce $\hat{\tilde{X}}_i(t)$, and use the augmented state estimation error model in (11) to produce the estimation error $\tilde{X}_i(t)$ to calculate $\bar{X}_i(t)$. Therefore, we can also obtain the tracking error $\bar{e}_i(t)$ by $\bar{X}_i(t)$ minus $\bar{r}_i(t)$. After that, $\hat{\tilde{X}}_i(t)$ and $\bar{e}_i(t)$ are employed as inputs of DNN to produce $(\frac{\partial V(\tilde{X}_i(t),\bar{e}_i(t),t)}{\partial[\tilde{X}_i^T(t)\ \bar{e}_i^T(t)\ t]^T})_\varepsilon$ at the output of DNN. Then, the output $(\frac{\partial V(\tilde{X}_i(t),\bar{e}_i(t),t)}{\partial[\tilde{X}_i^T(t)\ \bar{e}_i^T(t)\ t]^T})_\varepsilon$ of DNN will be sent back to calculate the value of HJIE_i as follows:

$$
\begin{aligned}
HJIE_{i,\varepsilon} &= \tilde{\bar{X}}_i^T(t)\bar{Q}_i\tilde{\bar{X}}_i(t) - \tfrac{1}{4}(\tfrac{\partial V(\tilde{X}_i(t),\bar{e}_i(t),t)}{\partial[\tilde{X}_i^T(t)\ \bar{e}_i^T(t)\ t]^T})_\varepsilon^T \\
&\times \begin{bmatrix} \tilde{\bar{G}}_i(\tilde{X}_i(t),\bar{e}_i(t),t) \\ 0 \end{bmatrix} R_i^{-1} \begin{bmatrix} \tilde{\bar{G}}_i(\tilde{X}_i(t),\bar{e}_i(t),t) \\ 0 \end{bmatrix}^T \\
&\times (\tfrac{\partial V(\tilde{X}_i(t),\bar{e}_i(t),t)}{\partial[\tilde{X}_i^T(t)\ \bar{e}_i^T(t)\ t]^T})_\varepsilon + (\tfrac{\partial V(\tilde{X}_i(t),\bar{e}_i(t),t)}{\partial[\tilde{X}_i^T(t)\ \bar{e}_i^T(t)\ t]^T})_\varepsilon^T \\
&\times \begin{bmatrix} \tilde{\bar{F}}_i(\tilde{X}_i(t),\bar{e}_i(t),t) \\ 1 \end{bmatrix} + \tfrac{1}{4\rho_i^2}(\tfrac{\partial V(\tilde{X}_i(t),\bar{e}_i(t),t)}{\partial[\tilde{X}_i^T(t)\ \bar{e}_i^T(t)\ t]^T})_\varepsilon^T \\
&\times \begin{bmatrix} \tilde{\bar{D}}_i(\tilde{X}_i(t),\bar{e}_i(t),t) & 0 \\ 0 & 0 \end{bmatrix} (\tfrac{\partial V(\tilde{X}_i(t),\bar{e}_i(t),t)}{\partial[\tilde{X}_i^T(t)\ \bar{e}_i^T(t)\ t]^T})_\varepsilon \\
&+ \tfrac{1}{4\rho_i^2}(\tfrac{\partial V(\tilde{X}_i(t),\bar{e}_i(t),t)}{\partial[\tilde{X}_i^T(t)\ \bar{e}_i^T(t)\ t]^T})_\varepsilon^T \begin{bmatrix} \tilde{\bar{F}}_i(\tilde{X}_i(t),\bar{e}_i(t),t) & 0 \\ 0 & 0 \end{bmatrix} \\
&\times (\tfrac{\partial V(\tilde{X}_i(t),\bar{e}_i(t),t)}{\partial[\tilde{X}_i^T(t)\ \bar{e}_i^T(t)\ t]^T})_\varepsilon - \tfrac{1}{16\rho_i^2}\tilde{C}_i^T(\tilde{X}_i(t))\tilde{C}_i(\tilde{X}_i(t)) \\
&= \varepsilon_i(\theta_p^i(t)), for\ i = 1,\ldots,N
\end{aligned} \tag{23}
$$

Next, $\varepsilon_i(\theta_p^i(t))$ is sent back to train the DNN weighting parameters until $\varepsilon_i(\theta_p^i(t))$ converges to zero or below a small threshold. Therefore, the output of the HJIE-reinforcement DNN is expected to approximate $\frac{\partial V(\tilde{X}_i(t),\bar{e}_i(t),t)}{\partial[\tilde{X}_i^T(t)\ \bar{e}_i^T(t)\ t]^T}$ after the offline training phase. Furthermore, the output of DNN $(\frac{\partial V(\tilde{X}_i(t),\bar{e}_i(t),t)}{\partial[\tilde{X}_i^T(t)\ \bar{e}_i^T(t)\ t]^T})_\varepsilon$ is taken to calculate $(U_i^*(t))_\varepsilon$, $(L_i^*(\hat{\tilde{X}}_i(t)))_\varepsilon$, $(\tilde{\bar{v}}_i^*(t))_\varepsilon$, and $(\tilde{\bar{X}}_{-i}^*(t-\tau_{-i}(t)))_\varepsilon$ as follows:

$$
\begin{aligned}
(\tilde{\bar{v}}_i^*(t))_\varepsilon &= \tfrac{1}{2\rho_i^2}\begin{bmatrix} \bar{D}_i(\bar{X}_i(t)) & -L_i(\hat{\tilde{X}}_i(t)) \\ D_{e,i}(\bar{e}_i(t),t) & 0 \end{bmatrix}^T \\
&\times (\tfrac{\partial V(\tilde{X}_i(t),\bar{e}_i(t),t)}{\partial[\tilde{X}_i^T(t)\ \bar{e}_i^T(t)]^T})_\varepsilon \\
(U_i^*(t))_\varepsilon &= K_i^*(\hat{\tilde{X}}_i(t),\bar{e}_i(t)) \\
&= -\tfrac{1}{2}R_i^{-1}\begin{bmatrix} \tilde{G}_i(\tilde{X}_i(t)) \\ G_{e,i}(\bar{e}_i(t),t) \end{bmatrix}^T \\
&\times (\tfrac{\partial V(\tilde{X}_i(t),\bar{e}_i(t),t)}{\partial[\tilde{X}_i^T(t)\ \bar{e}_i^T(t)]^T})_\varepsilon \\
(\tilde{\bar{X}}_{-i}^*(t-\tau_{-i}(t)))_\varepsilon &= \tfrac{1}{2\rho_i^2}\begin{bmatrix} \bar{F}_{-i}(\bar{X}_i(t)) \\ F_{e,-i}(\bar{e}_i(t),t) \end{bmatrix}^T \\
&\times (\tfrac{\partial V(\tilde{X}_i(t),\bar{e}_i(t),t)}{\partial[\tilde{X}_i^T(t)\ \bar{e}_i^T(t)]^T})_\varepsilon \\
(L_i^*(\hat{\tilde{X}}_i(t)))_\varepsilon &= \frac{1}{2}\frac{(\frac{\partial V(\tilde{X}_i(t),\bar{e}_i(t),t)}{\partial\tilde{X}_i(t)})_\varepsilon}{\left\|(\frac{\partial V(\tilde{X}_i(t),\bar{e}_i(t),t)}{\partial\tilde{X}_i(t)})_\varepsilon\right\|^2}\tilde{C}_i^T(\tilde{X}_i(t)), \\
&for\ i = 1,\ldots,N
\end{aligned} \tag{24}
$$

Then the H_∞ control input, observer gain, and worst-case disturbance are sent to our quadrotor UAV system in (7) to generate the training data for the next training step. Consequently, repeat the above DNN learning procedure until $\varepsilon_i(\theta_p^i(t)) \to 0$ and $(\frac{\partial V(\tilde{X}_i(t),\bar{e}_i(t),t)}{\partial[\tilde{X}_i^T(t)\ \bar{e}_i^T(t)\ t]^T})_\varepsilon$ in (23) approach the theoretical solution $(\frac{\partial V(\tilde{X}_i(t),\bar{e}_i(t),t)}{\partial[\tilde{X}_i^T(t)\ \bar{e}_i^T(t)\ t]^T})$ in (22), then the offline training is over, and we can switch the offline training phase to the online operation phase.

In the online operation phase, as shown in Fig.2, the observer can receive the output $Y_i(t)$ from each quadrotor UAV on the local side with authentic external disturbance, malicious attacks, coupling effects, measurement noise, and $U_i^*(t)$. Hence, we do not need the worst-case $\bar{v}_i^*(t)$, $n_i^*(t)$, and $\tilde{\bar{X}}_{-i}^*(t-\tau_{-i}(t))$ to produce $Y_i(t)$ from the stochastic model of the ith quadrotor UAV. The other procedure to output $(\frac{\partial V(\tilde{X}_i(t),\bar{e}_i(t),t)}{\partial[\tilde{X}_i^T(t)\ \bar{e}_i^T(t)\ t]^T})$ by DNN to produce control $K_i(\hat{\tilde{X}}_i(t),\bar{e}_i(t))$ and observer gain $L_i(\hat{\tilde{X}}_i(t))$ is in a similar way as the offline training phase. In general, we don't have to train DNN by the reinforcement learning scheme again as in the online operation phase. Nevertheless, in some situations, if $\varepsilon_i(\theta_p^i(t)) > \kappa$ for a specified little value κ, we can start the reinforcement learning-based Adam algorithm to continue training without affecting the online operation process.

The DNN architecture of HJIE-reinforcement learning in the robust decentralized H_∞ attack-tolerant observer-based team formation tracking control scheme is composed of an input layer, multiple hidden layers, an output layer, and HJIE-reinforcement learning, as shown in Fig.4. In hidden layers, we adopted LeakyReLU instead of ReLU as an activation function to avoid the dead neuron problem. If the input to a ReLU neuron is negative, the output will be zero, which means those neurons may never get updated. It can also avoid the gradient-vanishing problem that other activation functions such as hyperbolic tangent or sigmoid functions may have. The LeakyReLU function is formulated as follows:

$$
l(X(t)) = \begin{cases} \mu_1 X(t), if X(t) > 0 \\ \mu_2 X(t), if X(t) \le 0 \end{cases}
$$

where μ_1 and μ_2 are some constants with $\mu_1, \mu_2 \in (0,1]$.

As shown in the offline training phase in Fig.3 at the remote side, the error $\varepsilon_i(\theta_p^i(t))$ of HJIE-reinforcement learning will be sent back to update the weighting parameters of DNN through Adam learning algorithm [34], [36],

$$\theta_p^i(t) = \theta_{p-1}^i(t) - \frac{\iota}{\sqrt{\hat{v}_p^i(t)+\zeta}}\hat{m}_p^i(t), p = 1, \ldots, P \tag{25}$$

$$\hat{m}_p^i(t) = \frac{m_p^i(t)}{1-\alpha_1^p},\ \hat{v}_p^i(t) = \frac{v_p^i(t)}{1-\alpha_2^p} \tag{26}$$

$$m_p^i(t) = \alpha_1 m_{p-1}^i(t) + (1-\alpha_1)\nabla_p^i(t)$$

$$v_p^i(t) = \alpha_2 v_{p-1}^i(t) + (1-\alpha_2)\nabla_p^{i\,2}(t) \tag{27}$$

$$\nabla_p^i(t) = \frac{\partial}{\partial\theta_p^i(t)}\sqrt{\frac{1}{B}\sum_{p=1}^{B}\varepsilon_i^2(\theta_p^i(t))}$$

$$= \frac{\partial}{\partial\theta_p^i(t)}\sqrt{\frac{1}{B}\sum_{p=1}^{B}HJIE_{i,\varepsilon}^2} \tag{28}$$

where $\theta_p^i(t)$ represents the vector of DNN parameters in the hidden layers at time t, ι represents the learning rate of the learning algorithm, and P represents the number of training steps at time t. ζ denotes a small number to prevent a zero denominator. $\hat{v}_p^i(t)$ and $\hat{m}_p^i(t)$ denote bias-corrected estimators defined as (26). $\nabla_p^i(t)$ is the gradient, that is, the vector of the derivative of the root mean square error $\varepsilon_i(\theta_p^i(t))$ of HJIE$_i$ in (23) w.r.t. $\theta_p^i(t)$ in time step p at time t. B is the batch size of the input data. $\alpha_1, \alpha_2 \in [0, 1]$ in (27) denotes the degree of influence of the previous impact on the current direction. The designer specifies these two parameters to prevent DNN parameters from being captured by local minima [34], [36]. Moreover, if the current gradient $\nabla_p^i(t)$ direction is the same as the accumulated gradient, then the gradient will conduct a larger update. Conversely, it will conduct a smaller update. α_1^p and α_2^p are the p-th power of α_1 and α_2, respectively. $m_p^i(t)$ and $v_p^i(t)$ in (27) are the moving average of the gradient and the squared gradient of $\nabla_p^i(t)$ at time t, respectivly. The HJIE-reinforcement learning-based Adam algorithm combines the advantages of momentum and RMSProp [36] and is an adaptive gradient descent algorithm. This method is easy to use and does not require a lot of memory. Overall, it is a robust optimizer and suitable for non-convex optimization problems in the field of Machine Learning and Deep Learning [37].

Remark 3: If the time steps and the number of hidden neurons are large enough, then the Adam learning algorithm is employed for updating the weighted parameter vector $\theta_p^i(t)$ of DNN can converge to a globally optimal $\theta_p^{i*}(t)$ with a linear convergence rate as $p \to \infty$ in (25)-(28). It has been proven in [34].

The flow chart of the offline training phase for the robust decentralized H_∞ attack-tolerant observer-based team formation tracking control scheme of large-scale quadrotor UAV NCS via HJIE-reinforcement Adam learning algorithm (25)-(28) is described as follows: The worst-case $U_i^*(t)$, $\tilde{\bar{v}}_i^*(t)$, and $\tilde{\bar{X}}_{-i}^*(t-\tau_{-i}(t))$ are fed back to the model of the ith quadrotor UAV in the team formation to produce $Y_i(t)$. Then $Y_i(t)$ is inputted to the augmented Luenberger observer in (8) to produce $\hat{\tilde{X}}_i(t)$ with observer gain $L_i^*(\hat{\tilde{X}}_i(t))$. Further $U_i^*(t)$, $\tilde{\bar{v}}_i^*(t)$, $L_i^*(\hat{\tilde{X}}_i(t))$, and $\tilde{\bar{X}}_{-i}^*(t-\tau_{ij}(t))$ are also inputted to the estimation error system in (11) to produce $\tilde{\tilde{X}}_i(t)$. After that, we can acquire $\bar{\tilde{X}}_i(t) = \hat{\tilde{X}}_i(t) + \tilde{\tilde{X}}_i(t)$ to get the tracking error by $\bar{\tilde{e}}_i(t) = \bar{\tilde{X}}_i(t) - \bar{\tilde{r}}_i(t)$. Eventually, the estimation error $\tilde{\tilde{X}}_i(t)$ and reference tracking error $\bar{\tilde{e}}_i(t)$ are both inputted to DNN to output $\frac{\partial V(\tilde{\tilde{X}}_i(t),\bar{\tilde{e}}_i(t),t)}{\partial[\tilde{\tilde{X}}_i^T(t)\ \bar{\tilde{e}}_i^T(t)\ t]^T}$ to solve the HJIE$_i$ (Please see Fig.4 in detail). The error $\varepsilon_i(\theta_p^i(t))$ of HJIE$_i$ will be back-propagated to train DNN by HJIE-reinforcement Adam learning algorithm (25)-(28). In the online operation phase, $\tilde{\bar{v}}_i^*(t)$ and $\tilde{\bar{X}}_{-i}^*(t-\tau_{-i}(t))$ are replaced by the real external disturbance $\tilde{\bar{v}}_i(t)$ and coupling $\tilde{\bar{X}}_{-i}(t-\tau_{-i}(t))$ of the real ith quadrotor UAV. The remote side only needs to receive $Y_i(t)$ from the ith quadrotor UAV on the local side and sent $U_i^*(t)$ to the ith quadrotor UAV as shown in Fig.2. In general, the reinforcement learning-based Adam algorithm is stopped during the online operation phase. However, when $\left|\varepsilon_i(\theta_p^i(t))\right| > \kappa$ for prescribed small κ, the reinforcement learning-based Adam algorithm can be performed to enhance DNN performance without effect on the observer and tracking controller in the online operation phase.

When the error $\varepsilon_i(\theta_p^i(t))$ approaches to zero using the HJIE-reinforcement-based Adam learning algorithm in (25)-(28), it can be proven that the output $(\frac{\partial V(\tilde{\tilde{X}}_i(t),\bar{\tilde{e}}_i(t),t)}{\partial[\tilde{\tilde{X}}_i^T(t)\ \bar{\tilde{e}}_i^T(t)\ t]^T})_\varepsilon$ in (23) of DNN can approach $(\frac{\partial V(\tilde{\tilde{X}}_i(t),\bar{\tilde{e}}_i(t),t)}{\partial[\tilde{\tilde{X}}_i^T(t)\ \bar{\tilde{e}}_i^T(t)\ t]^T})$ of HJIE$_i$ in (22) using the following theorem.

Theorem 2: If $\varepsilon_i(\theta_p^i(t)) \to 0$ in (23) by HJIE-reinforcement learning-based Adam algorithm in (25)-(28), then $(\frac{\partial V(\tilde{\tilde{X}}_i(t),\bar{\tilde{e}}_i(t),t)}{\partial[\tilde{\tilde{X}}_i^T(t)\ \bar{\tilde{e}}_i^T(t)\ t]^T})_\varepsilon$ will approach to $\frac{\partial V(\tilde{\tilde{X}}_i(t),\bar{\tilde{e}}_i(t),t)}{\partial[\tilde{\tilde{X}}_i^T(t)\ \bar{\tilde{e}}_i^T(t)\ t]^T}$ in (20), i.e.,the proposed HJIE-reinforcement learning DNN decentralized $H\infty$ attack-tolerant observer-based team formation tracking control scheme via Adam learning algorithm (25)-(28) will approach to the theoretical decentralized $H\infty$ attack-tolerant observer-based team formation tracking control design (16)-(19) of large-scale quadrotor UAV NCS in Theorem 1.

Proof: Please refer to Appendix B. □

Remark 4: (i) In Theorem 2, we can obtain the output $\frac{\partial V(\tilde{\tilde{X}}_i(t),\bar{\tilde{e}}_i(t),t)}{\partial[\tilde{\tilde{X}}_i^T(t)\ \bar{\tilde{e}}_i^T(t)\ t]^T}$ by training DNN with the Adam learning algorithm of HJIE-reinforcement to calculate the H_∞ control $U_i^*(t)$ and H_∞ observer gain $L_i^*(\hat{\tilde{X}}_i(t))$ if the error $\varepsilon_i(\theta_p^i(t))$ of HJIE$_{\varepsilon,i}$ in (23) approaches to zero in the offline training phase, as shown in Fig.3. Nevertheless, for the practical design, if $\left|\varepsilon(\theta_p^i(t))\right| \le \kappa$ for a little prescribed κ, we will stop the reinforcement learning-based Adam algorithm in the offline training phase and switch to the online operation phase. (ii) The existing neural network-based reference tracking control results always need to update their weightings parameters at very time instant [40], i.e., the conventional adaptive neural network control schemes need

a recursine algorithm to update their parameters to achieve a desired reference tracking performance. However, after the off-line training by deep Adam learning in (25)-(28), the proposed DNN-based H_∞ attack-tolerant observer-based team formation network tracking control can achieve the desired reference tracking control without training again.

Remark 5: $Y_i(t)$ can be obtained through the actual quadrotor UAV system in (2) with real $v_i(t)$, coupling effect $X_j(t-\tau_{ij}(t))$ and malicious attacks by the decentralized H_∞ attack-tolerant observer-based team formation tracking control $U_i^*(t)$ in the online operation phase as shown in Fig.2. We take $\tilde{X}_i(t)$ and $\bar{e}_i(t)$ as input in a well-trained DNN to obtain $\frac{\partial V(\tilde{X}_i(t),\bar{e}_i(t),t)}{\partial[\tilde{X}_i^T(t)\ \bar{e}_i^T(t)\ t]^T}$ to calculate $U_i^*(t)$ and $L_i^*(\hat{\tilde{X}}_i(t))$ for the robust decentralized H_∞ attack-tolerant observer-based team formation tracking control of the large-scale quadrotor UAV NCS. However, the weighting parameter $\theta_p^i(t)$ of the DNN can still be updated by the HJIE-reinforced Adam learning algorithm in (25)-(28) if $\left|\varepsilon(\theta_p^i(t))\right| > \kappa$ during the online operation phase, without any impact on the HJIE-reinforcement learning-based DNN observer-based team formation tracking control scheme of large-scale quadrotor UAV NCS.

The state information is transmitted through the wireless network channel in the form of data packets in practical applications. Therefore, the quadrotor UAV formation NCS in (2) can be reformulated by the nonlinear sampled-data system as follows:

$$\begin{aligned} S_i: \tfrac{X_i(t+h)-X_i(t)}{h} &= F_i(X_i(t)) + G_i(X_i(t))(U_i(t) \\ &\quad + \gamma_a^i(t)) + D_i(X_i(t))v_i(t) \\ &\quad + \sum_{j\in N_i} F_{ij}(X_i(t))X_j(t-\tau_{ij}(t)) \\ Y_i(t) &= C_i(X_i(t)) + n_i(t) + D_s^i(t)\gamma_s^i(t) \end{aligned} \tag{29}$$

where h is the sampling time. Or we can rewrite (29) as follows:

$$\begin{aligned} S_i: X_i(t+h) &= (X_i(t) + hF_i(X_i(t))) + hG_i(X_i(t))(U_i(t) \\ &\quad + \gamma_a^i(t)) + hD_i(X_i(t))v_i(t) \\ &\quad + h\sum_{j\in N_i} F_{ij}(X_i(t))X_j(t-\tau_{ij}(t)) \\ Y_i(t) &= C_i(X_i(t)) + n_i(t) + D_s^i(t)\gamma_s^i(t) \end{aligned} \tag{30}$$

From smoothed models of actuator malicious attacks in (5) and the sensor malicious attacks in (6), the augmented system (7) can be reformulated as follows:

$$\begin{aligned} \bar{X}_i(t+h) &= (\bar{X}_i(t) + h\bar{F}_i(\bar{X}_i(t))) + h\bar{G}_i(\bar{X}_i(t))U_i(t) \\ &\quad + h\bar{D}_i(\bar{X}_i(t))\bar{v}_i(t) \\ &\quad + h\sum_{j\in N_i} \bar{F}_{ij}(\bar{X}_i(t))\bar{X}_j(t-\tau_{ij}(t)) \\ Y_i(t) &= \bar{C}_i(\bar{X}_i(t)) + n_i(t) \end{aligned} \tag{31}$$

In this case, the observer dynamic model in (8) is reformulated as

$$\begin{aligned} \hat{\bar{X}}_i(t+h) &= (\hat{\bar{X}}_i(t) + h\bar{F}_i(\hat{\bar{X}}_i(t))) + h\bar{G}_i(\hat{\bar{X}}_i(t))U_i(t) \\ &\quad + hL_i(\hat{\bar{X}}_i(t))\left(Y_i(t) - \hat{Y}_i(t)\right) \\ \hat{Y}_i(t) &= \bar{C}_i(\hat{\bar{X}}_i(t)) \end{aligned} \tag{32}$$

Correspondingly, the tracking error dynamic equation in (9) and the state estimation error dynamic equation in (11) are reformulated as follows:

$$\begin{aligned} \bar{e}_i(t+h) &= (e(t) + hF_{e,i}(\bar{e}_i(t),t)) + hG_{e,i}(\bar{e}_i(t),t)U_i(t) \\ &\quad + hD_{e,i}(\bar{e}_i(t),t)\bar{v}_i(t) \\ &\quad + h\sum_{j\in N_i} F_{e,ij}(\bar{e}_i(t),t)\bar{X}_j(t-\tau_{ij}(t)) \end{aligned} \tag{33}$$

and

$$\begin{aligned} \tilde{X}_i(t+h) &= (\tilde{X}_i(t) + h\tilde{F}_i(\tilde{X}_i(t))) + h\tilde{G}_i(\tilde{X}_i(t))U_i(t) \\ &\quad - hL_i(\hat{\tilde{X}}_i(t))\tilde{C}_i(\tilde{X}_i(t)) \\ &\quad + h\sum_{j\in N_i} \bar{F}_{ij}(\bar{X}_i(t))\bar{X}_j(t-\tau_{ij}(t)) \\ &\quad + h\left[\bar{D}_i(\bar{X}_i(t)) - L_i(\hat{\tilde{X}}_i(t))\right]\tilde{\bar{v}}_i(t) \end{aligned} \tag{34}$$

respectively.

The above sampled-data quadrotor UAV systems will be employed for the simulation of the reinforcement learning-based DNN robust decentralized H_∞ attack-tolerant observer-based team formation tracking of large-scale quadrotor UAVs network control strategy in the following section. Before the simulation example is given to illustrate the design procedure and to confirm the performance of proposed method, the pseudo-code of the proposed algorithm is provided for better understand of the proposed method.

V. SIMULATION RESULTS

In order to validate the effectiveness of the proposed reinforcement learning-based DNN robust decentralized H_∞ attack-tolerant observer-based team formation tracking control of large-scale quadrotor UAV NCS under external disturbances, malicious attacks, measurement noises, and couplings, a simulation example of a team formation NCS of 25 quadrotor UAVs under external disturbances, malicious attack, measurement noises, and couplings is provided in this section. The parameters of the ith quadrotor UAV in NCS are given as [33]

$$\begin{aligned} &m = 2\ (\text{kg}),\ g = 9.8\ (\text{m/s}^2),\ J_x = J_y = J_z = 0.1(\text{Ns}^2/\text{rad}), \\ &K_x = K_y = K_z = 0.01(\text{Ns/m}), \\ &K_\phi = K_\theta = K_\psi = 0.01\ (\text{Ns/m}). \end{aligned}$$

The weighting matrices are set as $Q_{1,i} = 0.02diag\{I_{20}\}$, $Q_{2,i} = 0.01diag\{I_{20}\}$ and $R = 10^{-4}I_4$ in the robust decentralized H_∞ attack-tolerant observer-based team formation tracking control strategy in (10).

Algorithm 1 HJIE-Embedded DNN-Based H_∞ Observer-Based Decentralized Team Formation Reference Tracking Control of Each UAV

Input: $t, \bar{Q}_i, R_i, \rho_i, \kappa, P$

1: $Y_i(t) \leftarrow$ Measure the output of the i-th UAV by sensors.
2: $\hat{\tilde{X}}_i(t) \leftarrow$ Estimate the augmented states of the i-th UAV using Luenberger H_∞ observer in Eq.(3).
3: $\tilde{\tilde{X}}_i(t) \leftarrow$ Compute the estimation error by estimation error dynamic system with $Y_i(t)$ and $\hat{\tilde{X}}_i(t)$ in Eq.(11).
4: $\bar{X}_i(t), \bar{e}_i(t) \leftarrow$ Compute the states and the tracking errors of the i-th UAV with $\hat{\tilde{X}}_i(t), \tilde{\tilde{X}}_i(t), \bar{r}_i(t), \dot{\bar{r}}_i(t)$.
5: $\tilde{\tilde{X}}_i^T(t)\bar{Q}_i\tilde{\tilde{X}}_i(t)$, $\tilde{\tilde{G}}_i(\tilde{X}_i(t), \bar{e}_i(t), t)$, $\tilde{\tilde{F}}_i(\tilde{X}_i(t), \bar{e}_i(t), t)$, $\tilde{\tilde{D}}_i(\tilde{X}_i(t), \bar{e}_i(t), t)$, $\bar{C}_i(\tilde{X}_i(t)) \leftarrow$ Compute the parameters which will be imported to $\text{HJIE}_{i,\epsilon}$ in Eq.(23).
6: $(\frac{\partial V(\tilde{X}_i(t),\bar{e}_i(t),t)}{\partial[\tilde{X}_i^T(t),\bar{e}_i^T(t),t]^T}) \leftarrow$ Obtain the partial differential of a Lyapunov function using DNN with the inputs, $\tilde{X}_i(t)$ and $\bar{e}_i(t)$.
7: $\text{HJIE}_{i,\epsilon} \leftarrow$ Calculate $\text{HJIE}_{i,\epsilon}$ using Eq.(23) with $\tilde{\tilde{X}}_i^T(t)\bar{Q}_i\tilde{\tilde{X}}_i(t)$, $\tilde{\tilde{G}}_i(\tilde{X}_i(t), \bar{e}_i(t), t)$, $\tilde{\tilde{F}}_i(\tilde{X}_i(t), \bar{e}_i(t), t)$, $\tilde{\tilde{D}}_i(\tilde{X}_i(t), \bar{e}_i(t), t)$, $\bar{C}_i(\tilde{X}_i(t))$ and $(\frac{\partial V(\tilde{X}_i(t),\bar{e}_i(t),t)}{\partial[\tilde{X}_i^T(t),\bar{e}_i^T(t),t]^T})$
8: **if** $\text{HJIE}_{i,\epsilon} - 0 > \kappa$ **then**
9: **while** $p \le P$ **do**
10: Train the DNN using Adam optimizer in Eq.(25) -Eq.(28) by taking $\tilde{X}_i(t)$ and $\bar{e}_i(t)$ as inputs once, and then calculate $\text{HJIE}_{i,\epsilon}$ using its outputs.
11: **if** $\text{HJIE}_{i,\epsilon} - 0 \le \kappa$ **then**
12: **break**
13: **end if**
14: **end while**
15: **end if**
16: $(U_i^*(t))_\epsilon, (L_i^*(\hat{\tilde{X}}_i(t)))_\epsilon \leftarrow$ Compute the control gain and the observer gain in Eq.(24).
17: Send $(U_i^*(t))_\epsilon$ to the controller.
18: Send $(L_i^*(\hat{\tilde{X}}_i(t)))_\epsilon$ to the observer and the estimation error dynamic system.
19: $(\tilde{\tilde{v}}_i^*(t))_{i,\epsilon}, (\tilde{\tilde{X}}_{-i}^*(t-\tau_{-i}(t)))_\epsilon \leftarrow$ Compute the disturbance and the coupling of the worst-case in Eq.(24).
20: Send $(\tilde{\tilde{v}}_i^*(t))_{i,\epsilon}, (\tilde{\tilde{X}}_{-i}^*(t-\tau_{-i}(t)))_\epsilon$ to the estimation error dynamic system.

Remark 6: In general, the poor state estimation will deteriorate the observer-based tracking performance. Consequently, the weighting on the state estimation error should be more significant than the weighting on the tracking error. Therefore $Q_{1,i}$ is double of $Q_{i,2}$. Further, in order to achieve a better reference team formation tracking performance, more control effort is needed for each UAV, therefore, a more weighting R is needed.

The sampling time h is set as $0.01s$ and the terminal time t_f is $30s$. The quadrotor UAV NCS may suffer interference from external disturbances in the system plant and measurement noise in the measurement output. Therefore, the external disturbances are given in the following:

$$v_i(t) = 0.1[\sin(0.5t), \sin(0.5t), \cos(0.5t), \cos(0.5t), \sin(0.5t), \sin(0.5t)]^T$$

and the measurement noise $n(t) \doteq N(0, 0.1I_{20})$. Since there are only four control inputs in $U_i(t)$ for each quadrotor UAV in (1), the desired position and the yaw angle for the reference input $r_i(t)$ of each quadrotor UAV are given in Table 1.

TABLE 1. The reference $r_i(t)$ of 25 quadrotor UAVs.

Quadrotor UAV	The reference $r_i(t)$
UAV 1	$x_1 = 15\sin(0.5t), y_1 = 15\cos(0.5t), z_1 = t, \psi_1 = 0$
UAV 2	$x_2 = 17\sin(0.5t), y_2 = 17\cos(0.5t), z_2 = t, \psi_2 = 0$
UAV 3	$x_3 = 19\sin(0.5t), y_3 = 19\cos(0.5t), z_3 = t, \psi_3 = 0$
UAV 4	$x_4 = 21\sin(0.5t), y_4 = 21\cos(0.5t), z_4 = t, \psi_4 = 0$
UAV 5	$x_5 = 13\sin(0.5t), y_5 = 13\cos(0.5t), z_5 = t, \psi_5 = 0$
UAV 6	$x_6 = 15\sin(0.5t), y_6 = 15\cos(0.5t), z_6 = t+2, \psi_6 = 0$
UAV 7	$x_7 = 17\sin(0.5t), y_7 = 17\cos(0.5t), z_7 = t+2, \psi_7 = 0$
UAV 8	$x_8 = 19\sin(0.5t), y_8 = 19\cos(0.5t), z_8 = t+2, \psi_8 = 0$
UAV 9	$x_9 = 21\sin(0.5t), y_9 = 21\cos(0.5t), z_9 = t+2, \psi_9 = 0$
UAV 10	$x_{10} = 13\sin(0.5t), y_{10} = 13\cos(0.5t), z_{10} = t+2, \psi_{10} = 0$
UAV 11	$x_{11} = 15\sin(0.5t), y_{11} = 15\cos(0.5t), z_{11} = t+1, \psi_{11} = 0$
UAV 12	$x_{12} = 17\sin(0.5t), y_{12} = 17\cos(0.5t), z_{12} = t+1, \psi_{12} = 0$
UAV 13	$x_{13} = 19\sin(0.5t), y_{13} = 19\cos(0.5t), z_{13} = t+1, \psi_{13} = 0$
UAV 14	$x_{14} = 21\sin(0.5t), y_{14} = 21\cos(0.5t), z_{14} = t+1, \psi_{14} = 0$
UAV 15	$x_{15} = 13\sin(0.5t), y_{15} = 13\cos(0.5t), z_{15} = t+1, \psi_{15} = 0$
UAV 16	$x_{16} = 15\sin(0.5t), y_{16} = 15\cos(0.5t), z_{16} = t+3, \psi_{16} = 0$
UAV 17	$x_{17} = 17\sin(0.5t), y_{17} = 17\cos(0.5t), z_{17} = t+3, \psi_{17} = 0$
UAV 18	$x_{18} = 19\sin(0.5t), y_{18} = 19\cos(0.5t), z_{18} = t+3, \psi_{18} = 0$
UAV 19	$x_{19} = 21\sin(0.5t), y_{19} = 21\cos(0.5t), z_{19} = t+3, \psi_{19} = 0$
UAV 20	$x_{20} = 13\sin(0.5t), y_{20} = 13\cos(0.5t), z_{20} = t+3, \psi_{20} = 0$
UAV 21	$x_{21} = 15\sin(0.5t), y_{21} = 15\cos(0.5t), z_{21} = t+4, \psi_{21} = 0$
UAV 22	$x_{22} = 17\sin(0.5t), y_{22} = 17\cos(0.5t), z_{22} = t+4, \psi_{22} = 0$
UAV 23	$x_{23} = 19\sin(0.5t), y_{23} = 19\cos(0.5t), z_{23} = t+4, \psi_{23} = 0$
UAV 24	$x_{24} = 21\sin(0.5t), y_{24} = 21\cos(0.5t), z_{24} = t+4, \psi_{24} = 0$
UAV 25	$x_{25} = 13\sin(0.5t), y_{25} = 13\cos(0.5t), z_{25} = t+4, \psi_{25} = 0$

Furthermore, the attitude of the quadrotor UAV depends on its corresponding position information. Therefore, the reference attitudes of ϕ_i and θ_i are given as follows:

$$\phi_i = \sin^{-1}\left(\frac{m}{F(t)}(\ddot{x}_i \sin\psi_i - \ddot{y}_i \cos\psi_i)\right),$$
$$\theta_i = \tan^{-1}\left(\frac{1}{\ddot{z}_i + g}(\ddot{x}_i \cos\psi_i + \ddot{y}_i \sin\psi_i)\right)$$

where $\ddot{x}_i, \ddot{y}_i, \ddot{z}_i$ are the double derivative of x_i, y_i, z_i representing acceleration, respectively.

From the perspective of the network, the observation of the position will be affected by the sensor attack $\gamma_s^i(t)$ via the wireless network channel. On the other hand, the actuator attack signal $\gamma_a^i(t)$ will be transmitted to the actuator with control signals to destroy the tracking control of the quadrotor UAV. To construct the smoothed model in (5) and (6) for the estimation of the actuator attack signal $\gamma_a^i(t)$ and the sensor attack signal $\gamma_s^i(t)$ as shown in Fig.5, the extrapolation coefficients are specified, respectively, as follows:

$$a_1 = 0.9, a_2 = 0.06, a_3 = 0.03, a_4 = 0.01$$

$$b_1 = 0.96, b_2 = 0.02, b_3 = 0.01, b_4 = 0.01$$

Due to a large-scale team of quadrotor UAVs among 25-quadrotor-UAV NCS, some interconnected coupling effects will occur, such as trailing vortex couplings of neighboring quadrotor UAVs. The strength of the trailing vortex couplings is given below to affect the shape of the quadrotor UAV:

$$\begin{aligned} &F_{ij}(X_i(t))X_j(t-\tau_{ij}(t)) \\ &\quad = [0, 0.01x_2^i(t)x_2^j(t), 0, 0, 0, \\ &\quad 0.01z_2^i(t)z_2^j(t), 0, 0, 0, 0, 0, 0]^T, j \in N_i \end{aligned}$$

where N_i denotes the neighboring quadrotor UAVs of the ith quadrotor UAV.

According to Theorem 1, to achieve the decentralized H_∞ attack-tolerant observer-based team formation tracking control for 25 quadrotor UAVs must solve the following 25 independent HJIE$_i$ to obtain the decentralized H_∞ team formation control $U_i^*(t)$ in (17) and observer gain $L_i^*(\hat{\tilde{X}}_i(t))$ in (19) to track the desired reference path and attenuate the effect of unknown external disturbance, malicious attacks, coupling from neighboring quadrotor UAV and measurement noise.

$$\begin{aligned} HJIE_i = &\frac{\partial V(\tilde{X}_i(t),\bar{e}_i(t),t)}{\partial t} + \tilde{\tilde{X}}_i^T(t)\bar{Q}_i\tilde{\tilde{X}}_i(t) \\ &- \frac{1}{4}(\frac{\partial V(\tilde{X}_i(t),\bar{e}_i(t),t)}{\partial[\tilde{X}_i^T(t)\ \bar{e}_i^T(t)]^T})^T \tilde{\tilde{G}}_i(\tilde{X}_i(t),\bar{e}_i(t),t)R_i^{-1} \\ &\times \tilde{\tilde{G}}_i^T(\tilde{X}_i(t),\bar{e}_i(t),t)(\frac{\partial V(\tilde{X}_i(t),\bar{e}_i(t),t)}{\partial[\tilde{X}_i^T(t)\ \bar{e}_i^T(t)]^T}) \\ &+ (\frac{\partial V(\tilde{X}_i(t),\bar{e}_i(t),t)}{\partial[\tilde{X}_i^T(t)\ \bar{e}_i^T(t)]^T})^T \tilde{\tilde{F}}_i(\tilde{X}_i(t),\bar{e}_i(t),t) \\ &+ \frac{1}{4\rho_i^2}(\frac{\partial V(\tilde{X}_i(t),\bar{e}_i(t),t)}{\partial[\tilde{X}_i^T(t)\ \bar{e}_i^T(t)]^T})^T \tilde{\tilde{D}}_i(\tilde{X}_i(t),\bar{e}_i(t),t) \\ &\times (\frac{\partial V(\tilde{X}_i(t),\bar{e}_i(t),t)}{\partial[\tilde{X}_i^T(t)\ \bar{e}_i^T(t)]^T}) + \frac{1}{4\rho_i^2}(\frac{\partial V(\tilde{X}_i(t),\bar{e}_i(t),t)}{\partial[\tilde{X}_i^T(t)\ \bar{e}_i^T(t)]^T})^T \\ &\times \tilde{F}_{-i}(\tilde{\tilde{X}}_i(t))(\frac{\partial V(\tilde{X}_i(t),\bar{e}_i(t),t)}{\partial[\tilde{X}_i^T(t)\ \bar{e}_i^T(t)]^T}) \\ &- \frac{1}{16\rho_i^2}\tilde{C}_i^T(\tilde{X}_i(t))\tilde{C}_i(\tilde{X}_i(t)) = 0, i = 1, 2, \ldots, 25. \end{aligned} \tag{35}$$

It is nearly impossible to solve $\frac{\partial V(\tilde{X}_i(t),\bar{e}_i(t),t)}{\partial[\tilde{X}_i^T(t)\ \bar{e}_i^T(t)]^T}$ analytically or numerically for $U_i^*(t)$ in (17) and $L_i^*(\hat{\tilde{X}}_i(t))$ in (19) directly, since $HJIE_i$ in (35) is a highly nonlinear time-varying partial differential equation. Thus, the HJIE-reinforcement DNN-based observer-based tracking control scheme in Fig.2 is proposed to be derived from quadrotor UAV sample data systems in (29)-(34) with sampling time $h = 0.01$ in Fig.3 is adopted to solve $\frac{\partial V(\tilde{X}_i(t),\bar{e}_i(t),t)}{\partial[\tilde{X}_i^T(t)\ \bar{e}_i^T(t)\ t]^T}$ for $U_i^*(t)$, $\tilde{\bar{v}}_i^*(t)$ and $\tilde{\tilde{X}}_{-i}^*(t-\tau_{-i}(t))$ to accomplish the robust decentralized H_∞ observer-based team formation control design of 25 quadrotor UAVs. In the flow chart in Fig.3, the HJIE-reinforcement DNN is trained offline via the Adam learning algorithm in (25)-(28) by the approximation error HJIE$_{i,\varepsilon} = \varepsilon_i(\theta_p^i(t))$ in (23).In this case, the robust decentralized H_∞ control input $(U_i^*(t))_\varepsilon$, observer gain $(L_i^*(\hat{\tilde{X}}_i(t)))_\varepsilon$, worst-case effects $(\bar{v}_i^*(t))_\varepsilon$ and $(\tilde{\tilde{X}}_{-i}^*(t-\tau_{-i}(t)))_\varepsilon$ can be obtained, and they are sent to the quadrotor UAV system in (7) to generate the next state for the next training epoch.

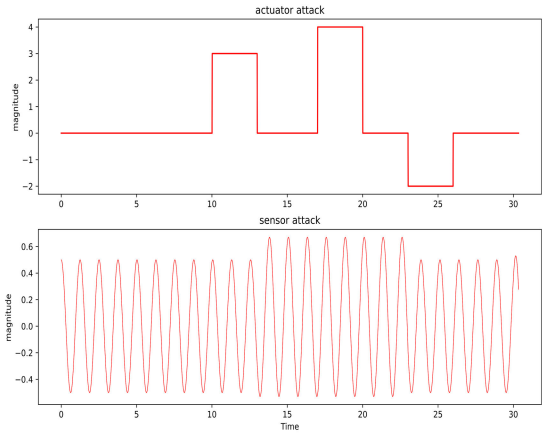

FIGURE 5. (a) The square actuator attack signal on each quadrotor UAV in the team formation. (b)the cosine-type sensor attack signal on each quadrotor UAV in the team formation.

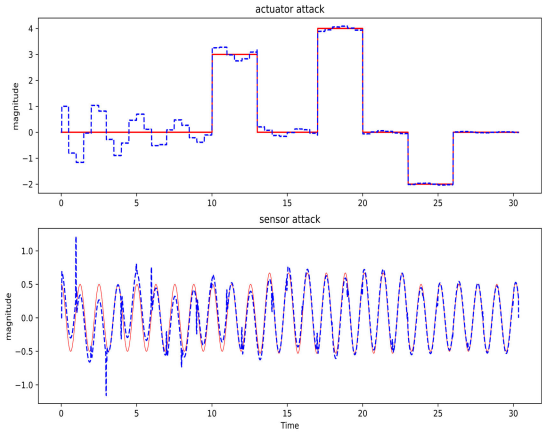

FIGURE 6. (a) The square actuator attack signal and its estimation of each quadrotor UAV.(b)the cosine-type sensor attack signal and its estimation of each quadrotor UAV.

In the simulation example, the HJIE-reinforcement DNN architecture in Fig.4 contains an input layer with input $\tilde{X}_i(t)$, $\bar{e}_i(t)$, four hidden layers, an output layer, and a feedback HJIE layer for reinforcement learning. Each hidden layer is sequentially with 256, 128, 32 and 12 neurons. The parameters of the Adam learning algorithm in (25)-(28) are specified as $\alpha_1 = 0.9$, $\alpha_2 = 0.999$, $\zeta = 10^{-7}$, and $\iota = 10^{-3}$. The training steps are specified as $P = 30$ and batch size B is 800. In the offline training phase as shown in Fig.4, we randomly select a set of training inputs, which are 20000 initial tracking errors $\bar{e}_i(0)$ and estimation errors $\tilde{X}_i(0)$ around the origin $X(0)$.

The simulation results are shown in Figs.7-12. Since the effect of actuator attack signals is more like the actuator fault and the square actuator fault has been widely considered in simulations, consequently the square wave in Fig.5 is considered as attack signal on actuator. On the other hand, sensor always suffer from high frequency attack

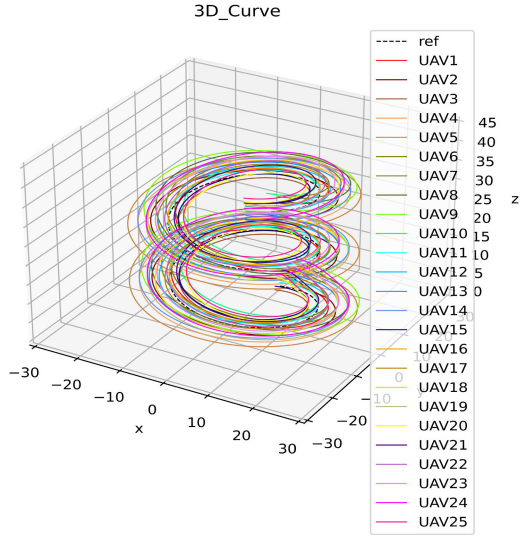

FIGURE 7. The flight trajectories of NCS team formation of 25 quadrotor UAVs using the proposed HJIE-reinforcement DNN-based H_∞ attack-tolerant observer-based team formation tracking control scheme are given based on the flight/hardware-in-the loop results.

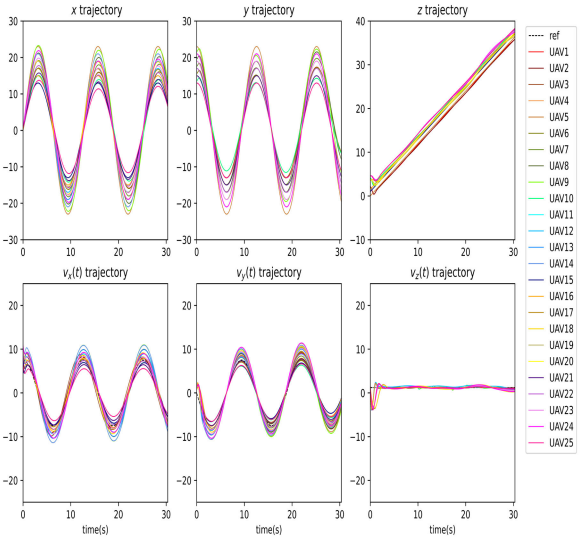

FIGURE 8. The position/velocity trajectories of 25 quadrotor UAVs using the proposed robust decentralized H_∞ attack-tolerant observer-based team formation control strategy via HJIE-reinforcement learning-based DNN approach.

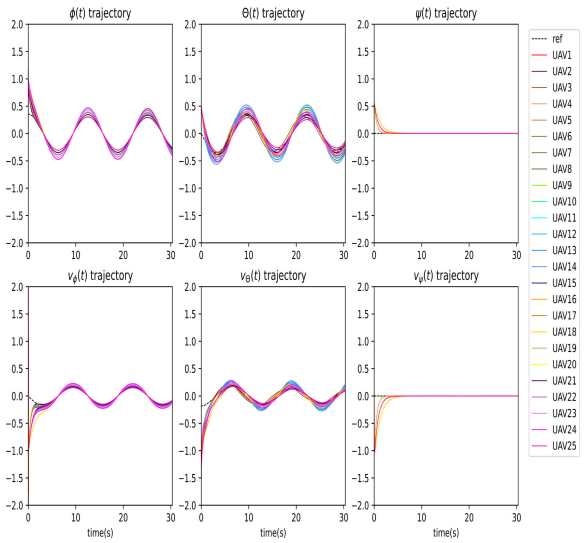

FIGURE 9. The angular/angular velocity trajectories of 25 quadrotor UAVs using the proposed robust decentralized H_∞ attack-tolerant observer-based team formation control strategy via HJIE-reinforcement learning-based DNN approach.

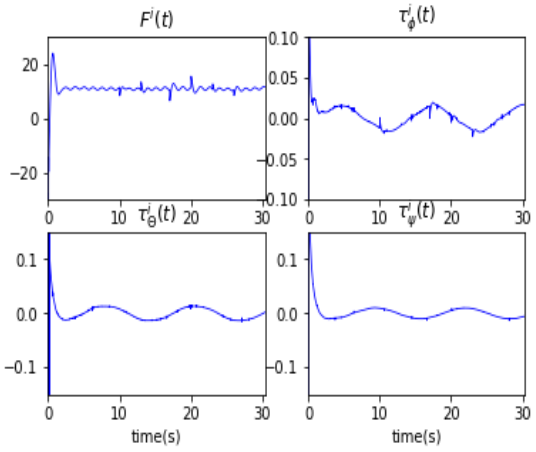

FIGURE 10. The control inputs of the 1st quadrotor UAV using the proposed robust decentralized H_∞ attack-tolerant observer-based team formation control strategy via HJIE-reinforcement learning-based DNN approach.

signals, therefore high frequency sinusoidal signal in Fig.5 is considered as sensor attack signal in the simulation. The malicious attack signals $\gamma_a^i(t)$ and $\gamma_s^i(t)$ on the ith quadrotor UAV and their estimation are shown in Fig.6. It can be shown in Fig.7 that the team of 25 quadrotor UAVs is capable of tracking a spiral trajectory formation along the virtual leader reference trajectory $r_i(t)$. In Figs.8-9, the trajectories of the large-scale quadrotor UAV NCS can track the reference trajectories by the HJIE-reinforcement DNN-based decentralized H_∞ attack-tolerant observer-based team formation tracking control approach. The control inputs of the 1st quadrotor UAV are shown in Fig.10. Additionally, using the estimation of malicious attack signals, the total thrust $F^i(t)$ which automatically changes its control amplitude to compensate for malicious attacks on the NCS actuator of the 1st quadrotor UAV is shown in Fig.10. On the other hand, since output measurement $Y_i(t)$ of the ith quadrotor UAV is transmitted to the observer on the remote side directly via the wireless network channel, it will be affected by the sensor attack signal $\gamma_s^i(t)$. Then, the sensor attack signal $\gamma_s^i(t)$ will affect the observer state $\tilde{X}_i(t)$ which in turn affects $U_i(t)$. In Figs.11-12, the estimation error of 1st quadrotor UAV quickly approaches to zero, which means that accurate estimation can be efficiently achieved by the proposed HJIE-reinforcement DNN-based decentralized H_∞ attack-tolerant observer-based tracking control approach under external disturbance, malicious attacks, coupling effects, and measurement noise. Robust decentralized H_∞ team

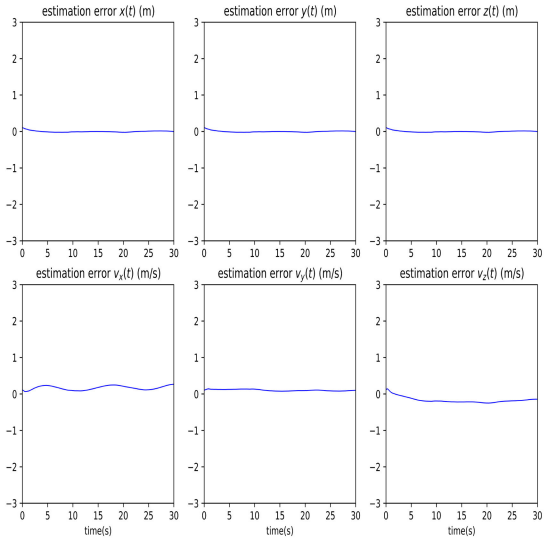

FIGURE 11. Estimation errors of the position/velocity of the 1st quadrotor UAV using the proposed robust decentralized H_∞ attack-tolerant observer-based team formation control strategy via HJIE-reinforcement learning-based DNN approach.

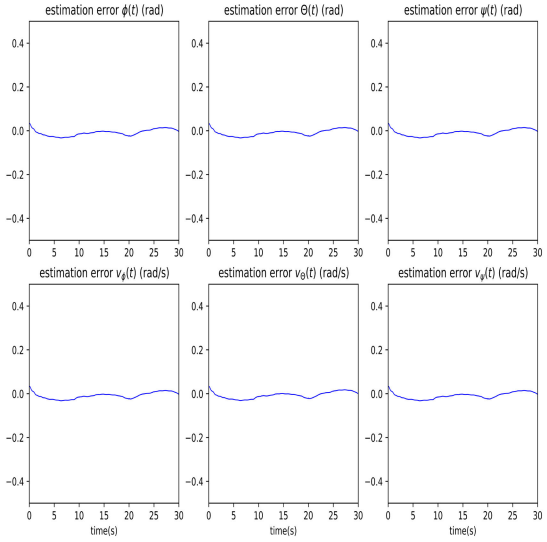

FIGURE 12. Estimation errors of the attitude/angular velocity of the 1st quadrotor UAV using the proposed robust decentralized H_∞ attack-tolerant observer-based team formation control strategy via HJIE-reinforcement learning-based DNN approach.

formation tracking control of the large-scale UAV network system by the T-S fuzzy controller in [9] is carried out for performance comparison with the proposed method and the results are also shown in Fig.13. However, the T-S fuzzy method needs to interpolate 128 local linearized UAV systems to approximate a nonlinear UAV system. In order to improve the formation tracking performance, the number of fuzzy rules must be increased. For a highly nonlinear system such as a quadrotor UAV, a large number of 128×128 locally linearized observer-based controllers need to be interpolated by fuzzy bases and need to be computed at every time instant for the observer-based control signal, which will increase the computational complexity dramatically. Furthermore,

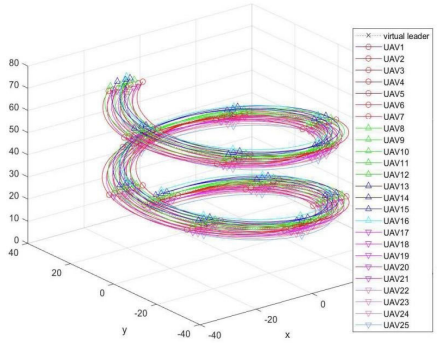

FIGURE 13. The flight trajectories of NCS formation of 25 quadrotor UAVs by the decentralized H_∞ T-S fuzzy team formation tracking control scheme in [9] are given based on the flight/hardware-in-the loop results.

the T-S fuzzy interpolation solution of the HJIE is based on a quadratic Lyapunov function, resulting in a more conservative solution of the nonlinear HJIE. The average attenuation level of the 25-quadrotor-UAV $\rho \approx 2.3112$ by the decentralized $H\infty$ fuzzy team formation control in [9] is poor than the proposed method which is calculated as $\rho \approx 2$.

VI. CONCLUSION

In this paper, an HJIE-reinforcement learning-based DNN robust decentralized H_∞ attack-tolerant observer-based team formation tracking control strategy is proposed to deal with a large-scale quadrotor UAV NCS under external disturbance, measurement noise, malicious attack, and coupling effect. First, a dynamic model of the position and attitude of the quadrotor UAV NCS under malicious attack, external disturbance, measurement noise, and coupling has been constructed. Then, with the aid of the virtual leader team formation structure, the large-scale quadrotor UAV team formation tracking control problem can be reformulated as the decentralized H_∞ attack-tolerant observer-based team formation tracking control design problem of large-scale quadrotor UAVs. To estimate the state variables of the system and the malicious attack signals on the sensors and actuators in the large-scale quadrotor UAV NCS, these malicious attack signals are augmented with each UAV NCS through a smooth dynamic model to simplify the estimation of the attack signals and state of the system. Through the smooth dynamic model embedded in the system model of the quadrotor UAV NCS, we can avoid its corruption and efficiently estimate the augmented system state by a traditional nonlinear Lunberger observer. Furthermore, by the proposed robust decentralized H_∞ attack-tolerant observer-based team formation tracking control strategy, the decentralized observer-based controller of each UAV can effectively attenuate the worst-case effect of external disturbance, measurement noise, malicious attacks, and couplings from other UAVs on the state estimation and reference team formation control of large-scale quadrotor UAVs NCS to achieve robust H_∞ state estimation performance and reference tracking performance of each quadrotor UAV in the team formation. To address the difficulties in solving the $HJIE_i$ of each quadrotor UAV for robust

decentralized H_∞ attack-tolerant observer-based team formation tracking control, an HJIE-reinforcement learning DNN observer-based control scheme has been proposed in Fig.3. Using the output $\frac{\partial V(\tilde{X}_i(t),\bar{e}_i(t),t)}{\partial[\tilde{X}_i^T(t)\ \bar{e}_i^T(t)\ t]^T}$ of DNN, H_∞ control input, the worst-case augmented external disturbance, and coupling are sent back to the ith quadrotor UAV model to produce the next system output to start a new training period without affecting H_∞ team formation tracking performance. Then, a DNN based on HJIE-reinforcement learning is used as a dynamic model-based learning scheme with great potential to solve nonlinear partial differential HJIE$_i$ for complicated decentralized H_∞ attack-tolerant observer-based team formation tracking control design problems of large-scale quadrotor UAVs. We have also proven that if the reinforcement learning-based DNN Adam algorithm makes the HJIE$_i$ error $\varepsilon_i(\theta_p^i(t))$ approach to zero, the proposed HJIE-reinforcement learning-based DNN robust decentralized H_∞ attack-tolerant observer-based team formation tracking control scheme can approach to the theoretical robust decentralized H_∞ attack-tolerant observer-based team formation tracking control performance of large-scale quadrotor UAVs. Eventually, the simulation example of decentralized H_∞ attack-tolerant observer-based team formation tracking control of 25 quadrotor UAVs NCS is also given to validate the effectiveness of the proposed method with comparison. The flight/hardware-in-loop results are very important to further demonstrate the practical effectiveness of the proposed method and will be the future work of my lab.

APPENDIX A
PROOF OF THEOREM 1

(a) Through the two-step procedure of the indirect method, we should first solve the Nash min-max quadratic game problem in (15) in step (i) to guarantee $J_i \le E\{V(\tilde{X}_i(0), \bar{e}_i(0), 0)\}$ in step (ii). Thus, Theorem 1 can be proved as follows:

From (15), we can obtain

$$\begin{aligned} J_i = & \min_{\substack{K_i(\hat{\tilde{X}}_i(t),\bar{e}_i(t)),\\ L_i(\hat{\tilde{x}}_i(t))}} \ \max_{\substack{\tilde{\tilde{v}}_i(t),\\ \tilde{\tilde{X}}_{-i}(t-\tau_{-i}(t))\\ \in \pounds_2[0,t_f]}} \ E\{-V(\tilde{X}_i(t_f), \bar{e}_i(t_f), t_f) \\ & + V(\tilde{X}_i(0), \bar{e}_i(0), 0) + \int_0^{t_f} (\tilde{\tilde{X}}_i^T(t)\bar{Q}_i\tilde{\tilde{X}}_i(t) \\ & + U_i(t)R_iU_i(t) - \rho_i^2(\tilde{\tilde{X}}_{-i}^T(t-\tau_{-i}(t))\tilde{\tilde{X}}_{-i}(t-\tau_{-i}(t))) \\ & + \tilde{\tilde{v}}_i(t)\tilde{\tilde{v}}_i(t)) + \tfrac{d}{dt}V(\tilde{X}_i(t), \bar{e}_i(t), t))dt\}, \\ & \text{for } i = 1, \ldots, N \end{aligned} \tag{36}$$

By chain rule from the nonlinear augmented time-varying system in (13), we have

$$\begin{aligned} \frac{dV(\tilde{X}_i(t), \bar{e}_i(t), t))}{dt} = & \frac{\partial V(\tilde{X}_i(t), \bar{e}_i(t), t)}{\partial t} \\ & + (\frac{\partial V(\tilde{X}_i(t), \bar{e}_i(t), t)}{\partial[\tilde{X}_i^T(t)\ \bar{e}_i^T(t)]^T})^T \\ & \times (\begin{bmatrix} \tilde{F}_i(\tilde{X}_i(t)) - L_i(\hat{\tilde{X}}_i(t))\tilde{C}_i(\tilde{X}_i(t)) \\ F_{e,i}(\bar{e}_i(t), t) \end{bmatrix} \\ & + \begin{bmatrix} \tilde{G}_i(\tilde{X}_i(t)) \\ G_{e,i}(\bar{e}_i(t), t) \end{bmatrix} U_i(t) \\ & + \begin{bmatrix} \bar{D}_i(\bar{X}_i(t)) & -L_i(\hat{\tilde{X}}_i(t)) \\ D_{e,i}(\bar{e}_i(t), t) & 0 \end{bmatrix} \tilde{\tilde{v}}_i^T(t) \\ & + \begin{bmatrix} \bar{F}_{-i}(\bar{X}_i(t)) \\ F_{e,-i}(\bar{e}_i(t), t) \end{bmatrix} \tilde{\tilde{X}}_{-i}(t-\tau_{-i}(t))), \\ & \text{for } i = 1, \ldots, N \end{aligned} \tag{37}$$

Substituting (37) and $\tilde{\tilde{G}}_i(\tilde{X}_i(t), \bar{e}_i(t), t) = \begin{bmatrix} \tilde{G}_i(\tilde{X}_i(t)) \\ G_{e,i}(\bar{e}_i(t), t) \end{bmatrix}$ into (36), we have

$$\begin{aligned} J_i = & \min_{\substack{K_i(\hat{\tilde{X}}_i(t),\bar{e}_i(t)),\\ L_i(\hat{\tilde{x}}_i(t))}} \ \max_{\substack{\tilde{\tilde{v}}_i(t),\\ \tilde{\tilde{X}}_{-i}(t-\tau_{-i}(t))\\ \in \pounds_2[0,t_f]}} \ E\{-V(\tilde{X}_i(t_f), \bar{e}_i(t_f), t_f) \\ & + V(\tilde{X}_i(0), \bar{e}_i(0), 0) + \int_0^{t_f} (\frac{\partial V(\tilde{X}_i(t),\bar{e}_i(t),t)}{\partial t} \\ & + \tilde{\tilde{X}}_i^T(t)\bar{Q}_i\tilde{\tilde{X}}_i(t) + U_i(t)R_iU_i(t) + (\frac{\partial V(\tilde{X}_i(t),\bar{e}_i(t),t)}{\partial[\tilde{X}_i^T(t)\ \bar{e}_i^T(t)]^T})^T \\ & \times \begin{bmatrix} \tilde{F}_i(\tilde{X}_i(t)) - L_i(\hat{\tilde{X}}_i(t))(\tilde{C}_i(\tilde{X}_i(t))) \\ F_{e,i}(\bar{e}_i(t), t) \end{bmatrix} \\ & + (\frac{\partial V(\tilde{X}_i(t),\bar{e}_i(t),t)}{\partial[\tilde{X}_i^T(t)\ \bar{e}_i^T(t)]^T})^T \tilde{\tilde{G}}_i(\tilde{X}_i(t), \bar{e}_i(t), t)U_i(t) \\ & + (\frac{\partial V(\tilde{X}_i(t),\bar{e}_i(t),t)}{\partial[\tilde{X}_i^T(t)\ \bar{e}_i^T(t)]^T})^T \begin{bmatrix} \bar{D}_i(\bar{X}_i(t)) & -L_i(\hat{\tilde{X}}_i(t)) \\ D_{e,i}(\bar{e}_i(t), t) & 0 \end{bmatrix} \\ & \times \tilde{\tilde{v}}_i(t) + (\frac{\partial V(\tilde{X}_i(t),\bar{e}_i(t),t)}{\partial[\tilde{X}_i^T(t)\ \bar{e}_i^T(t)]^T})^T \begin{bmatrix} \bar{F}_{-i}(\bar{X}_i(t)) \\ F_{e,-i}(\bar{e}_i(t), t) \end{bmatrix} \\ & \times \tilde{\tilde{X}}_{-i}(t-\tau_{-i}(t) - \rho_i^2\tilde{\tilde{v}}_i^T(t)\tilde{\tilde{v}}_i(t) \\ & - \rho_i^2\tilde{\tilde{X}}_{-i}(t-\tau_{-i}(t)\tilde{\tilde{X}}_{-i}(t-\tau_{-i}(t))dt\}, \\ & \text{for } i = 1, \ldots, N \end{aligned} \tag{38}$$

By the completing square method, we get

$$\begin{aligned} J_i = & \min_{\substack{K_i(\hat{\tilde{X}}_i(t),\bar{e}_i(t)),\\ L_i(\hat{\tilde{x}}_i(t))}} \ \max_{\substack{\tilde{\tilde{v}}_i(t),\\ \tilde{\tilde{X}}_{-i}(t-\tau_{-i}(t))\\ \in \pounds_2[0,t_f]}} \ E\{-V(\tilde{X}_i(t_f), \bar{e}_i(t_f), t_f) \\ & + V(\tilde{X}_i(0), \bar{e}_i(0), 0) + \int_0^{t_f} (\frac{\partial V(\tilde{X}_i(t),\bar{e}_i(t),t)}{\partial t} \\ & + \tilde{\tilde{X}}_i^T(t)\bar{Q}_i\tilde{\tilde{X}}_i(t) - \tfrac{1}{4}(\frac{\partial V(\tilde{X}_i(t),\bar{e}_i(t),t)}{\partial[\tilde{X}_i^T(t)\ \bar{e}_i^T(t)]^T})^T \\ & \times \tilde{\tilde{G}}_i(\tilde{X}_i(t), \bar{e}_i(t), t)R_i^{-1}\tilde{\tilde{G}}_i^T(\tilde{X}_i(t), \bar{e}_i(t), t) \\ & \times (\frac{\partial V(\tilde{X}_i(t),\bar{e}_i(t),t)}{\partial[\tilde{X}_i^T(t)\ \bar{e}_i^T(t)]^T}) + (\tfrac{1}{2}\tilde{\tilde{G}}_i^T(\tilde{X}_i(t), \bar{e}_i(t), t) \\ & \times (\frac{\partial V(\tilde{X}_i(t),\bar{e}_i(t),t)}{\partial[\tilde{X}_i^T(t)\ \bar{e}_i^T(t)]^T}) + R_iU_i(t))^TR_i^{-1} \\ & \times (\tfrac{1}{2}\tilde{\tilde{G}}_i^T(\tilde{X}_i(t), \bar{e}_i(t), t)(\frac{\partial V(\tilde{X}_i(t),\bar{e}_i(t),t)}{\partial[\tilde{X}_i^T(t)\ \bar{e}_i^T(t)]^T}) \\ & + R_iU_i(t)) + (\frac{\partial V(\tilde{X}_i(t),\bar{e}_i(t),t)}{\partial[\tilde{X}_i^T(t)\ \bar{e}_i^T(t)]^T})^T \\ & \times \begin{bmatrix} \tilde{F}_i(\tilde{X}_i(t)) - L_i(\hat{\tilde{X}}_i(t))(\tilde{C}_i(\tilde{X}_i(t))) \\ F_{e,i}(\bar{e}_i(t), t) \end{bmatrix} + \tfrac{1}{4\rho_i^2} \end{aligned}$$

$$\times \left(\frac{\partial V(\tilde{X}_i(t),\bar{e}_i(t),t)}{\partial[\tilde{X}_i^T(t)\ \bar{e}_i^T(t)]^T}\right)^T \begin{bmatrix} \bar{D}_i(\bar{X}_i(t)) & -L_i(\hat{\bar{X}}_i(t)) \\ D_{e,i}(\bar{e}_i(t),t) & 0 \end{bmatrix}$$
$$\times \begin{bmatrix} \bar{D}_i(\bar{X}_i(t)) & -L_i(\hat{\bar{X}}_i(t)) \\ D_{e,i}(\bar{e}_i(t),t) & 0 \end{bmatrix}^T \left(\frac{\partial V(\tilde{X}_i(t),\bar{e}_i(t),t)}{\partial[\tilde{X}_i^T(t)\ \bar{e}_i^T(t)]^T}\right)$$
$$-\frac{1}{4\rho_i^2}\left(\frac{\partial V(\tilde{X}_i(t),\bar{e}_i(t),t)}{\partial[\tilde{X}_i^T(t)\ \bar{e}_i^T(t)]^T}\right)^T \begin{bmatrix} \bar{F}_{-i}(\bar{X}_i(t)) \\ F_{e,-i}(\bar{e}_i(t),t) \end{bmatrix}$$
$$\times \begin{bmatrix} \bar{F}_{-i}(\bar{X}_i(t)) \\ F_{e,-i}(\bar{e}_i(t),t) \end{bmatrix}^T \left(\frac{\partial V(\tilde{X}_i(t),\bar{e}_i(t),t)}{\partial[\tilde{X}_i^T(t)\ \bar{e}_i^T(t)]^T}\right) - \left(\frac{1}{2\rho_i^2}\right.$$
$$\times \begin{bmatrix} \bar{D}_i(\bar{X}_i(t)) & -L_i(\hat{\bar{X}}_i(t)) \\ D_{e,i}(\bar{e}_i(t),t) & 0 \end{bmatrix}^T \left(\frac{\partial V(\tilde{X}_i(t),\bar{e}_i(t),t)}{\partial[\tilde{X}_i^T(t)\ \bar{e}_i^T(t)]^T}\right)$$
$$-\rho_i\tilde{\bar{v}}_i(t))^T \times \left(\frac{1}{2\rho_i^2}\begin{bmatrix} \bar{D}_i(\bar{X}_i(t)) & -L_i(\hat{\bar{X}}_i(t)) \\ D_{e,i}(\bar{e}_i(t),t) & 0 \end{bmatrix}^T\right.$$
$$\times \left(\frac{\partial V(\tilde{X}_i(t),\bar{e}_i(t),t)}{\partial[\tilde{X}_i^T(t)\ \bar{e}_i^T(t)]^T}\right) - \rho_i\tilde{\bar{v}}_i(t))$$
$$-\left(\frac{1}{2\rho_i^2}\begin{bmatrix} \bar{F}_{-i}(\bar{X}_i(t)) \\ F_{e,-i}(\bar{e}_i(t),t) \end{bmatrix}^T \left(\frac{\partial V(\tilde{X}_i(t),\bar{e}_i(t),t)}{\partial[\tilde{X}_i^T(t)\ \bar{e}_i^T(t)]^T}\right)\right.$$
$$-\rho_i\tilde{\bar{X}}_{-i}(t-\tau_{-i}))^T\left(\frac{1}{2\rho_i^2}\begin{bmatrix} \bar{F}_{-i}(\bar{X}_i(t)) \\ F_{e,-i}(\bar{e}_i(t),t) \end{bmatrix}^T\right.$$
$$\left.\left.\times \left(\frac{\partial V(\tilde{X}_i(t),\bar{e}_i(t),t)}{\partial[\tilde{X}_i^T(t)\ \bar{e}_i^T(t)]^T}\right) - \rho_i\tilde{\bar{X}}_{-i}(t-\tau_{-i}))\right)dt\right\},$$
$$for\ i = 1,\ldots,N \tag{39}$$

In (39) the optimal $U_i^*(t) = K_i^*(\hat{\bar{X}}_i(t),\bar{e}_i(t))$ in (17), the worst-case $\tilde{\bar{v}}_i^*(t)$ in (16) and $\tilde{\bar{X}}_{-i}^*(t-\tau_{-i}(t))$ in (18) make the square terms involved in (39) become zero to achieve $\min_{U_i(t)=K_i(\hat{\bar{X}}_i(t),\bar{e}_i(t))} \max_{\tilde{\bar{v}}_i(t),\tilde{\bar{X}}_{-i}(t-\tau_{-i}(t))}$. Then we can get

$$J_i = \min_{L_i(\hat{\bar{x}}_i(t))} E\{-V(\tilde{X}_i(t_f),\bar{e}_i(t_f),t_f) + V(\tilde{X}_i(0),\bar{e}_i(0),0)$$
$$+\int_0^{t_f}\left(\frac{\partial V(\tilde{X}_i(t),\bar{e}_i(t),t)}{\partial t} + \tilde{\bar{X}}_i^T(t)\bar{Q}_i\tilde{\bar{X}}_i(t)\right.$$
$$-\frac{1}{4}\left(\frac{\partial V(\tilde{X}_i(t),\bar{e}_i(t),t)}{\partial[\tilde{X}_i^T(t)\ \bar{e}_i^T(t)]^T}\right)^T\tilde{\bar{G}}_i(\tilde{X}_i(t),\bar{e}_i(t),t)R_i^{-1}$$
$$\times\tilde{\bar{G}}_i^T(\tilde{X}_i(t),\bar{e}_i(t),t)\left(\frac{\partial V(\tilde{X}_i(t),\bar{e}_i(t),t)}{\partial[\tilde{X}_i^T(t)\ \bar{e}_i^T(t)]^T}\right)$$
$$+\left(\frac{\partial V(\tilde{X}_i(t),\bar{e}_i(t),t)}{\partial[\tilde{X}_i^T(t)\ \bar{e}_i^T(t)]^T}\right)^T\begin{bmatrix} \tilde{F}_i(\tilde{X}_i(t)) - L_i(\hat{\bar{X}}_i(t))\tilde{C}_i(\tilde{X}_i(t)) \\ F_{e,i}(\bar{e}_i(t),t) \end{bmatrix}$$
$$+\frac{1}{4\rho_i^2}\left(\frac{\partial V(\tilde{X}_i(t),\bar{e}_i(t),t)}{\partial[\tilde{X}_i^T(t)\ \bar{e}_i^T(t)]^T}\right)^T\begin{bmatrix} \bar{D}_i(\bar{X}_i(t)) & -L_i(\hat{\bar{X}}_i(t)) \\ D_{e,i}(\bar{e}_i(t),t) & 0 \end{bmatrix}$$
$$\times\begin{bmatrix} \bar{D}_i(\bar{X}_i(t)) & -L_i(\hat{\bar{X}}_i(t)) \\ D_{e,i}(\bar{e}_i(t),t) & 0 \end{bmatrix}^T\left(\frac{\partial V(\tilde{X}_i(t),\bar{e}_i(t),t)}{\partial[[\tilde{X}_i^T(t)\ \bar{e}_i^T(t)]^T}\right)$$
$$+\frac{1}{4\rho_i^2}\left(\frac{\partial V(\tilde{X}_i(t),\bar{e}_i(t),t)}{\partial[[\tilde{X}_i^T(t)\ \bar{e}_i^T(t)]^T}\right)^T\begin{bmatrix} \bar{F}_{-i}(\bar{X}_i(t)) \\ F_{e,-i}(\bar{e}_i(t),t) \end{bmatrix}$$
$$\left.\times\begin{bmatrix} \bar{F}_{-i}(\bar{X}_i(t)) \\ F_{e,-i}(\bar{e}_i(t),t) \end{bmatrix}^T\left(\frac{\partial V(\tilde{X}_i(t),\bar{e}_i(t),t)}{\partial[\tilde{X}_i^T(t)\ \bar{e}_i^T(t)]^T}\right)dt\right\},$$
$$for\ i = 1,\ldots,N \tag{40}$$

By the fact

$$\frac{\partial V(\tilde{X}_i(t),\bar{e}_i(t),t)}{\partial[\tilde{X}_i^T(t)\ \bar{e}_i^T(t)]^T} = \begin{bmatrix} \frac{\partial V(\tilde{X}_i(t),\bar{e}_i(t),t)}{\partial\tilde{X}_i(t)} \\ \frac{\partial V(\tilde{X}_i(t),\bar{e}_i(t),t)}{\partial\bar{e}_i(t)} \end{bmatrix} \tag{41}$$

we get

$$\left(\frac{\partial V(\tilde{X}_i(t),\bar{e}_i(t),t)}{\partial[\tilde{X}_i^T(t),\bar{e}_i^T(t)]^T}\right)^T\begin{bmatrix} \tilde{F}_i(\tilde{X}_i(t)) - L_i(\hat{\bar{X}}_i(t))\tilde{C}_i(\tilde{X}_i(t)) \\ F_{e,i}(\bar{e}_i(t),t) \end{bmatrix}$$
$$= \left(\frac{\partial V(\tilde{X}_i(t),\bar{e}_i(t),t)}{\partial\tilde{X}_i(t)}\right)^T(\tilde{F}_i(\tilde{X}_i(t)) - L_i(\hat{\bar{X}}_i(t))\tilde{C}_i(\tilde{X}_i(t)))$$
$$+\left(\frac{\partial V(\tilde{X}_i(t),\bar{e}_i(t),t)}{\partial\bar{e}_i(t)}\right)^T F_{e,i}(\bar{e}_i(t),t),$$
$$for\ i = 1,\ldots,N \tag{42}$$

and

$$\left(\frac{\partial V(\tilde{X}_i(t),\bar{e}_i(t),t)}{\partial[\tilde{X}_i^T(t)\ \bar{e}_i^T(t)]^T}\right)^T\begin{bmatrix} \bar{D}_i(\bar{X}_i(t)) & -L_i(\hat{\bar{X}}_i(t)) \\ D_{e,i}(\bar{e}_i(t),t) & 0 \end{bmatrix}$$
$$\times\begin{bmatrix} \bar{D}_i(\bar{X}_i(t)) & -L_i(\hat{\bar{X}}_i(t)) \\ D_{e,i}(\bar{e}_i(t),t) & 0 \end{bmatrix}^T\left(\frac{\partial V(\tilde{X}_i(t),\bar{e}_i(t),t)}{\partial[\tilde{X}_i^T(t)\ \bar{e}_i^T(t)]^T}\right)$$
$$=\begin{bmatrix}\left(\frac{\partial V(\tilde{X}_i(t),\bar{e}_i(t),t)}{\partial\tilde{X}_i(t)}\right)^T & \left(\frac{\partial V(\tilde{X}_i(t),\bar{e}_i(t),t)}{\partial\bar{e}_i(t)}\right)^T\end{bmatrix}$$
$$\times\begin{bmatrix} \bar{D}_i(\bar{X}_i(t))\bar{D}_i^T(\bar{X}_i(t))+L_i(\hat{\bar{X}}_i(t))L_i^T(\hat{\bar{X}}_i(t)) & \bar{D}_i(\bar{X}_i(t))D_{e,i}^T(\bar{e}_i(t),t) \\ D_{e,i}(\bar{e}_i(t),t)\bar{D}_i^T(\bar{X}_i(t)) & D_{e,i}(\bar{e}_i(t),t)D_{e,i}^T(\bar{e}_i(t),t) \end{bmatrix}$$
$$\times\begin{bmatrix} \frac{\partial V(\tilde{X}_i(t),\bar{e}_i(t),t)}{\partial\tilde{X}_i(t)} \\ \frac{\partial V(\tilde{X}_i(t),\bar{e}_i(t),t)}{\partial\bar{e}_i(t)} \end{bmatrix} = \left(\frac{\partial V(\tilde{X}_i(t),\bar{e}_i(t),t)}{\partial\tilde{X}_i(t)}\right)^T$$
$$\times(\bar{D}_i(\bar{X}_i(t))\bar{D}_i^T(\bar{X}_i(t)) + L_i(\hat{\bar{X}}_i(t))L_i^T(\hat{\bar{X}}_i(t)))$$
$$\times\left(\frac{\partial V(\tilde{X}_i(t),\bar{e}_i(t),t)}{\partial\tilde{X}_i(t)}\right) + \left(\frac{\partial V(\tilde{X}_i(t),\bar{e}_i(t),t)}{\partial\tilde{X}_i(t)}\right)^T$$
$$\times\bar{D}_i(X_i(t))D_{e,i}(\bar{e}_i(t),t)^T\left(\frac{\partial V(\tilde{X}_i(t),\bar{e}_i(t),t)}{\partial\bar{e}_i(t)}\right)$$
$$+\left(\frac{\partial V(\tilde{X}_i(t),\bar{e}_i(t),t)}{\partial\tilde{X}_i(t)}\right)D_{e,i}(\bar{e}_i(t),t)\bar{D}_i^T(\bar{X}_i(t))$$
$$\times\left(\frac{\partial V(\tilde{X}_i(t),\bar{e}_i(t),t)}{\partial\bar{e}_i(t)}\right) + \left(\frac{\partial V(\tilde{X}_i(t),\bar{e}_i(t),t)}{\partial\tilde{X}_i(t)}\right)^T$$
$$\times D_{e,i}(\bar{e}_i(t),t)D_{e,i}(\bar{e}_i(t),t)^T\left(\frac{\partial V(\tilde{X}_i(t),\bar{e}_i(t),t)}{\partial\bar{e}_i(t)}\right),$$
$$for\ i = 1,\ldots,N \tag{43}$$

and

$$\left(\frac{\partial V(\tilde{X}_i(t),\bar{e}_i(t),t)}{\partial[\tilde{X}_i^T(t)\ \bar{e}_i^T(t)]^T}\right)^T\begin{bmatrix} \bar{F}_{-i}(\bar{X}_i(t)) \\ F_{e,-i}(\bar{e}_i(t),t) \end{bmatrix}$$
$$\times\begin{bmatrix} \bar{F}_{-i}(\bar{X}_i(t)) \\ F_{e,-i}(\bar{e}_i(t),t) \end{bmatrix}^T\left(\frac{\partial V(\tilde{X}_i(t),\bar{e}_i(t),t)}{\partial[\tilde{X}_i^T(t)\ \bar{e}_i^T(t)]^T}\right)$$
$$=\begin{bmatrix}\left(\frac{\partial V(\tilde{X}_i(t),\bar{e}_i(t),t)}{\partial\tilde{X}_i(t)}\right)^T & \left(\frac{\partial V(\tilde{X}_i(t),\bar{e}_i(t),t)}{\partial\bar{e}_i(t)}\right)^T\end{bmatrix}$$
$$\times\begin{bmatrix} \bar{F}_{-i}(\bar{X}_i(t))\bar{F}_{-i}^T(\bar{X}_i(t)) & \bar{F}_{-i}(\bar{X}_i(t))F_{e,-i}^T(\bar{e}_i(t),t) \\ F_{e,-i}(\bar{e}_i(t),t)\bar{F}_{-i}^T(\bar{X}_i(t)) & F_{e,-i}(\bar{e}_i(t),t)F_{e,-i}^T(\bar{e}_i(t),t) \end{bmatrix}$$
$$\times\begin{bmatrix} \frac{\partial V(\tilde{X}_i(t),\bar{e}_i(t),t)}{\partial\tilde{X}_i(t)} \\ \frac{\partial V(\tilde{X}_i(t),\bar{e}_i(t),t)}{\partial\bar{e}_i(t)} \end{bmatrix} = \left(\frac{\partial V(\tilde{X}_i(t),\bar{e}_i(t),t)}{\partial\tilde{X}_i(t)}\right)^T$$
$$\times\bar{F}_{-i}(\bar{X}_i(t))\bar{F}_{-i}^T(\bar{X}_i(t))\left(\frac{\partial V(\tilde{X}_i(t),\bar{e}_i(t),t)}{\partial\tilde{X}_i(t)}\right)$$
$$+\left(\frac{\partial V(\tilde{X}_i(t),\bar{e}_i(t),t)}{\partial\tilde{X}_i(t)}\right)^T\bar{F}_{-i}(\bar{X}_i(t))$$

$$\times F_{e,-i}^T(\bar{e}_i(t),t)(\tfrac{\partial V(\tilde{X}_i(t),\bar{e}_i(t),t)}{\partial \bar{e}_i(t)})$$
$$+(\tfrac{\partial V(\tilde{X}_i(t),\bar{e}_i(t),t)}{\partial \tilde{X}_i(t)})^T F_{e,-i}(\bar{e}_i(t),t)\bar{F}_{-i}^T(\bar{X}_i(t))$$
$$\times(\tfrac{\partial V(\tilde{X}_i(t),\bar{e}_i(t),t)}{\partial \bar{e}_i(t)})+(\tfrac{\partial V(\tilde{X}_i(t),\bar{e}_i(t),t)}{\partial \tilde{X}_i(t)})^T$$
$$\times F_{e,-i}(\bar{e}_i(t),t)F_{e,-i}^T(\bar{e}_i(t),t)(\tfrac{\partial V(\tilde{X}_i(t),\bar{e}_i(t),t)}{\partial \bar{e}_i(t)}),$$
$$for\ i=1,\ldots,N \tag{44}$$

Substituting (41),(42),(43),and(44) into (40), we can get

$$\begin{aligned}
J_i = \min_{L_i(\hat{\tilde{X}}_i(t))} & E\{-V(\tilde{X}_i(t_f),\bar{e}_i(t_f),t_f)+V(\tilde{X}_i(0),\bar{e}_i(0),0)\\
&+\int_0^{t_f}(\tfrac{\partial V(\tilde{X}_i(t),\bar{e}_i(t),t)}{\partial t}+\tilde{\bar{X}}_i^T(t)\bar{Q}_i\tilde{\bar{X}}_i(t)\\
&-\tfrac{1}{4}(\tfrac{\partial V(\tilde{X}_i(t),\bar{e}_i(t),t)}{\partial[\tilde{X}_i^T(t)\ \bar{e}_i^T(t)]^T})^T\tilde{\bar{G}}_i(\tilde{X}_i(t),\bar{e}_i(t),t)R_i^{-1}\\
&\times\tilde{\bar{G}}_i^T(\tilde{X}_i(t),\bar{e}_i(t),t)(\tfrac{\partial V(\tilde{X}_i(t),\bar{e}_i(t),t)}{\partial[\tilde{X}_i^T(t)\ \bar{e}_i^T(t)]^T})\\
&+(\tfrac{\partial V(\tilde{X}_i(t),\bar{e}_i(t),t)}{\partial \tilde{X}_i(t)})^T(\tilde{F}_i(\tilde{X}_i(t))-L_i(\hat{\tilde{X}}_i(t))\\
&\times\tilde{C}_i(\tilde{X}_i(t))+(\tfrac{\partial V(\tilde{X}_i(t),\bar{e}_i(t),t)}{\partial \bar{e}_i(t)})^T F_{e,i}(\bar{e}_i(t),t)\\
&+\tfrac{1}{4\rho_i^2}(\tfrac{\partial V(\tilde{X}_i(t),\bar{e}_i(t),t)}{\partial \tilde{X}_i(t)})^T(\bar{D}_i\bar{X}_i(t)\bar{D}_i^T(\bar{X}_i(t))\\
&+L_i(\hat{\tilde{X}}_i(t))L_i^T\hat{\tilde{X}}_i(t))(\tfrac{\partial V(\tilde{X}_i(t),\bar{e}_i(t),t)}{\partial \tilde{X}_i(t)})\\
&+\tfrac{1}{4\rho_i^2}(\tfrac{\partial V(\tilde{X}_i(t),\bar{e}_i(t),t)}{\partial \tilde{X}_i(t)})^T\bar{D}_i(\bar{X}_i(t))D_{e,i}^T(\bar{e}_i(t),t)\\
&\times(\tfrac{\partial V(\tilde{X}_i(t),\bar{e}_i(t),t)}{\partial \bar{e}_i(t)})+\tfrac{1}{4\rho_i^2}(\tfrac{\partial V(\tilde{X}_i(t),\bar{e}_i(t),t)}{\partial \tilde{X}_i(t)})^T\\
&\times D_{e,i}(\bar{e}_i(t),t)\bar{D}_i^T\bar{X}_i(t)(\tfrac{\partial V(\tilde{X}_i(t),\bar{e}_i(t),t)}{\partial \bar{e}_i(t)})\\
&+\tfrac{1}{4\rho_i^2}(\tfrac{\partial V(\tilde{X}_i(t),\bar{e}_i(t),t)}{\partial \tilde{X}_i(t)})^T D_{e,i}(\bar{e}_i(t),t)D_{e,i}^T(\bar{e}_i(t),t)\\
&\times(\tfrac{\partial V(\tilde{X}_i(t),\bar{e}_i(t),t)}{\partial \bar{e}_i(t)})+\tfrac{1}{4\rho_i^2}(\tfrac{\partial V(\tilde{X}_i(t),\bar{e}_i(t),t)}{\partial \tilde{X}_i(t)})^T\\
&\times\bar{F}_{-i}(\bar{X}_i(t))\bar{F}_{-i}^T(\bar{X}_i(t))(\tfrac{\partial V(\tilde{X}_i(t),\bar{e}_i(t),t)}{\partial \tilde{X}_i(t)})\\
&+\tfrac{1}{4\rho_i^2}(\tfrac{\partial V(\tilde{X}_i(t),\bar{e}_i(t),t)}{\partial \tilde{X}_i(t)})^T\bar{F}_{-i}(\bar{X}_i(t))F_{e,-i}^T(\bar{e}_i(t),t)\\
&\times(\tfrac{\partial V(\tilde{X}_i(t),\bar{e}_i(t),t)}{\partial \bar{e}_i(t)})+\tfrac{1}{4\rho_i^2}(\tfrac{\partial V(\tilde{X}_i(t),\bar{e}_i(t),t)}{\partial \tilde{X}_i(t)})^T\\
&\times F_{e,-i}(\bar{e}_i(t),t)\bar{F}_{-i}^T(\bar{X}_i(t))(\tfrac{\partial V(\tilde{X}_i(t),\bar{e}_i(t),t)}{\partial \bar{e}_i(t)})\\
&+\tfrac{1}{4\rho_i^2}(\tfrac{\partial V(\tilde{X}_i(t),\bar{e}_i(t),t)}{\partial \tilde{X}_i(t)})^T F_{e,-i}(\bar{e}_i(t),t)\\
&\times F_{e,-i}^T(\bar{e}_i(t),t)(\tfrac{\partial V(\tilde{X}_i(t),\bar{e}_i(t),t)}{\partial \bar{e}_i(t)})dt\}\\
= \min_{L_i(\hat{\tilde{X}}_i(t))} & E\{-V(\tilde{X}_i(t_f),\bar{e}_i(t_f),t_f)+V(\tilde{X}_i(0),\bar{e}_i(0),0)\\
&+\int_0^{t_f}(\tfrac{\partial V(\tilde{X}_i(t),\bar{e}_i(t),t)}{\partial t}+\tilde{\bar{X}}_i^T(t)\bar{Q}_i\tilde{\bar{X}}_i(t)\\
&-\tfrac{1}{4}(\tfrac{\partial V(\tilde{X}_i(t),\bar{e}_i(t),t)}{\partial[\tilde{X}_i^T(t)\ \bar{e}_i^T(t)]^T}^T)^T\tilde{\bar{G}}_i(\tilde{X}_i(t),\bar{e}_i(t),t)R_i^{-1}\\
&\times\tilde{\bar{G}}_i^T(\tilde{X}_i(t),\bar{e}_i(t),t)(\tfrac{\partial V(\tilde{X}_i(t),\bar{e}_i(t),t)}{\partial[\tilde{X}_i^T(t)\ \bar{e}_i^T(t)]^T}^T)\\
&+(\tfrac{\partial V(\tilde{X}_i(t),\bar{e}_i(t),t)}{\partial \tilde{X}_i(t)})^T\tilde{F}_i(\tilde{X}_i(t))\\
&+(\tfrac{\partial V(\tilde{X}_i(t),\bar{e}_i(t),t)}{\partial \bar{e}_i(t)})^T F_{e,i}(\bar{e}_i(t),t)\\
&+\tfrac{1}{4\rho_i^2}(\tfrac{\partial V(\tilde{X}_i(t),\bar{e}_i(t),t)}{\partial \tilde{X}_i(t)})^T\bar{D}_i(\bar{X}_i(t))\bar{D}_i^T(\bar{X}_i(t))\\
&\times(\tfrac{\partial V(\tilde{X}_i(t),\bar{e}_i(t),t)}{\partial \tilde{X}_i(t)})\\
&+\tfrac{1}{4\rho_i^2}(\tfrac{\partial V(\tilde{X}_i(t),\bar{e}_i(t),t)}{\partial \tilde{X}_i(t)})^T\bar{D}_i(\bar{X}_i(t))D_{e,i}^T(\bar{e}_i(t),t)\\
&\times(\tfrac{\partial V(\tilde{X}_i(t),\bar{e}_i(t),t)}{\partial \bar{e}_i(t)})+\tfrac{1}{4\rho_i^2}(\tfrac{\partial V(\tilde{X}_i(t),\bar{e}_i(t),t)}{\partial \tilde{X}_i(t)})^T\\
&\times D_{e,i}(\bar{e}_i(t),t)\bar{D}_i^T(\bar{X}_i(t))(\tfrac{\partial V(\tilde{X}_i(t),\bar{e}_i(t),t)}{\partial \bar{e}_i(t)})\\
&+\tfrac{1}{4\rho_i^2}(\tfrac{\partial V(\tilde{X}_i(t),\bar{e}_i(t),t)}{\partial \tilde{X}_i(t)})^T D_{e,i}(\bar{e}_i(t),t)D_{e,i}^T(\bar{e}_i(t),t)\\
&\times(\tfrac{\partial V(\tilde{X}_i(t),\bar{e}_i(t),t)}{\partial \bar{e}_i(t)})+\tfrac{1}{4\rho_i^2}(\tfrac{\partial V(\tilde{X}_i(t),\bar{e}_i(t),t)}{\partial \tilde{X}_i(t)})^T\\
&\times\bar{F}_{-i}(\bar{X}_i(t))\bar{F}_{-i}^T(\bar{X}_i(t))(\tfrac{\partial V(\tilde{X}_i(t),\bar{e}_i(t),t)}{\partial \tilde{X}_i(t)})\\
&+\tfrac{1}{4\rho_i^2}(\tfrac{\partial V(\tilde{X}_i(t),\bar{e}_i(t),t)}{\partial \tilde{X}_i(t)})^T\bar{F}_{-i}(\bar{X}_i(t))F_{e,-i}^T(\bar{e}_i(t),t)\\
&\times(\tfrac{\partial V(\tilde{X}_i(t),\bar{e}_i(t),t)}{\partial \bar{e}_i(t)})+\tfrac{1}{4\rho_i^2}(\tfrac{\partial V(\tilde{X}_i(t),\bar{e}_i(t),t)}{\partial \tilde{X}_i(t)})^T\\
&\times F_{e,-i}(\bar{e}_i(t),t)\bar{F}_{-i}^T(\bar{X}_i(t))(\tfrac{\partial V(\tilde{X}_i(t),\bar{e}_i(t),t)}{\partial \bar{e}_i(t)})\\
&+\tfrac{1}{4\rho_i^2}(\tfrac{\partial V(\tilde{X}_i(t),\bar{e}_i(t),t)}{\partial \tilde{X}_i(t)})^T F_{e,-i}(\bar{e}_i(t),t)\\
&\times F_{e,-i}^T(\bar{e}_i(t),t)(\tfrac{\partial V(\tilde{X}_i(t),\bar{e}_i(t),t)}{\partial \bar{e}_i(t)})+\tfrac{1}{4\rho_i^2}(L_i^T(\hat{\tilde{X}}_i(t))\\
&\times(\tfrac{\partial V(\tilde{X}_i(t),\bar{e}_i(t),t)}{\partial \tilde{X}_i(t)})-\tfrac{1}{2}\tilde{C}_i(\tilde{X}_i(t))^T)(L_i^T(\hat{\tilde{X}}_i(t))\\
&\times(\tfrac{\partial V(\tilde{X}_i(t),\bar{e}_i(t),t)}{\partial \tilde{X}_i(t)})-\tfrac{1}{2}\tilde{C}_i(\tilde{X}_i(t)))\\
&-\tfrac{1}{16\rho_i^2}\tilde{C}_i^T(\tilde{X}_i(t))\tilde{C}_i(\tilde{X}_i(t)))dt\},\\
&for\ i=1,\ldots,N
\end{aligned} \tag{45}$$

We can obtain the optimal observer gain $L_i^*(\hat{\tilde{X}}_i(t))$ as (19) from (45). After optimal $U_i^*(t)$ in (17), $L_i^*(\hat{\tilde{X}}_i(t))$ in (19), worst-case $\tilde{\bar{v}}_i^*(t)$ in (16) and $\tilde{\bar{X}}_{-i}^*(t-\tau_{-i}(t))$ in (18) are obtained and proof step (i) is completed. Then, J_i in (45), it can be rewritten as follows:

$$\begin{aligned}
J_i = & E\{-V(\tilde{X}_i(t_f),\bar{e}_i(t_f),t_f)+V(\tilde{X}_i(0),\bar{e}_i(0),0)\\
&+\int_0^{t_f}(\tfrac{\partial V(\tilde{X}_i(t),\bar{e}_i(t),t)}{\partial t}+\tilde{\bar{X}}_i^T(t)\bar{Q}_i\tilde{\bar{X}}_i(t)\\
&-\tfrac{1}{4}(\tfrac{\partial V(\tilde{X}_i(t),\bar{e}_i(t),t)}{\partial[\tilde{X}_i^T(t)\ \bar{e}_i^T(t)]^T})^T\tilde{\bar{G}}_i(\tilde{X}_i(t),\bar{e}_i(t),t)R_i^{-1}\\
&\times\tilde{\bar{G}}_i^T(\tilde{X}_i(t),\bar{e}_i(t),t)(\tfrac{\partial V(\tilde{X}_i(t),\bar{e}_i(t),t)}{\partial[\tilde{X}_i^T(t)\ \bar{e}_i^T(t)]^T})\\
&+(\tfrac{\partial V(\tilde{X}_i(t),\bar{e}_i(t),t)}{\partial[\tilde{X}_i^T(t)\ \bar{e}_i^T(t)]^T})^T\tilde{\bar{F}}_i(\tilde{X}_i(t),\bar{e}_i(t),t)\\
&+\tfrac{1}{4\rho_i^2}(\tfrac{\partial V(\tilde{X}_i(t),\bar{e}_i(t),t)}{\partial[\tilde{X}_i^T(t)\ \bar{e}_i^T(t)]^T})^T\tilde{\bar{D}}_i(\tilde{X}_i(t),\bar{e}_i(t),t)\\
&\times(\tfrac{\partial V(\tilde{X}_i(t),\bar{e}_i(t),t)}{\partial[\tilde{X}_i^T(t)\ \bar{e}_i^T(t)]^T})+\tfrac{1}{4\rho_i^2}(\tfrac{\partial V(\tilde{X}_i(t),\bar{e}_i(t),t)}{\partial[\tilde{X}_i^T(t)\ \bar{e}_i^T(t)]^T})^T\\
&\times\bar{F}_{-i}(\tilde{\bar{X}}_i(t))(\tfrac{\partial V(\tilde{X}_i(t),\bar{e}_i(t),t)}{\partial[\tilde{X}_i^T(t)\ \bar{e}_i^T(t)]^T})\\
&-\tfrac{1}{16\rho_i^2}\tilde{C}_i^T(\tilde{X}_i(t))\tilde{C}_i(\tilde{X}_i(t)))dt\},\\
&for\ i=1,\ldots,N
\end{aligned} \tag{46}$$

By HJIE$_i$ in (20) and (46), we get

$$J_i = E\{-V(\tilde{X}_i(t_f), \bar{e}_i(t_f), t_f) + V(\tilde{X}_i(0), \bar{e}_i(0), 0)\}, \quad for\ i = 1, \ldots, N \tag{47}$$

where $V(\tilde{X}_i(t), \bar{e}_i(t), t_f) \geq 0$, then

$$J_i \leq E\{V(\tilde{X}_i(0), \bar{e}_i(0), 0)\},\ for\ i = 1, \ldots, N \tag{48}$$

i.e., the second step in (ii) is also guaranteed.

(b) If $\tilde{\bar{v}}_i(t) \in \pounds_2[0, \infty)$ and $\tilde{\bar{X}}_{-i}(t - \tau_{-i}(t)) \in \pounds_2[0, \infty)$ and $V(\tilde{X}_i(0), \bar{e}_i(0), 0) < \infty$, from the definition of J_i in (15), then (48) becomes

$$\begin{aligned} &E\{\int_0^{t_f} (\tilde{\bar{X}}_i^T(t)\bar{Q}_i\tilde{\bar{X}}_i(t)) + U_i^T(t)R_i(t)U_i(t)\} \\ &\leq E\{V(\tilde{X}_i(0), \bar{e}_i(0), 0) + \rho_i^2 \int_0^{t_f} (\tilde{\bar{v}}_i^T(t)\tilde{\bar{v}}_i(t) \\ &\quad + \tilde{\bar{X}}_{-i}^T(t - \tau_{-i}(t)))\tilde{\bar{X}}_{-i}^T(t - \tau_{-i}(t)))dt\}, \\ &\quad for\ i = 1, \ldots, N \end{aligned} \tag{49}$$

Since $\rho_i^2 E\{\int_0^{t_f} (\tilde{\bar{v}}_i^T(t)\tilde{\bar{v}}_i(t) + \tilde{\bar{X}}_{-i}^T(t-\tau_{-i}(t)))\tilde{\bar{X}}_{-i}^T(t-\tau_{-i}(t)))dt\}$ is finite, from (49), it is seen that $E\{U_i^T(t)U_i(t)\}$, $E\{\tilde{X}_i^T(t))\tilde{X}_i(t)\}$ and $E\{\bar{e}_i^T(t)\bar{e}_i(t)\}$ approach to zero as $t_f \to \infty$ in the mean square error sense. This proof is finished.

APPENDIX B
PROOF OF THEOREM 2

First, we suppose

$$\begin{aligned} &(\tfrac{\partial V(\tilde{X}_i(t),\bar{e}_i(t),t)}{\partial[\tilde{X}_i^T(t)\ \bar{e}_i^T(t)\ t]^T})_\varepsilon \\ &= (\tfrac{\partial V(\tilde{X}_i(t),\bar{e}_i(t),t)}{\partial[\tilde{X}_i^T(t)\ \bar{e}_i^T(t)\ t]^T}) + \Xi_i(\tilde{X}_i(t), \bar{e}_i(t), t), \\ &\quad for\ i = 1, \ldots, N \end{aligned} \tag{50}$$

where $\Xi_i(\tilde{X}_i(t), \bar{e}_i(t), t)$ is the error function between $(\tfrac{\partial V(\tilde{X}_i(t),\bar{e}_i(t),t)}{\partial[\tilde{X}_i^T(t)\ \bar{e}_i^T(t)\ t]^T})_\varepsilon$ and $(\tfrac{\partial V(\tilde{X}_i(t),\bar{e}_i(t),t)}{\partial[\tilde{X}_i^T(t)\ \bar{e}_i^T(t)\ t]^T})$.

By the fact that HJIE$_{\varepsilon,i} = \varepsilon_i(\theta_p^i(t))$ and HJIE$_i = 0$, $\varepsilon_i(\theta_p^i(t))$ can be rewritten as follows:

$$\begin{aligned} \varepsilon_i(\theta_p^i(t)) &= HJIE_{i,\varepsilon} - HJIE_i \\ &= ((\tfrac{\partial V(\tilde{X}_i(t),\bar{e}_i(t),t)}{\partial[\tilde{X}_i^T(t)\ \bar{e}_i^T(t)\ t]^T})_\varepsilon^T - (\tfrac{\partial V(\tilde{X}_i(t),\bar{e}_i(t),t)}{\partial[\tilde{X}_i^T(t)\ \bar{e}_i^T(t)\ t]^T})^T) \\ &\quad \times \begin{bmatrix} \tilde{\bar{F}}_i(\tilde{X}_i(t), \bar{e}_i(t), t) \\ 1 \end{bmatrix} - \tfrac{1}{4}(\tfrac{\partial V(\tilde{X}_i(t),\bar{e}_i(t),t)}{\partial[\tilde{X}_i^T(t)\ \bar{e}_i^T(t)\ t]^T})_\varepsilon^T \\ &\quad \times \begin{bmatrix} \tilde{\bar{G}}_i(\tilde{X}_i(t), \bar{e}_i(t), t) \\ 0 \end{bmatrix} R_i^{-1} \begin{bmatrix} \tilde{\bar{G}}_i(\tilde{X}_i(t), \bar{e}_i(t), t) \\ 0 \end{bmatrix}^T \\ &\quad \times (\tfrac{\partial V(\tilde{X}_i(t),\bar{e}_i(t),t)}{\partial[\tilde{X}_i^T(t)\ \bar{e}_i^T(t)\ t]^T})_\varepsilon + \tfrac{1}{4}(\tfrac{\partial V(\tilde{X}_i(t),\bar{e}_i(t),t)}{\partial[\tilde{X}_i^T(t)\ \bar{e}_i^T(t)\ t]^T})^T \\ &\quad \times \begin{bmatrix} \tilde{\bar{G}}_i(\tilde{X}_i(t), \bar{e}_i(t), t) \\ 0 \end{bmatrix} R_i^{-1} \begin{bmatrix} \tilde{\bar{G}}_i(\tilde{X}_i(t), \bar{e}_i(t), t) \\ 0 \end{bmatrix}^T \\ &\quad \times (\tfrac{\partial V(\tilde{X}_i(t),\bar{e}_i(t),t)}{\partial[\tilde{X}_i^T(t)\ \bar{e}_i^T(t)\ t]^T}) + \tfrac{1}{4\rho_i^2}(\tfrac{\partial V(\tilde{X}_i(t),\bar{e}_i(t),t)}{\partial[\tilde{X}_i^T(t)\ \bar{e}_i^T(t)\ t]^T})_\varepsilon^T \\ &\quad \times \begin{bmatrix} \tilde{\bar{D}}_i(\tilde{X}_i(t), \bar{e}_i(t), t) & 0 \\ 0 & 0 \end{bmatrix} (\tfrac{\partial V(\tilde{X}_i(t),\bar{e}_i(t),t)}{\partial[\tilde{X}_i^T(t)\ \bar{e}_i^T(t)\ t]^T})_\varepsilon \\ &\quad - \tfrac{1}{4\rho_i^2}(\tfrac{\partial V(\tilde{X}_i(t),\bar{e}_i(t),t)}{\partial[\tilde{X}_i^T(t)\ \bar{e}_i^T(t)\ t]^T})^T \begin{bmatrix} \tilde{\bar{D}}_i(\tilde{X}_i(t), \bar{e}_i(t), t) & 0 \\ 0 & 0 \end{bmatrix} \\ &\quad \times (\tfrac{\partial V(\tilde{X}_i(t),\bar{e}_i(t),t)}{\partial[\tilde{X}_i^T(t)\ \bar{e}_i^T(t)\ t]^T}) + \tfrac{1}{4\rho_i^2}(\tfrac{\partial V(\tilde{X}_i(t),\bar{e}_i(t),t)}{\partial[\tilde{X}_i^T(t)\ \bar{e}_i^T(t)\ t]^T})_\varepsilon^T \\ &\quad \times \begin{bmatrix} \tilde{\bar{F}}_{-i}(\tilde{\bar{X}}_i(t), \bar{e}_i(t), t) & 0 \\ 0 & 0 \end{bmatrix} (\tfrac{\partial V(\tilde{X}_i(t),\bar{e}_i(t),t)}{\partial[\tilde{X}_i^T(t)\ \bar{e}_i^T(t)\ t]^T})_\varepsilon \\ &\quad - \tfrac{1}{4\rho_i^2}(\tfrac{\partial V(\tilde{X}_i(t),\bar{e}_i(t),t)}{\partial[\tilde{X}_i^T(t)\ \bar{e}_i^T(t)\ t]^T})^T \begin{bmatrix} \tilde{\bar{F}}_{-i}(\tilde{\bar{X}}_i(t), \bar{e}_i(t), t) & 0 \\ 0 & 0 \end{bmatrix} \\ &\quad \times (\tfrac{\partial V(\tilde{X}_i(t),\bar{e}_i(t),t)}{\partial[\tilde{X}_i^T(t)\ \bar{e}_i^T(t)\ t]^T}), \\ &\quad for\ i = 1, \ldots, N \end{aligned} \tag{51}$$

By (50), we get

$$\begin{aligned} \varepsilon_i(\theta_p^i(t)) &= \Xi_i^T(\tilde{X}_i(t), \bar{e}_i(t), t) \begin{bmatrix} \tilde{\bar{F}}_i(\tilde{X}_i(t), \bar{e}_i(t), t) \\ 1 \end{bmatrix} \\ &\quad - \tfrac{1}{4}\Xi_i^T(\tilde{X}_i(t), \bar{e}_i(t), t) \begin{bmatrix} \tilde{\bar{G}}_i(\tilde{X}_i(t), \bar{e}_i(t), t) \\ 0 \end{bmatrix} R_i^{-1} \\ &\quad \times \begin{bmatrix} \tilde{\bar{G}}_i(\tilde{X}_i(t), \bar{e}_i(t), t) \\ 0 \end{bmatrix}^T (\tfrac{\partial V(\tilde{X}_i(t),\bar{e}_i(t),t)}{\partial[\tilde{X}_i^T(t)\ \bar{e}_i^T(t)\ t]^T}) \\ &\quad - \tfrac{1}{4}(\tfrac{\partial V(\tilde{X}_i(t),\bar{e}_i(t),t)}{\partial[\tilde{X}_i^T(t)\ \bar{e}_i^T(t)\ t]^T})^T \begin{bmatrix} \tilde{\bar{G}}_i(\tilde{X}_i(t), \bar{e}_i(t), t) \\ 0 \end{bmatrix} R_i^{-1} \\ &\quad \times \begin{bmatrix} \tilde{\bar{G}}_i(\tilde{X}_i(t), \bar{e}_i(t), t) \\ 0 \end{bmatrix}^T \Xi_i(\tilde{X}_i(t), \bar{e}_i(t), t) \\ &\quad - \tfrac{1}{4}\Xi_i^T(\tilde{X}_i(t), \bar{e}_i(t), t) \begin{bmatrix} \tilde{\bar{G}}_i(\tilde{X}_i(t), \bar{e}_i(t), t) \\ 0 \end{bmatrix} R_i^{-1} \\ &\quad \times \begin{bmatrix} \tilde{\bar{G}}_i(\tilde{X}_i(t), \bar{e}_i(t), t) \\ 0 \end{bmatrix}^T \Xi_i(\tilde{X}_i(t), \bar{e}_i(t), t) \\ &\quad + \tfrac{1}{4\rho_i^2}\Xi_i^T(\tilde{X}_i(t), \bar{e}_i(t), t) \begin{bmatrix} \tilde{\bar{D}}_i(\tilde{X}_i(t), \bar{e}_i(t), t) & 0 \\ 0 & 0 \end{bmatrix} \\ &\quad \times (\tfrac{\partial V(\tilde{X}_i(t),\bar{e}_i(t),t)}{\partial[\tilde{X}_i^T(t)\ \bar{e}_i^T(t)\ t]^T}) + \tfrac{1}{4\rho_i^2}(\tfrac{\partial V(\tilde{X}_i(t),\bar{e}_i(t),t)}{\partial[\tilde{X}_i^T(t)\ \bar{e}_i^T(t)\ t]^T})^T \\ &\quad \times \begin{bmatrix} \tilde{\bar{D}}_i(\tilde{X}_i(t), \bar{e}_i(t), t) & 0 \\ 0 & 0 \end{bmatrix} \Xi_i(\tilde{X}_i(t), \bar{e}_i(t), t) \\ &\quad + \tfrac{1}{4\rho_i^2}\Xi_i^T(\tilde{X}_i(t), \bar{e}_i(t), t) \begin{bmatrix} \tilde{\bar{D}}_i(\tilde{X}_i(t), \bar{e}_i(t), t) & 0 \\ 0 & 0 \end{bmatrix} \\ &\quad \times \Xi_i(\tilde{X}_i(t), \bar{e}_i(t), t) + \tfrac{1}{4\rho_i^2}\Xi_i^T(\tilde{X}_i(t), \bar{e}_i(t), t) \\ &\quad \times \begin{bmatrix} \tilde{\bar{F}}_{-i}(\tilde{\bar{X}}_i(t), \bar{e}_i(t), t) & 0 \\ 0 & 0 \end{bmatrix} (\tfrac{\partial V(\tilde{X}_i(t),\bar{e}_i(t),t)}{\partial[\tilde{X}_i^T(t)\ \bar{e}_i^T(t)\ t]^T}) \\ &\quad + \tfrac{1}{4\rho_i^2}(\tfrac{\partial V(\tilde{X}_i(t),\bar{e}_i(t),t)}{\partial[\tilde{X}_i^T(t)\ \bar{e}_i^T(t)\ t]^T})^T \begin{bmatrix} \tilde{\bar{F}}_{-i}(\tilde{\bar{X}}_i(t), \bar{e}_i(t), t) & 0 \\ 0 & 0 \end{bmatrix} \\ &\quad \times \Xi_i(\tilde{X}_i(t), \bar{e}_i(t), t) + \tfrac{1}{4\rho_i^2}\Xi_i^T(\tilde{X}_i(t), \bar{e}_i(t), t) \\ &\quad \times \begin{bmatrix} \tilde{\bar{F}}_{-i}(\tilde{\bar{X}}_i(t), \bar{e}_i(t), t) & 0 \\ 0 & 0 \end{bmatrix} \Xi_i(\tilde{X}_i(t), \bar{e}_i(t), t), \end{aligned}$$

$$for\ i = 1, \ldots, N \tag{52}$$

By the symmetric property, we have following equations:

$$\begin{aligned}
&\Xi_i^T(\tilde{X}_i(t), \bar{e}_i(t), t)\begin{bmatrix}\tilde{\bar{G}}_i(\tilde{X}_i(t), \bar{e}_i(t), t)\\ 0\end{bmatrix}R_i^{-1}\\
&\times\begin{bmatrix}\tilde{\bar{G}}_i(\tilde{X}_i(t), \bar{e}_i(t), t)\\ 0\end{bmatrix}^T\left(\frac{\partial V(\tilde{X}_i(t),\bar{e}_i(t),t)}{\partial[\tilde{X}_i^T(t)\ \bar{e}_i^T(t)\ t]^T}\right)\\
&=\left(\frac{\partial V(\tilde{X}_i(t),\bar{e}_i(t),t)}{\partial[\tilde{X}_i^T(t)\ \bar{e}_i^T(t)\ t]^T}\right)^T\begin{bmatrix}\tilde{\bar{G}}_i(\tilde{X}_i(t), \bar{e}_i(t), t)\\ 0\end{bmatrix}R_i^{-1}\\
&\times\begin{bmatrix}\tilde{\bar{G}}_i(\tilde{X}_i(t), \bar{e}_i(t), t)\\ 0\end{bmatrix}^T\Xi_i(\tilde{X}_i(t), \bar{e}_i(t), t),\\
&\quad for\ i = 1, \ldots, N
\end{aligned} \tag{53}$$

$$\begin{aligned}
&\Xi_i^T(\tilde{X}_i(t), \bar{e}_i(t), t)\begin{bmatrix}\tilde{\bar{D}}_i(\tilde{X}_i(t), \bar{e}_i(t), t) & 0\\ 0 & 0\end{bmatrix}\\
&\times\left(\frac{\partial V(\tilde{X}_i(t),\bar{e}_i(t),t)}{\partial[\tilde{X}_i^T(t)\ \bar{e}_i^T(t)\ t]^T}\right)\\
&=\left(\frac{\partial V(\tilde{X}_i(t),\bar{e}_i(t),t)}{\partial[\tilde{X}_i^T(t)\ \bar{e}_i^T(t)\ t]^T}\right)^T\begin{bmatrix}\tilde{\bar{D}}_i(\tilde{X}_i(t), \bar{e}_i(t), t) & 0\\ 0 & 0\end{bmatrix}\\
&\Xi_i(\tilde{X}_i(t), \bar{e}_i(t), t),\\
&\quad for\ i = 1, \ldots, N
\end{aligned} \tag{54}$$

and

$$\begin{aligned}
&\Xi_i^T(\tilde{X}_i(t), \bar{e}_i(t), t)\begin{bmatrix}\tilde{\bar{F}}_{-i}(\tilde{\bar{X}}_i(t), \bar{e}_i(t), t) & 0\\ 0 & 0\end{bmatrix}\\
&\times\left(\frac{\partial V(\tilde{X}_i(t),\bar{e}_i(t),t)}{\partial[\tilde{X}_i^T(t)\ \bar{e}_i^T(t)\ t]^T}\right)\\
&=\left(\frac{\partial V(\tilde{X}_i(t),\bar{e}_i(t),t)}{\partial[\tilde{X}_i^T(t)\ \bar{e}_i^T(t)\ t]^T}\right)^T\begin{bmatrix}\tilde{\bar{F}}_{-i}(\tilde{\bar{X}}_i(t), \bar{e}_i(t), t) & 0\\ 0 & 0\end{bmatrix}\\
&\Xi_i(\tilde{X}_i(t), \bar{e}_i(t), t),\\
&\quad for\ i = 1, \ldots, N
\end{aligned} \tag{55}$$

By (53), (54), and (55), then (52) becomes

$$\begin{aligned}
\varepsilon_i(\theta_p^i(t)) = \Xi_i^T(\tilde{X}_i(t), \bar{e}_i(t), t)\{&\begin{bmatrix}\tilde{\bar{F}}_i(\tilde{X}_i(t), \bar{e}_i(t), t)\\ 1\end{bmatrix}\\
&-\frac{1}{2}\begin{bmatrix}\tilde{\bar{G}}_i(\tilde{X}_i(t), \bar{e}_i(t), t)\\ 0\end{bmatrix}R_i^{-1}\begin{bmatrix}\tilde{\bar{G}}_i(\tilde{X}_i(t), \bar{e}_i(t), t)\\ 0\end{bmatrix}^T\\
&\times\left(\frac{\partial V(\tilde{X}_i(t),\bar{e}_i(t),t)}{\partial[\tilde{X}_i^T(t)\ \bar{e}_i^T(t)\ t]^T}\right)-\frac{1}{4}\begin{bmatrix}\tilde{\bar{G}}_i(\tilde{X}_i(t), \bar{e}_i(t), t)\\ 0\end{bmatrix}R_i^{-1}\\
&\times\begin{bmatrix}\tilde{\bar{G}}_i(\tilde{X}_i(t), \bar{e}_i(t), t)\\ 0\end{bmatrix}^T\Xi_i(\tilde{X}_i(t), \bar{e}_i(t), t)+\frac{1}{2\rho_i^2}\\
&\times\begin{bmatrix}\tilde{\bar{D}}_i(\tilde{X}_i(t), \bar{e}_i(t), t) & 0\\ 0 & 0\end{bmatrix}\left(\frac{\partial V(\tilde{X}_i(t),\bar{e}_i(t),t)}{\partial[\tilde{X}_i^T(t)\ \bar{e}_i^T(t)\ t]^T}\right)\\
&+\frac{1}{4\rho_i^2}\begin{bmatrix}\tilde{\bar{D}}_i(\tilde{X}_i(t), \bar{e}_i(t), t) & 0\\ 0 & 0\end{bmatrix}\Xi_i(\tilde{X}_i(t), \bar{e}_i(t), t)\\
&+\frac{1}{2\rho_i^2}\begin{bmatrix}\tilde{\bar{F}}_i(\tilde{X}_i(t), \bar{e}_i(t), t)\\ 1\end{bmatrix}\left(\frac{\partial V(\tilde{X}_i(t),\bar{e}_i(t),t)}{\partial[\tilde{X}_i^T(t)\ \bar{e}_i^T(t)\ t]^T}\right)\\
&+\frac{1}{4\rho_i^2}\begin{bmatrix}\tilde{\bar{F}}_i(\tilde{X}_i(t), \bar{e}_i(t), t)\\ 1\end{bmatrix}\Xi_i(\tilde{X}_i(t), \bar{e}_i(t), t)\},\\
&for\ i = 1, \ldots, N
\end{aligned} \tag{56}$$

If $\varepsilon_i(\theta_p^i(t)) \to 0$ in (23), then (56) $\to 0$, too. Clearly, the term

$$\begin{aligned}
&\begin{bmatrix}\tilde{\bar{F}}_i(\tilde{X}_i(t), \bar{e}_i(t), t)\\ 1\end{bmatrix}-\frac{1}{2}\begin{bmatrix}\tilde{\bar{G}}_i(\tilde{X}_i(t), \bar{e}_i(t), t)\\ 0\end{bmatrix}R_i^{-1}\\
&\times\begin{bmatrix}\tilde{\bar{G}}_i(\tilde{X}_i(t), \bar{e}_i(t), t)\\ 0\end{bmatrix}^T\left(\frac{\partial V(\tilde{X}_i(t),\bar{e}_i(t),t)}{\partial[\tilde{X}_i^T(t)\ \bar{e}_i^T(t)\ t]^T}\right)\\
&-\frac{1}{4}\begin{bmatrix}\tilde{\bar{G}}_i(\tilde{X}_i(t), \bar{e}_i(t), t)\\ 0\end{bmatrix}R_i^{-1}\begin{bmatrix}\tilde{\bar{G}}_i(\tilde{X}_i(t), \bar{e}_i(t), t)\\ 0\end{bmatrix}^T\\
&\times\Xi_i(\tilde{X}_i(t), \bar{e}_i(t), t)+\frac{1}{2\rho_i^2}\begin{bmatrix}\tilde{\bar{D}}_i(\tilde{X}_i(t), \bar{e}_i(t), t) & 0\\ 0 & 0\end{bmatrix}\\
&\times\left(\frac{\partial V(\tilde{X}_i(t),\bar{e}_i(t),t)}{\partial[\tilde{X}_i^T(t)\ \bar{e}_i^T(t)\ t]^T}\right)+\frac{1}{4\rho_i^2}\begin{bmatrix}\tilde{\bar{D}}_i(\tilde{X}_i(t), \bar{e}_i(t), t) & 0\\ 0 & 0\end{bmatrix}\\
&\times\Xi_i(\tilde{X}_i(t), \bar{e}_i(t), t)+\frac{1}{2\rho_i^2}\begin{bmatrix}\tilde{\bar{F}}_i(\tilde{X}_i(t), \bar{e}_i(t), t)\\ 1\end{bmatrix}\\
&\times\left(\frac{\partial V(\tilde{X}_i(t),\bar{e}_i(t),t)}{\partial[\tilde{X}_i^T(t)\ \bar{e}_i^T(t)\ t]^T}\right)+\frac{1}{4\rho_i^2}\begin{bmatrix}\tilde{\bar{F}}_i(\tilde{X}_i(t), \bar{e}_i(t), t)\\ 1\end{bmatrix}\\
&\times\Xi_i(\tilde{X}_i(t), \bar{e}_i(t), t)
\end{aligned}$$

in {.} of (56) is not equal to zero for all $\tilde{X}_i(t)$ and $\bar{e}_i(t)$. If (56) is $\to 0$, $\Xi_i(\tilde{X}_i(t), \bar{e}_i(t), t)$ must approach to zero. In this situation, from (50), it is deduced that $\left(\frac{\partial V(\tilde{X}_i(t),\bar{e}_i(t),t)}{\partial[\tilde{X}_i^T(t)\ \bar{e}_i^T(t)\ t]^T}\right)_\varepsilon \to \left(\frac{\partial V(\tilde{X}_i(t),\bar{e}_i(t),t)}{\partial[\tilde{X}_i^T(t)\ \bar{e}_i^T(t)\ t]^T}\right)$. According to Theorem 1, the HJIE-reinforcement DNN-based robust decentralized H_∞ attack-tolerant observer-based tracking control scheme in Fig. 3 can approach to the theoretical robust decentralized H_∞ attack-tolerant observer-based team formation tracking control design. The proof is complete.

REFERENCES

[1] M. Zhu, X. Du, X. Zhang, H. Luo, and G. Wang, "Multi-UAV rapid-assessment task-assignment problem in a post-earthquake scenario," *IEEE Access*, vol. 7, pp. 74542–74557, 2019.
[2] N. H. Motlagh, M. Bagaa, and T. Taleb, "UAV-based IoT platform: A crowd surveillance use case," *IEEE Commun. Mag.*, vol. 55, no. 2, pp. 128–134, Feb. 2017.
[3] K. Dorling, J. Heinrichs, G. G. Messier, and S. Magierowski, "Vehicle routing problems for drone delivery," *IEEE Trans. Syst., Man, Cybern. Syst.*, vol. 47, no. 1, pp. 70–85, Jan. 2017.
[4] F. Liao, R. Teo, J. L. Wang, X. Dong, F. Lin, and K. Peng, "Distributed formation and reconfiguration control of VTOL UAVs," *IEEE Trans. Control Syst. Technol.*, vol. 25, no. 1, pp. 270–277, Jan. 2017.
[5] P. Ogren, M. Egerstedt, and X. Hu, "A control Lyapunov function approach to multiagent coordination," *IEEE Trans. Robot. Autom.*, vol. 18, no. 5, pp. 847–851, Oct. 2002.
[6] B.-S. Chen, C.-P. Wang, and M.-Y. Lee, "Stochastic robust team tracking control of multi-UAV networked system under Wiener and Poisson random fluctuations," *IEEE Trans. Cybern.*, vol. 51, no. 12, pp. 5786–5799, Dec. 2021.

[7] J. R. T. Lawton, R. W. Beard, and B. J. Young, "A decentralized approach to formation maneuvers," *IEEE Trans. Robot. Autom.*, vol. 19, no. 6, pp. 933–941, Dec. 2003.

[8] M.-Y. Lee, B.-S. Chen, Y. Chang, and C.-L. Hwang, "Stochastic robust team formation tracking design of multi-VTOL-UAV networked control system in smart city under time-varying delay and random fluctuation," *IEEE Access*, vol. 8, pp. 131310–131326, 2020.

[9] M.-Y. Lee, B.-S. Chen, C.-Y. Tsai, and C.-L. Hwang, "Stochastic H_∞ robust decentralized tracking control of large-scale team formation UAV network system with time-varying delay and packet dropout under interconnected couplings and Wiener fluctuations," *IEEE Access*, vol. 9, pp. 41976–41997, 2021, doi: 10.1109/ACCESS.2021.3065127.

[10] L. Chettri and R. Bera, "A comprehensive survey on Internet of Things (IoT) toward 5G wireless systems," *IEEE Internet Things J.*, vol. 7, no. 1, pp. 16–32, Jan. 2020.

[11] W. Cheng, X. Zhang, and H. Zhang, "Statistical-QoS driven energy-efficiency optimization over green 5G mobile wireless networks," *IEEE J. Sel. Areas Commun.*, vol. 34, no. 12, pp. 3092–3107, Dec. 2016.

[12] Y. Shi and B. Yu, "Output feedback stabilization of networked control systems with random delays modeled by Markov chains," *IEEE Trans. Autom. Control*, vol. 54, no. 7, pp. 1668–1674, Jul. 2009.

[13] G.-P. Liu, Y. Xia, D. Rees, and W. Hu, "Design and stability criteria of networked predictive control systems with random network delay in the feedback channel," *IEEE Trans. Syst., Man, Cybern. C, Appl. Rev.*, vol. 37, no. 2, pp. 173–184, Mar. 2007.

[14] H. Gao and T. Chen, "Network-based H_∞ output tracking control," *IEEE Trans. Autom. Control*, vol. 53, no. 3, pp. 655–667, Apr. 2008.

[15] B. Xue, S. Li, and Q. Zhu, "Moving horizon state estimation for networked control systems with multiple packet dropouts," *IEEE Trans. Autom. Control*, vol. 57, no. 9, pp. 2360–2366, Sep. 2012.

[16] R. Lu, Y. Xu, and R. Zhang, "A new design of model predictive tracking control for networked control system under random packet loss and uncertainties," *IEEE Trans. Ind. Electron.*, vol. 63, no. 11, pp. 6999–7007, Nov. 2016.

[17] B. Genge, P. Haller, and I. Kiss, "Cyber-security-aware network design of industrial control systems," *IEEE Syst. J.*, vol. 11, no. 3, pp. 1373–1384, Sep. 2017.

[18] H. Zhang, P. Cheng, L. Shi, and J. Chen, "Optimal DoS attack scheduling in wireless networked control system," *IEEE Trans. Control Syst. Technol.*, vol. 24, no. 3, pp. 843–852, May 2016.

[19] N. Liu, J. Zhang, H. Zhang, and W. Liu, "Security assessment for communication networks of power control systems using attack graph and MCDM," *IEEE Trans. Power Del.*, vol. 25, no. 3, pp. 1492–1500, Jul. 2010.

[20] A. Shui, W. Chen, P. Zhang, S. Hu, and X. Huang, "Review of fault diagnosis in control systems," in *Proc. Chin. Control Decis. Conf*, Guilin, China, 2009, pp. 5324–5329.

[21] S. Harshavarthini, R. Sakthivel, and C. K. Ahn, "Finite-time reliable attitude tracking control design for nonlinear quadrotor model with actuator faults," *Nonlinear Dyn.*, vol. 96, no. 4, pp. 2681–2692, Jun. 2019.

[22] H. Yang and S. Yin, "Descriptor observers design for Markov jump systems with simultaneous sensor and actuator faults," *IEEE Trans. Autom. Control*, vol. 64, no. 8, pp. 3370–3377, Aug. 2019.

[23] Q. Jia, W. Chen, Y. Zhang, and H. Li, "Fault reconstruction and fault-tolerant control via learning observers in Takagi–Sugeno fuzzy descriptor systems with time delays," *IEEE Trans. Ind. Electron.*, vol. 62, no. 6, pp. 3885–3895, Jun. 2015.

[24] J. Han, X. Liu, X. Gao, and X. Wei, "Intermediate observer-based robust distributed fault estimation for nonlinear multiagent systems with directed graphs," *IEEE Trans. Ind. Informat.*, vol. 16, no. 12, pp. 7426–7436, Dec. 2020.

[25] J. Han, X. Liu, X. Wei, and X. Hu, "Adaptive adjustable dimension observer based fault estimation for switched fuzzy systems with unmeasurable premise variables," *Fuzzy Sets Syst.*, vol. 452, pp. 149–167, Jan. 2023.

[26] J. W. Helton and M. R. James, *Extending H_∞ Control to Nonlinear Systems*. Philadelphia, PA, USA: SIAM, 1999.

[27] J. Yong and X. Y. Zhou, *Stochastic Control: Hamiltonian Systems and HJB Equation*. New York, NY, USA: Springer, 1999.

[28] W. Zhang, L. Xie, and B. S. Chen, *Stochasitc H_2/H_∞ Control: A Nash Game Approach*. Boca Raton, FL, USA: CRC Press, 2017.

[29] B. Chen, M. Lee, and X. Chen, "Security-enhanced filter design for stochastic systems under malicious attack via smoothed signal model and multiobjective estimation method," *IEEE Trans. Signal Process.*, vol. 68, pp. 4971–4986, 2020.

[30] H. J. Gao, J. Lam, L. H. Xie, and C. H. Wang, "New approach to mixed H_2/H_∞ filtering for polytopic discrete-time systems," *IEEE Trans. Signal Process.*, vol. 53, no. 8, pp. 3183–3192, Aug. 2005.

[31] X. Lin, C. Wu, and B. Chen, "Robust H_∞ adaptive fuzzy tracking control for MIMO nonlinear stochastic Poisson jump diffusion systems," *IEEE Trans. Cybern.*, vol. 49, no. 8, pp. 3116–3130, Aug. 2019.

[32] B. Chen, M. Lee, and T. Lin, "DNN-based H_∞ control scheme of nonlinear time-varying dynamic systems with external disturbance and its application to UAV tracking design," *IEEE Access*, vol. 9, pp. 69635–69653, 2021.

[33] B. Chen and P. Wu, "Robust H_∞ observer-based reference tracking control design of nonlinear stochastic systems: HJIE-embedded deep learning approach," *IEEE Access*, vol. 10, pp. 39889–39911, 2022.

[34] D. P. Kingma and J. Ba, "ADAM: A method for stochastic optimization," in *Proc. ICLR*, San Diego, CA, USA, Dec. 2014, pp. 1–15.

[35] S. X. Du, A. Dekka, and B. Wu, *Modular Multilevel Converters: Analysis, Control, and Applications*. Hoboken, NJ, USA: Wiley, Jan. 2018.

[36] Y. N. Dauphin, H. D. Vries, J. Chung, and Y. Bengio, "RMSProp and equilibrated adaptive learning rates for non-convex optimization," *Mach. Learn.*, Feb. 2015.

[37] A. H. Khan, X. Cao, S. Li, V. N. Katsikis, and L. Liao, "BAS-ADAM: An ADAM based approach to improve the performance of beetle antennae search optimizer," *IEEE/CAA J. Autom. Sinica*, vol. 7, no. 2, pp. 461–471, Mar. 2020.

[38] C.-S. Tseng and B.-S. Chen, "H_∞ decentralized fuzzy model reference tracking control design for nonlinear interconnected systems," *IEEE Trans. Fuzzy Syst.*, vol. 9, no. 6, pp. 795–809, Dec. 2001.

[39] S. R. Kou, D. L. Elliott, and T. J. Tarn, "Observability of nonlinear systems," *Inf. Control*, vol. 22, pp. 89–99, Feb. 1973.

[40] X. Yang, W. Deng, and J. Yao, "Neural adaptive dynamic surface asymptotic tracking control of hydraulic manipulators with guaranteed transient performance," *IEEE Trans. Neural Netw. Learn. Syst.*, early access, Jan. 28, 2022, doi: 10.1109/TNNLS.2022.3141463.

BOR-SEN CHEN (Life Fellow, IEEE) received the B.S. degree in electrical engineering from the Tatung Institute of Technology, Taipei, Taiwan, in 1970, the M.S. degree in geophysics from National Central University, Chungli, Taiwan, in 1973, and the Ph.D. degree in electrical engineering from the University of Southern California, Los Angeles, CA, USA, in 1982. He has been a Lecturer, an Associate Professor, and a Professor with the Tatung Institute of Technology, from 1973 to 1987. Currently, he is the Tsing Hua Distinguished Chair Professor of electrical engineering and computer science with National Tsing Hua University, Hsinchu, Taiwan. He is also the National Chair Professor of the Ministry of Education of Taiwan. His current research interests include control engineering, signal processing, and systems biology. He has received the Distinguished Research Award from the National Science Council of Taiwan four times.

PO-CHUN CHAO received the B.S. degree from the Department of Communications, Navigation and Control Engineering, National Taiwan Ocean University, Keelung, Taiwan, in 2020, and the M.S. degree from the Department of Electrical Engineering, National Tsing Hua University, Hsinchu, Taiwan, in 2022. His current research interests include robust control, fuzzy control, and nonlinear stochastic systems.